Alma Mater Studiorum – Università di Bologna

Dipartimento di Chimica Organica "A. Mangini"

DOTTORATO DI RICERCA IN

Scienze Chimiche

Ciclo XXIV

Settore Concorsuale di afferenza: 03/C1

Settore Scientifico disciplinare: CHIM/06

Sulfanyl Radical Addition to Alkynes: Revisiting an Old Reaction to Enter the Novel Realms of Green Chemistry, Bioconjugation, and Material Chemistry

Presentata da: Alessandro Monesi

Coordinatore Dottorato
Prof. Adriana Bigi

Relatore
Prof. Daniele Nanni

Correlatori
Prof. Piero Spagnolo
Dott. Mauro Boero,
CNRS Strasburgo
Dott. Carlo Massobrio,
CNRS Strasburgo
Dott. Alessandro Massi,
Università di Ferrara

Esame finale anno 2012

Abstract

In the last decade considerable attention has been devoted to the rewarding use of Green Chemistry in various synthetic processes and applications.

Green Chemistry is of special interest in the synthesis of expensive pharmaceutical products, where suitable adoption of “green” reagents and conditions is highly desirable. Our project especially focused in a search for new green radical processes which might also find useful applications in the industry. In particular, we have explored the possible adoption of green solvents in radical Thiol-Ene and Thiol-Yne coupling reactions, which to date have been normally performed in “ordinary” organic solvents such as benzene and toluene, with the primary aim of applying those coupling reactions to the construction of biological substrates. We have additionally tuned adequate reaction conditions which might enable achievement of highly functionalised materials and/or complex bioconjugation via homo/heterosequence. Furthermore, we have performed suitable theoretical studies to gain useful chemical information concerning mechanistic implications of the use of green solvents in the radical Thiol-Yne coupling reactions.

Table of Contents

CHAPTER 1 7

Introduction 7

1.1 Green and Click chemistry : concept 7

1.2 Basics of the radical chemistry 16

1.3 Thiol radical coupling 37

1.4 Theoretical approach 45

CHAPTER 2 55

Radical Additions of Thiols to Alkenes and Alkynes in Ionic Liquids 55

2.1 Introduction 55

2.2 Result and discussion 56

2.3 Conclusions 63

2.4 Experimental Section 63

CHAPTER 3 71

Thiol/Yne Coupling for Peptide Glycosidation 71

3.1 Introduction 71

3.2 Result and Discussion 71

3.3 Conclusions 82

3.4 Experimental Section 83

CHAPTER 4 95

Theorical approach for radical additions Computational Methods 95

4.1 Theoretical approach 95

4.1.1 Density Functional Theory 95

4.1.2 Car-Parinello Method 102

4.1.3 Blue Moon 105

4.2 Introduction of our problem 106

4.3 Computational Section 107

4.4 Result and Discussion 109

4.5 Conclusion 122

List of Publications 127

CHAPTER 1
Introduction

1.1 Green and Click chemistry : concept

In 1998 Warner and P. Anastas first coined the concept of "Green Chemistry", in a the seminal book "Green Chemistry: Theory and Practice[1]", where a precise definition of Green Chemistry was provided together with the Twelve Principles which were taken as the basis of the Green Chemistry itself (Table 1). The original guidelines of Green Chemistry have become generally accepted and the field has since seen a rapid expansion, with numerous innovative scientific developments associated with the production and utilization of chemical products.

The concept and philosophy of green chemistry now go beyond chemistry and actually involve different fields ranging from energy to societal sustainability. The main topic is "efficiency"[2] and "security", including material, energy, work force and property efficiency; any waste is to be addressed through innovative green chemistry means. Low efficiency in organic synthesis causes great challenges in resource conservation and draws environmental and health concerns related to the chemical wastes.

The majority of the processes that make use of chemicals cause a potential negative impact on the environment. Therefore, it is extremely important to eliminate, or, at least, reduce any possible risk to an acceptable level. Risk can be expressed as:

Risk = Hazard * Exposure

Traditionally, the risks connected with chemical processes have been minimized by controlling the so-called "circumstantial" factors, such as the use, handling, treatment, and disposal of chemicals. In contrast with the tradition, the Green Chemistry aims to minimize the risk by minimizing the hazard. It therefore shifts control from circumstantial to intrinsic factors, such as the design or selection of chemicals with reduced toxicity and the use of reaction pathways that tend to eliminate by-products or ensure that they are benign.

To improve the security of a synthetic process, it is necessary to operate on different directions such as feedstock of chemical(s), type of reaction and solvent, and product separation.

The main feedstock of chemical products comes from nonrenewable petroleum that is being depleted rapidly both for chemical and energy needs. However, nature provides a vast amount of biomass in the renewable forms of carbohydrates, amino acids, and triglycerides to obtain organic products[3], but a major obstacle to using renewable biomass as feedstock is the need for novel chemistry able to transform large amounts of biomass in its natural state, without the need of extensive functionalisation or protection.

Table 1. The most widely accepted definition of green chemistry (*1*) is "the design, development and implementation of chemical processes and products to reduce or eliminate substances hazardous to human health and the environment." This definition has been expanded into 12 principles listed in the table.

Green chemistry principles
1. It is better to prevent waste than to treat or clean up waste after it is formed.
2. Synthetic methods should be designed to maximize the incorporation of all materials used in the process into the final product.
3. Wherever practicable, synthetic methodologies should be designed to use and generate substances that possess little or no toxicity to human health and the environment.
4. Chemical products should be designed to preserve efficacy of function while reducing toxicity.
5. The use of auxiliary substances (e.g., solvents, separation agents, and so forth) should be made unnecessary wherever possible and innocuous when used.
6. Energy requirements should be recognized for their environmental and economic impacts and should be minimized. Synthetic methods should be conducted at ambient temperature and pressure.
7. A raw material or feedstock should be renewable rather than depleting wherever technically and economically practicable.
8. Unnecessary derivatization (blocking group, protection/deprotection, temporary modification of physical/chemical processes) should be avoided whenever possible.
9. Catalytic reagents (as selective as possible) are superior to stoichiometric reagents.
10. Chemical products should be designed so that at the end of their function they do not persist in the environment and break down into innocuous degradation products.
11. Analytical methodologies need to be developed further to allow for real-time in-process monitoring and control before the formation of hazardous substances.
12. Substances and the form of a substance used in a chemical process should be chosen so as to minimize the potential for chemical accidents, including releases, explosions, and fires.

Solvents represent the largest amount of auxiliary wastes in most chemical productions (approximately 80%)[4], they are used extensively for dissolving reactants, extracting and washing products, separating mixtures, cleaning reaction apparatus and dispersing products for practical applications; efficient control can produce a substantial improvement in the environmental impact of a process[5]. The primary function of solvents in classical chemical syntheses is to facilitate mass transfer to modulate chemical reactions in terms of reaction rate, yields, conversions, and selectivity. They do this by dissolving the reactants in dilute homogeneous mixtures; but, after the reaction, the final products have to be separated from the solvent through energy-intensive means. The

development of Green Chemistry redefines the role of a solvent: An "ideal solvent facilitates the mass transfer but does not dissolve!"[2a] In addition, an ideal green solvent should be natural, non-toxic, cheap and also readily available.

Furthermore, it should have the additional ability of favoring reaction, product separation, and/or catalyst recycling. The most elegant way to avoid any problem with solvents is avoiding their use, which approach has been widely exploited in the paints and coatings industries and also, in most recent years, in the arduous sphere of organic chemistry[6]. Most reactions, however, require solvent: a green chemical process must therefore involve an environmentally acceptable solvent, but, unfortunately, there is no green solvent suitable for every need.

Among the most widely explored greener solvents are ionic liquids[7], supercritical CO_2[8], and water[9]. Ionic liquids are salts of highly asymmetrical organic ions with melting points below or close to room temperature[10], while supercritical fluids are gases that are nearly as dense as liquids[11].

A supercritical fluid is a gas that has been brought above its critical temperature and pressure. At the critical point all the properties of the two phases are equal and the two phases become a single continuous phase. The diffusivity, while being lower than that of a gas, is significantly higher than that of a liquid. The combination of these two properties makes supercritical fluids much better solvents than they would be expected to be. This is particularly true when the temperature and pressure are not too far above the critical temperature and pressure. It is therefore possible to tune the density, and as a consequence the solvent power (Figure 1).

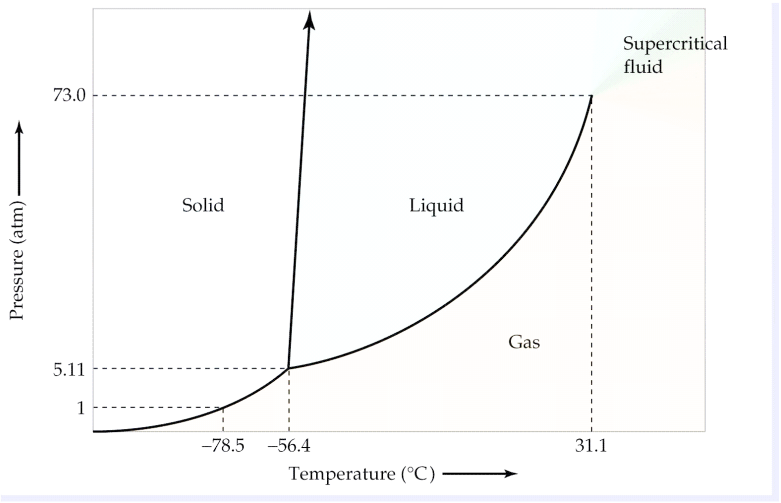

Figure 1. Carbon dioxide phase diagram

Processes that make use of supercritical fluid solvents occur necessarily at elevated pressures. In certain cases, they may also occur at elevated temperatures. Solvents are often chosen on the basis of the suitability of the temperatures and pressures corresponding to the supercritical region. However, other factors are important as well. These include toxicity and other hazards, cost, availability, and environmental friendliness (or lack thereof) of the solvent itself. On these bases, carbon dioxide is the most preferred solvent: in fact, besides being the cheapest natural solvent, it is renewable, nonflammable, and highly volatile. Moreover, it has solvent properties similar to light hydrocarbons, apart from an unusually high affinity with fluorocarbons[12]. Supercritical CO_2 has found numerous applications in synthesis, and, more interestingly, in certain industrial processes. The first example of its industrial use is offered by the extraction of caffeine from coffee, by SFE in the 1970s,[13] which led to an explosive interest in the 1980s for food treatment (tea decaffeination, extraction of fats from foods and of essential oils and spices from plants). The recent literature reflects the wide variety of current applications of CO_2 supercritical fluid: dry cleaning[14], precision-cleaning of inorganic surfaces[15], deposition media for the production of metallic powders and thin films[16] and other numerous applications. In a recent book Leitner and Jessop and Anastas[17] highlighted the versatile use of this medium in chemical and industrial processes.

In addition to natural solvents, other non-natural ones have been extensively adopted as green solvents. Ionic liquids[18] are probably the most studied ones. Ionic liquids are organic salts with melting points below ambient (or reaction) temperature: such solvents generally have very low vapor pressures and hence present much lower toxicity than low-boiling solvents, which fact makes them especially safe for microwave synthesis methods.[19] Importantly, ionic liquids present high thermal and chemical stability (in Table 2 are summarized the main properties of a modern ionic liquid). An attractive feature of ionic liquids is that, depending on the nature of their organic cations and inorganic counter anions, they can be readily separated from organics as well from water; moreover, their peculiar properties enable ready solubility of even complex systems like carbohydrates[20] or polymer[21]. For this reason, ionic liquids have been termed "designer solvents".

A salt	Cation and or anion quite large
Freezing point	Preferably below 100°C
Liquidus range	Often > 200°C
Thermal stability	Usually high
Viscosity	Normally < 100 cP, workable
Dielectric constant	Implied ≤ 30
Polarity	Moderate
Specific conductivity	Usually < 10 $mScm^{-1}$, "Good"
Molar conductivity	< 10 $Scm^2\ mol^{-1}$
Electrochemical window	> 2V, even 4.5 V, except for Brønsted acidic systems
Solvent and/or catalyst	Excellent for many organic reactions
Vapor pressure	Usually negligible

Table 2. Properties of a modern ionic liquid

Ionic liquid has been used in different research fields: chemical engineering (extraction and separation process, ands also build selective membranes)[22], for normal organic synthesis (like chiral synthesis, polymerization, nano materials, surfactants)[23] and in biotechnology (biocatalysis and purification of proteins)[24].

The only natural solvent on earth is water. Water is the most inexpensive, safe and green solvent in nature. This points have attracted the attention of scientists for many years: the first use of water for an organic reaction could be dated back to Wohler's synthesis of urea from ammonium cyanate[25].

Water possesses unique physical and chemical properties: a large temperature window in which it remains in the liquid state, extensive hydrogen

bonding, high heat capacity, large dielectric constant, and optimum oxygen solubility (it could to maintain aquatic life forms). These distinctive properties are the consequence of the unique structure of water.

However, unfortunately, water presents limited chemical compatibility: in fact, many (organic) reactants and reagents, including most organometallic compounds, are totally incompatible with water. Hydrophilicity can be properly enhanced by introduction of polar functional soluble[26], but the need of possible manipulations can seriously reduce the advantages (low cost, simplicity of reaction conditions, ease of workup and product isolation) connected with the use of water in place of the traditional organic solvents. Since the solubility of any reacting species and product in water can be dramatically changed, leading to homogeneous or heterogeneous reaction mixtures, recent publications describe reactions in water under very different conditions[27].

The green solvents so far studied complement one another in properties and applications: perhaps one day, already known and others new green solvents will become the most used ones in synthesis. Green Chemistry seems to be based on new exotic solvents and new technologies; however, running reactions in the latest green solvents or water instead rather than in organic solvents does not necessarily improve the environmental impact of a synthetic sequence.

A measure of the efficiency of a process is furnished by the so-called E-factor, which is actually due to the ratio of the amount of waste produced with respect to that of the desired material which is achieved.

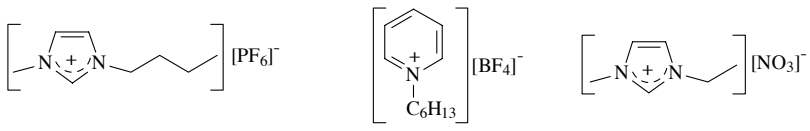

Figure 2. Tipical Ionic liquid used for organic synthesis.

E-factor = mass of waste ÷ mass of product

Since it is not easy to perform a direct determination of the waste generated, it is usual to measure the quantity of material put into the system and

subtract the mass of material output from the system. In the simplest case, the only output from the system would be the final product. If materials (e.g. solvents or catalysts) are recycled, however, then the output of the system would also include those materials.

In parallel of the green chemistry concept, Kolb, Finn and Sharpless, in 2001[28] have published a review where was introduced the **"Click Chemistry"** concept. The click chemistry's principles overlaps in different sections the green chemistry: atom economy, simple purification procedures, and benign solvents and side products.

$$\text{Atom Economy} = \frac{\text{molecular wt. of desired product}}{\text{molecular weight of all products}} \times 100\%$$

Click chemistry is based on the philosophy that the any reaction must be modular, wide in scope, give very high yields, generate only inoffensive by-products, and also be stereospecific (but not necessarily enantio-selective). The features of a click process also include simple reaction conditions (ideally, the process should be insensitive to oxygen and water), readily available starting materials and reagents, the use of benign solvents (green solvents and/or water) as well as simple product isolation. Moreover, product purification (when required) should entail crystallization or distillation (not chromatography) and the ensuing product should be stable under physiological conditions. Finally, a click process should have a high thermodynamic driving force, usually greater than 20 kcal/mol. Most common examples of click reaction are:

- Cycloadditions[29] of unsaturated species, Huisgen 1,3-dipolar cycloaddition reactions of azides and alkynes, and hetero-Diels-Alder transformation.

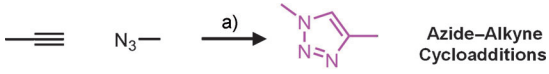

The classical [3+2] cycloaddition of unactivated alkynes and azides requires high temperatures or pressures and was relatively ignored for decades after its discovery by Huisgen[30]. When Sharpless[31] and Meldal[32] independently reported a Cu(I)-catalyzed variant that proceeds rapidly at room temperature to

regiospecifically form 1,4-disubstituted 1,2,3-triazoles the reaction back to-life. The success of the CuAAC reaction is now well recognised by the chemical community, but its biological applications remain seriously limited by toxicity of the copper catalyst. This fact has led to the recent discovery of copper-free cycloadditions[33], which nonetheless occur at comparably fast rates. The groups of Fokin and Jia [34] used a ruthenium(II) catalyst, but under more severe conditions.

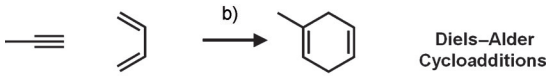

The Diels-Alder reaction is legendary in organic chemistry[35]. The solid-state Diels–Alder proposed by Kochi ten years ago[36], besides providing 100% atom economy with no solvent required, and affords a single product with no purification. The Diels–Alder reaction is certainly modular and wide in its scope: its ability to function as a click reaction in different fields is being well recognized.

- Nucleophilic ring-openings, these refer to the openings of strained heterocyclic electrophiles, such as aziridines, epoxides, cyclic sulfates, aziridinium ions, episulfonium ions

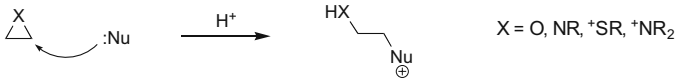

- B carbonyl chemistry of the “non-aldol” type, such as formation of ureas, thioureas, aromatic heterocycles, oxime ethers, hydrazones, and amides;

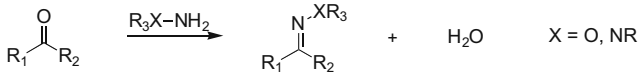

(Hydrazone/oxime ether formation)

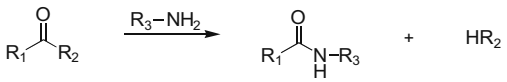

(Amide/isourea formation)

- Additions to carbon - carbon multiple bonds, especially oxidative cases such as epoxidation, dihydroxylation, aziridination, and sulfenyl halide addition, but also Michael additions of Nu-H reactants.

• Highly efficient reactions of thiols with reactive carbon–carbon double/ triple bonds (TEC-TYC)

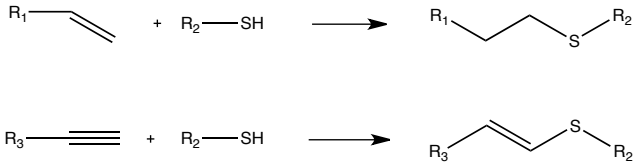

1.2 Basics of the radical chemistry [37,38]

Heterolysis 'versus' homolysis

"Common" organic reactions are envisioned to occur by displacement of electron pairs: this dissociative process entails unsymmetrical cleavage of covalent bonds (heterolysis), in which both bonding electrons remain with one partner and there is consequent formation of charged species (ions).

The alternative possibility is a symmetrical bond breaking (homolysis), in which case each atom carries away one of the two original bonding electrons. In this way, neutral species bearing an unpaired electron (radical intermediates) are generated. Most radical reactions involve homolytic cleavage (Scheme 1), but exceptions are usually encountered with electron-transfer processes.

Scheme 1. Heterolysis vs. Homolysis

It is worth noting that, at least in gas phase, more familiar heterolysis is generally less feasible than homolysis. However, under more usual solution conditions, especially when (highly) polar solvents are employed, ionic solvatations become so important as to allow most reactions to proceed through heterolytic pathways. Since free radicals are often electrically neutral, solvent stabilization on those species are usually meaningless: consequently, only bonds with (particularly) low Bond Dissociation Energy (BDE) such as, for instance, Sn-H bonds (≈310 kJ mol-1 at 300 K in gas-phase), can be involved in alternative radical pathways. A main solvent effect is that "solvatated" ions have a low tendency to recombine and, therefore, can occur in somewhat high concentrations; on the other side, radical intermediates tend to recombine very quickly to non-radical products and so they usually occur in very low concentrations.

This is the main reason why radical intermediates are often not easily detectable even by spectroscopic methods and why free radical reactions have long been believed to be very poorly selective. Nevertheless, through a careful choice of the experimental conditions (solvent, temperature, reagent ratio and

reagent concentration), radical reactions can allow highly useful synthetic transformations both in terms of product yield and by-product minimization.

Structure and stability of radicals

The structure and stability of free (carbon) radicals roughly resemble those of the corresponding (carbo)cations. In general, lowering of BDE values favour production of radical species which are therefore regarded as being more stable (Table 3). Progressive substitution at the radical centre can usually enhance radical stability owing to inherent hyperconjugation and/or resonance effects (carbon radical stability follows the order: benzyl > tertiary > secondary > primary > methyl).

Table 3. Approximate dissociation energies of selected bonds (kJ mol^{-1} at 300 K in gas-phase)

CH_3-H	439	Cl_3C-H	402	$((CH_3)_3Si)_3Si$-H	331
CH_3CH_2-H	423	F-H	569	$(CH_3)_3Sn$-H	310
$(CH_3)_2CH$-H	410	Cl-H	431	C_2H_5-Cl	339
$(CH_3)_3C$-H	397	Br-H	366	C_2H_5-Br	289
CH_2=CH-H	431	I-H	297	C_2H_5-I	222
HC≡C-H	544	HO-H	498	RO-OR	155
C_6H_5-H	464	HOO-H	368	CH_3-CH_3	372
CH_2=$CHCH_2$-H	364	CH_3O-H	439	CH_3CH_2-CH_3	364
$C_6H_5CH_2$-H	372	C_6H_5O-H	360	$(CH_3)_2CH$-CH_3	360
RC(=O)-H	364	R_2NO-H	310	$(CH_3)_3C$-CH_3	351
$EtOCH(CH_3)$-H	385	CH_3S-H	385	Cl-Cl	243
N≡CCH_2-H	360	C_6H_5S-H	343	Br-Br	192
CH_3COCH_2-H	385	$(CH_3)_3Si$-H	377	I-I	151

The unpaired electron can occupy a *p* orbital or a hybrid orbital having some *s*-character: the corresponding radicals are referred to as π- and σ-radicals, respectively. Ethyl radical 1 as well as primary, secondary and tertiary alkyl radicals usually are "planar" π-radicals, but their geometry is affected by the presence of strongly electronegative substituents like fluorine or alkoxyl. In fact, trifluoromethyl 2 is a pyramidal σ-radical bearing its electron in a sp^3-orbital. Benzyl radical 3 also is a π-radical where the unpaired electron is delocalized onto the adjacent aromatic ring (Figure 3). Similar to benzyl radical 3, other π-

radicals bearing an adjacent unsaturated substituent like the vinyl, cyano or carbonyl group are stabilized by conjugation with the adjacent π bond.

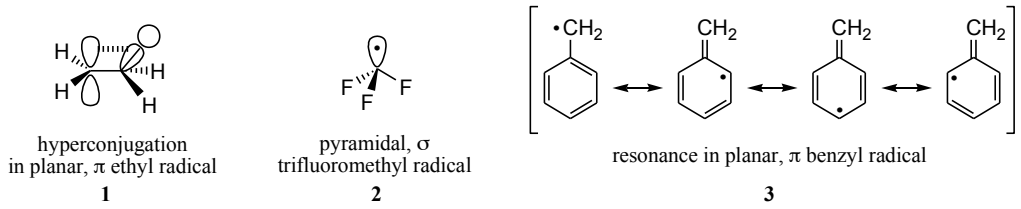

Figure 3. Stucture and stabilisation effects in radicals

Stabilization can additionally arise from overlapping of the orbital of the π-radical with the lone pair of a vicinal heteroatom including *inter alia* oxygen, nitrogen and, to a lesser extent, halogen atom; such interaction in fact leads to a resonance-stabilized 'three-electron bonding' where there is a separation of charge since an electron is donated from the heteroatom (Scheme 2). Consequently, the extent of such lone pair stabilization is expected to decrease with increasing the electronegativity of the heteroatom involved.

The concomitant presence of an electron-donating and electron-withdrawing group brings about a synergistic effect between the two groups and radical stabilization becomes greater than might be expected based on the sum of the effects of the two separate groups. The effect has been referred to as "*captodative*" stabilization, where the electron-withdrawing group is the "capto" group and the electron-donating group is the "dative" one. For instance, such effect is responsible for the very low BDE displayed by the α-C–H bond of glycine (318 kJ mol–1, Scheme 2)[39]

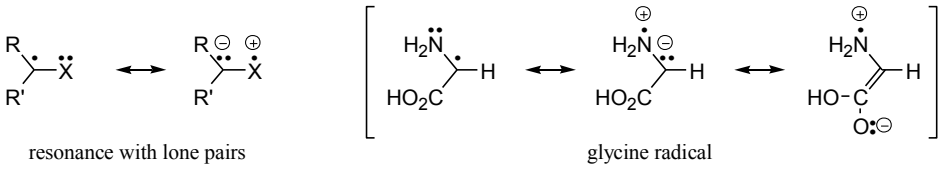

Scheme 2 . Stabilization by lone pairs and captodative

'Stability' versus 'persistence'

There is a further, important point concerning "radical stability" which is worth note: the difference between thermodynamic stability (or "**stability**") and lifetime (or "**persistence**") of a radical species.

Stability largely depends on electronic effects such as the mesomeric and inductive ones discussed above. On the other side, persistence is a general result of steric factors: the more congested is the radical centre the greater will be the radical lifetime. This is reflected in relatively high concentrations of radicals species occurring in solution and/or in self-reactions significantly less than the diffusion limit.

For example, methyl radical 4 has a half-life of 0.2 × 10−3 s at a 10−6 M concentration, whereas tri(iso-propyl)methyl radical 5 (a relatively 'persistent' radical), at the same concentration, has a half-life of 21 h! The longer the lifetime, the less reactive a radical intermediate will be, since its persistency will slow down the reaction rate with itself and other species. It is worth note that benzyl 6, even though being 'stabilized' by resonance delocalization, undergoes diffusion-controlled self-reaction and hence is not at all a "persistent' radical (Figure 4).[40]

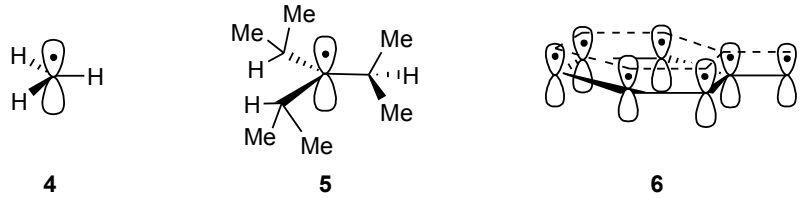

Figure 4. Stability vs. persistence: benzyl radical 6 is thermodynamically more 'stable' than 5, but kinetically less persistent

In certain cases of noteworthy persistency (due to both thermodynamic and kinetic factors), the lifetimes of radical species can be so long that they can survive for a very long time (like some biologically or industrially important phenoxyls) or even almost indefinitely as do some commercially available free-radicals such as TEMPO and DPPH) (Figure 5).

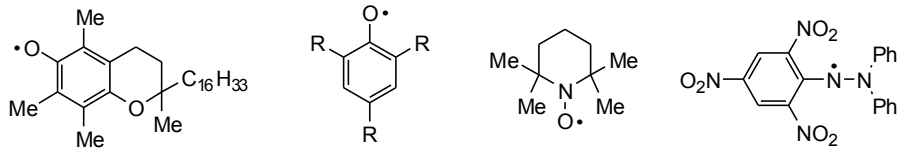

Vitamin E | 2,4,6-trisubstituted phenoxyls | TEMPO | DPPH

Figure 5. Stable and persistent free-radicals

The idea of persistency is hence strongly related to the mechanism of action of popular antioxidants which play a crucial role in the fields of food conservation and cell protection. Moreover, the concept of radical persistency is also very important in organic synthesis as a radical generation method coupled with efficient trapping control: infact, radical persistency is exploited in the achievement of living-radical polymerization.[41]

'Philicity' of radicals and 'Hydrogen Abstraction''

The presence of electron-donating (EDG) and electron-withdrawing (EWG) substituents also affects the 'philicity' of radicals species with important consequences for their chemical behaviour. Indeed, although radical reactions have long been considered to be independent of polar effects owing to the intervention of neutral intermediates, more recent studies have clearly established that those reactions can be largely governed by an appropriate choice of radical/molecule partners having opposite philicity.

This concept can be simply accounted for by considering that EDG groups can actually enhance the electron density on the radical centre, whereas EWG groups can behave in an opposite fashion. In fact, the oxidation/reduction potentials of radicals are largely affected by the electronic properties of their substituents: the presence of an EDG group will lower the oxidation potential of a radical centre, thus favoring possible occurrence of a corresponding (carbo) cation, while the presence of an EWG will lower the reduction potential, thus encouraging alternative occurrence of a corresponding (carb)anion. In the former cases 'electrophilic' radicals will arise and in the latter 'nucleophilic' ones (Scheme 3).

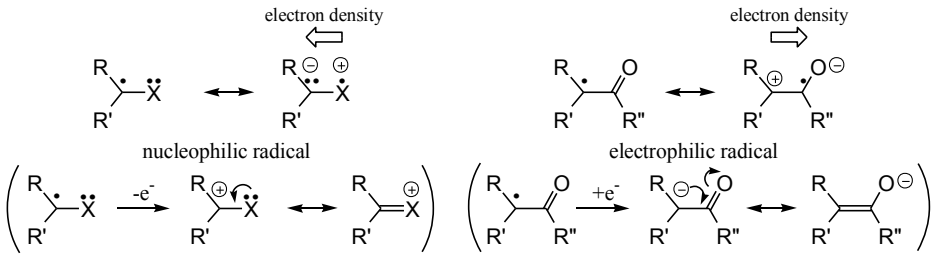

Scheme 3. Radical philicity

The radical philicity can be explained more rigorously in terms of a frontier molecular orbital (FMO) approach.[42,43]

For a radical having a vicinal EDG substituent with a lone pair, interaction of the p-orbital containing the unpaired electron (SOMO) with the adjacent lone pair gives rise to two new molecular orbitals: two of the three electrons occupy the new lower energy orbital, while the third electron occupies the new SOMO which is higher in energy than that of the original one (Scheme 4a). On the contrary, a radical bearing an unsaturated EWG substituent has a SOMO that is very close in energy to the antibonding π*-orbital (LUMO) of the substituent: in this case, the interaction between the SOMO and the empty LUMO gives rise to a new SOMO that is lower in energy than the original one (Scheme 4b). Accordingly, unlike ions, radicals are stabilized by both EDG and EWG substituents.

Furthermore, the FMO approach also explains the high selectivity of most radical reactions. Since in fast reactions small energy differences are required in SOMO-LUMO or SOMO-HOMO interactions, radicals with a high-energy SOMO have a tendency to interact with unfilled LUMO orbitals (such as those of electron-deficient olefins), and hence behave as electron-donating (nucleophilic) species. On the contrary, radicals with a low-energy SOMO tend to interact with SOMO filled orbitals (like those of electron-rich alkenes) and then behave as electrophilic species (Scheme 4c,d).

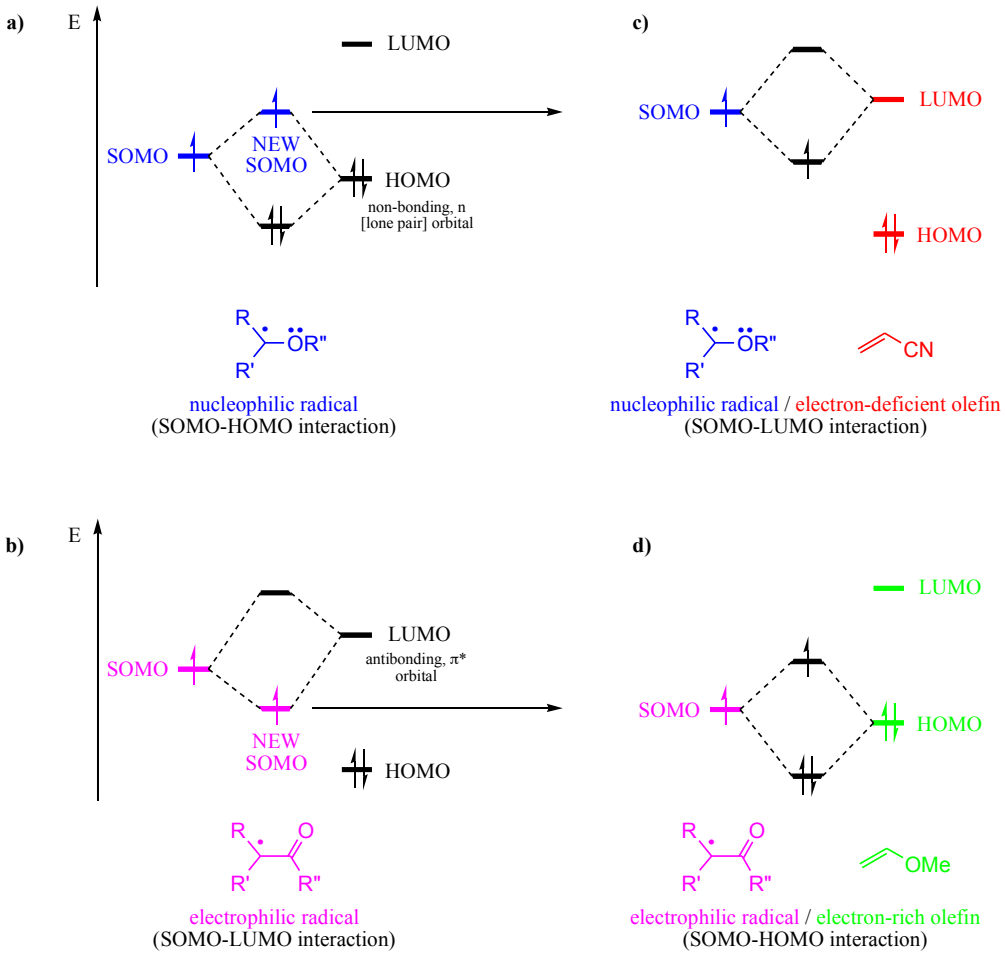

Scheme 4 . Molecular orbitals and radical philicity

An analogous explanation can account for the very high selectivity often observed in hydrogen abstractions. These reactions are known to be highly affected by polar factors and substituents capable to stabilize a partial charge separation in the transition state increase the reaction rate (Scheme 5). For example, nucleophilic alkyl radicals abstract a hydrogen atom from a thiol with a kinetic constant of ≅ 107 – 108 M^{-1} s^{-1}, whereas the same reaction with a silicon hydride has a kinetic constant of ≅ 103 M^{-1} s^{-1} only. Since the sulfur–hydrogen bond (370 kJ mol^{-1}) has a similar strength to the silicon–hydrogen one (375 kJ mol^{-1}), the reaction is clearly not influenced by thermodynamic factors. Indeed, the reaction with thiols is fast because the nucleophilic alkyl radical rapidly abstracts the thiol hydrogen through a transition state with partial charge separation in which the carbon radical donates an electron to sulfur. With nucleophilic silanes analogous charge separation in the transition state is

evidently discouraged (Scheme 5a). Of course, the opposite applies to for electrophilic radicals, which can rapidly abstract hydrogen from nucleophilic silanes but not from electrophilic thiols (Scheme 5b).

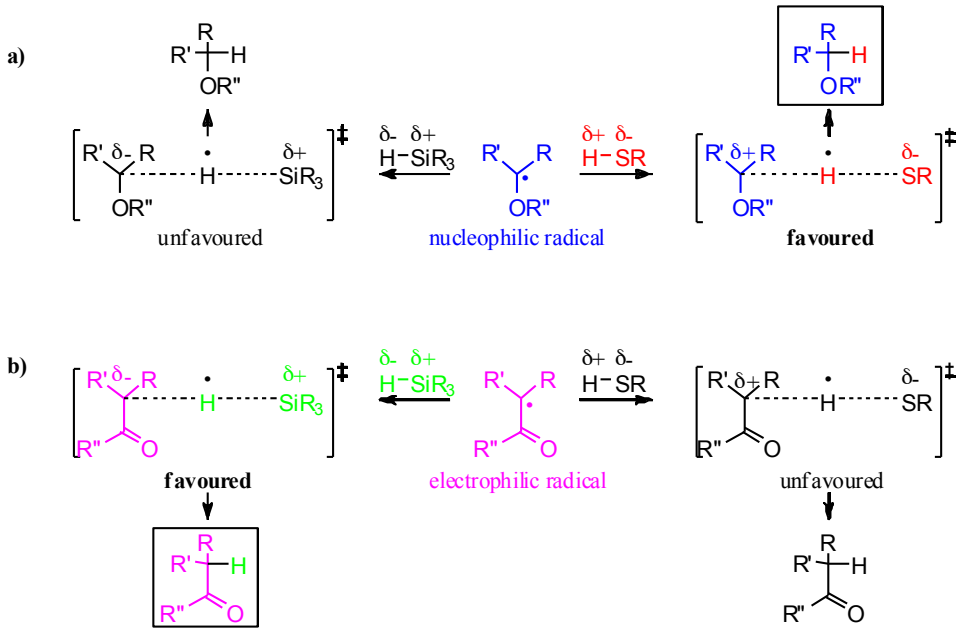

Scheme 5. Polar effects in hydrogen abstraction

We can obtain the same rationale by the frontier molecular orbital approach. The hydrogen abstraction reaction is the result of the interaction between the SOMO of the radical and either the HOMO (σ) or the LUMO (σ*) of the C–H bond. Electron-withdrawing groups attached to the C–H bond will lower the HOMO and LUMO energies, whereas electron-donating groups will have the opposite effect. Therefore, electrophilic radicals will react faster with the electron-rich C–H bond of silanes through SOMO-HOMO interaction (see Scheme 4d), whereas nucleophilic radicals will prefer to react with the electron-deficient C–H bond of thiols through SOMO-LUMO interaction (see Scheme 4c).

Mechanism of radical transformations: "chain reactions" and unit steps

Many radical reactions are "chain reactions" and they are characterized by three fundamental steps: initiation, propagation and termination of chain. For better understanding these concepts, we shall examine the radical reaction of

methane with molecular chlorine leading to formation of methyl chloride upon photochemical irradiation (Reaction 1).

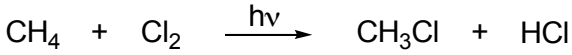

Reaction 1. Chlorination of methane

The first step of this reaction is the initiation of a radical chain: suitable irradiation causes initial fragmentation of molecular chlorine to chlorine atoms (Reaction 2).

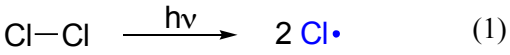

Reaction 2. Initiation step of radical chain

Like in this case, an initiation step generally entails generation of some radical species from non-radical precursors (initiators)[44].

The second step involves propagation of a radical chain: an initially-formed chlorine abstracts a hydrogen atom from methane to form hydrochloric acid and a methyl radical (CH3•) which then reacts with molecular chlorine to form chloromethane with regeneration of a chlorine atom (Scheme 6).

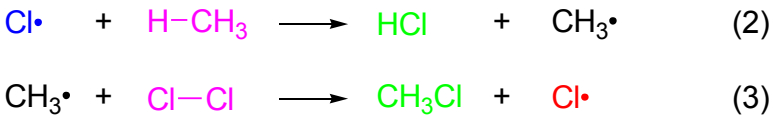

Scheme 6 . Propagation step of radical chain

The repetitive character of Scheme 6 is referred to as propagation of a "radical chain": through radical chain propagation the starting reagents (molecular chlorine and methane) are consumed and chloromethane and hydrogen chloride products are formed.

The third and last step, occurring in competition with the propagation step, entails termination of a radical chain: pairs of radical species formed in Equation 2 (Cl• and CH3•) interact to form non-radical products[45] according to Scheme 7.

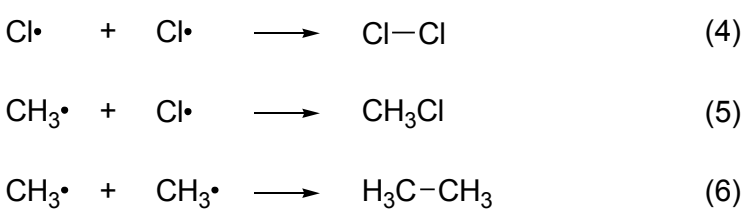

Scheme 7. Termination step of radical chain

We will now analyze more in details these three processes which are very important for successful applications of radical reactions in organic synthesis.

Radical Initiation

Radical reactions are commonly initiated by thermolysis or photolysis of suitable precursors, but radicals can also be produced by redox reactions (oxidations and reductions).[46] Also dioxygen can initiate radical processes, since the ground state of O_2 is a triplet with two unpaired electrons one of which is accommodated into two degenerate π*-orbitals. Dioxygen is therefore a stable biradical and can, for instance, abstract hydrogen atoms from weak carbon –hydrogen bonds or act as a radical scavenger: these processes are of basic importance for example in lipid and polymer autoxidations.[47]

Radical generation by ***thermolysis*** can occur in solution at relatively low temperatures from molecules having suitably low BDEs (125-165 kJ mol^{-1}). Low BDEs are usually encountered with carbon–heteroatom, heteroatom –heteroatom, or metal–metal bonds, but carbon–carbon or carbon–hydrogen bonds are normally too strong to be thermally broken. Suitable molecules include diacyl and dialkyl peroxides, where O–O bonds are broken (125-150 kJ mol^{-1}), and azo-compounds, which undergo cleavage of two N–C bonds with concomitant formation of molecular nitrogen. Peroxides like di-tert-butyl, dilauroyl, or dibenzoyl peroxide and azobis-iso-butyronitrile (AIBN) are the most commonly used radical initiators, also employed in industrial applications (e.g. polymerisations) (Scheme 8a). The decomposition temperature of a radical initiator largely depends on structural features and electronic properties of substituents: its decomposition can range from room temperature (hyponitrites, peroxyoxalates, or V-70 [azobis(4-methoxy-2,4-dimethylvaleronitrile]) up to 140-150 °C.

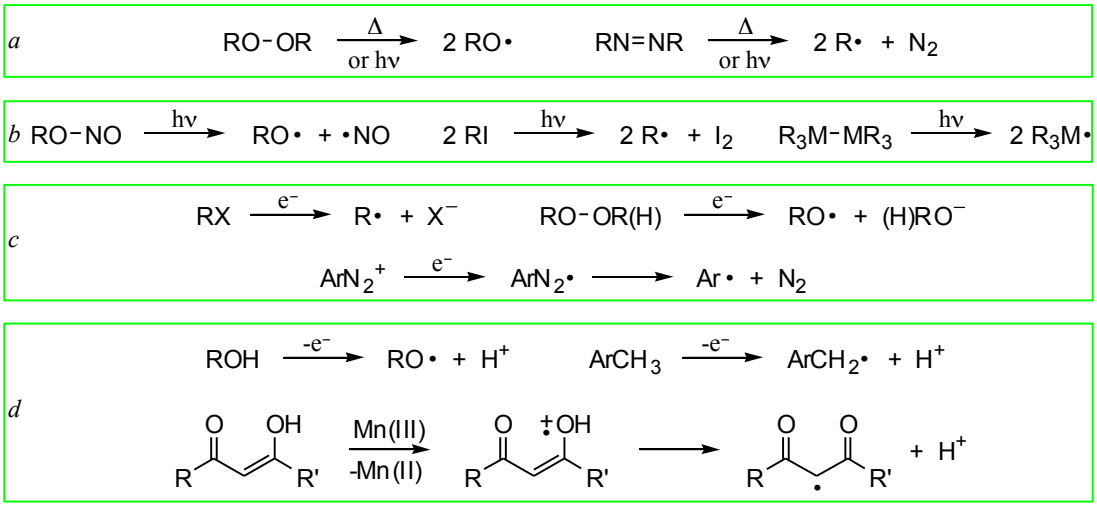

Scheme 8. Radical initiation methods

Visible or UV light can promote low-energy or non-bonding electrons to antibonding orbitals, giving rise to excited states characterized by weaker bonds with respect to the ground states. Light can therefore be used to break bonds, providing that the molecule is able to absorb it. Under mild thermal conditions ***Photolysis*** can cleave even strong bonds, which would be otherwise broken at elevated temperatures, in a very selective way through selected choice of light of requisite energy. However, photolysis (especially UV irradiation) often requires special apparatus, reactors, and vessels, and is hence not as practical as other usual experimental procedures. Substrates that can be broken photolytically include peroxides, azo-compounds, halides (especially iodides), nitrites, and organometallics (to give metal-centred radicals) (Scheme 8 a,b). Carbonyl compounds absorb UV light (270-300 nm) yielding singlet excited states, through n → π* transitions, that next form triplet states through intersystem crossing processes: the resulting di-radicals can participate in many radical reactions.

Neutral molecules can also be converted into radicals by ***electron-transfer*** routes: addition of an electron gives a radical anion that usually fragments to a radical and an anion, whereas extrusion loss of an electron generates a radical cation that commonly breaks into a radical and a cation. Alternatively, radicals can be directly generated from anions or cations by removal or addition of an electron, respectively. These redox reactions are usually carried out by means of metal ions that change their oxidation state and thus behave like one-electron

oxidizing or reducing agents. These processes normally occur under very mild conditions and are very selective. Single-electron transfer can also take place in electrolytic cells, where neutral molecules can be either reduced to radical anions at the cathode or oxidized to radical cations at the anode (in the same way, cations can add an electron at the cathode or anions can lose an electron at the anode). Radical generation by one-electron reduction can be easily accomplished with halides (which fragment to carbon radical and halide anion), peroxides or hydroperoxides (which break into alkoxyl radical and alkoxide or hydroxide anion) as well as with arenediazonium salts giving rise to diazenyl radicals that rapidly extrude dinitrogen (Scheme 8c). Radical generation by one-electron oxidation can be achieved with carboxylic acids and alcohols (whose radical cations lose a proton to give acyloxyl or alkoxyl radicals, respectively), alkylarenes (which give rise to benzylic-type radicals by loss of a proton), and carbonyl compounds (mainly di-carbonyls, whose enolic form can be especially oxidized with Mn(III) salts), to give resonance-stabilized α–carbonyl or α,α-dicarbonyl radicals (Scheme 8d)[48].

Radical propagation

Propagation reactions are processes in which a radical intermediate is converted into a new radical by means of either unimolecular (rearrangements and fragmentations) or bimolecular processes (intermolecular reactions with non-radical molecules); a number of these reactions can take place in sequence until a termination step pairs all of the electrons[49].

Unimolecular propagation reactions encompass rearrangements and fragmentations. The former involve transformation of a precursor radical into a more stable (or more reactive!)[50] radical intermediate and usually occur through migration of atoms (e.g. 1,5-H shifts) or groups (e.g. 1,2-aryl shift), or by intramolecular addition[51] to C-C double and triple bonds and carbonyl moieties (Scheme 9). Atom transfers are typically limited to 1,5 and 1,6 shifts, since lower-order migrations require strained transition states, whereas group translocations may occur also between vicinal atoms, like in the cases of neophyl rearrangement (1,2-aryl shift) and 1,2-acyloxy migration.

Fragmentations occur by β– (or α–) elimination of a radical species with concomitant formation of an unsaturated molecule. The driving force, besides the obvious increase in entropy, can be due to generation of a stable radical, formation of a strong π–system like a carbonyl group or an aromatic ring, or release of a very stable molecule (CO_2, CO, N_2). Alkyl radicals can suffer β–fragmentation only in the presence of a weak σ–bond in the β–position, since the resulting alkene bond is not enough strong as to provide a suitable driving force (suitable β–substituents are halogen atoms, sulfanyl and stannyl groups). On the contrary, the fragmentation of alkoxyl or cyclohexadienyl radicals is strongly favoured by the formation of strong carbonyl groups or aromatic rings, respectively. Acyloxyl and diazenyl radicals have a high propensity to extrude carbon dioxide and nitrogen, respectively: with these radicals even aryl radicals can be generated in an efficient fashion.

As far as ***bimolecular*** propagation reactions are concerned, they include atom abstractions (S_H2 reactions) and addition reactions to unsaturated moieties (alkenes, alkynes, carbonyls and their derivatives) and aromatic compounds (Scheme 9).

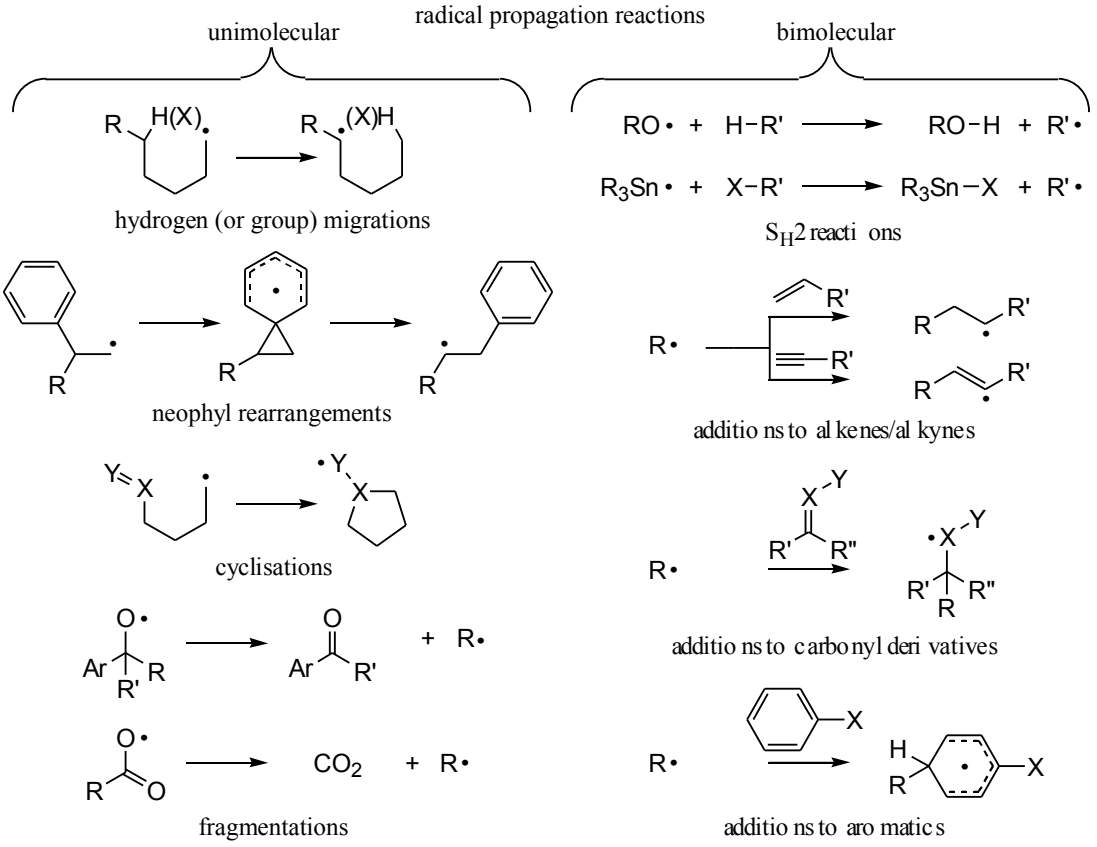

Scheme 9. Intra- and intermolecular radical propagation reactions

Atom abstractions are analogous to the ionic S_N2 reactions: indeed, S_H2 stands for **S**ubstitution **H**omolytic **B**imolecular (2) and the unimolecular analogue discussed above is often called S_Hi (**S**ubstitution **H**omolytic **i**ntramolecular). They are concerted displacement reactions where a hydrogen or halogen atom (but sometimes sulfanyl, stannyl, and other groups) is transferred from a molecule to a radical through the involvement of a linear transition state in which the radical orbital overlaps with the vacant σ* orbital of the bond being broken. Hydrogen abstractions are typically performed with alkoxyl radicals, which form alcohols having a strong O–H bond, whereas halogen abstractions are usually achieved with tin or silicon radicals in which cases the driving force arises from the formation of a strong metal-halogen bond at the expense of a weaker carbon-halogen bond.

Radical addition to unsaturated moieties is very common in the case of alkenes (e.g. in polymerisations), since the formation of a new C–C σ-bond (≅ 370 kJ mol^{-1}) at the expense of a weaker π–bond (≅ 235 kJ mol^{-1}) is usually a

good driving force. With mono-or unsymmetrically-substituted alkenes, addition takes place preferentially at the less hindered position: such regiochemical outcome is probably a result of steric factors rather than stability of the ensuing radical adduct. The most popular reaction of this type is the *anti*-Markovnikov, peroxide-mediated addition of hydrobromic acid to alkenes (Scheme 10).

Unlike charged intermediates, radicals can add to both electron-rich and electron-poor multiple bonds, although the addition rate strongly depends on polar effects (see above) and bulkiness of the reactants. Alkenes and alkynes exhibit analogous regioselectivity, but alkyne reactions are usually slower due to ensuing generation of less stable vinyl radical adducts.

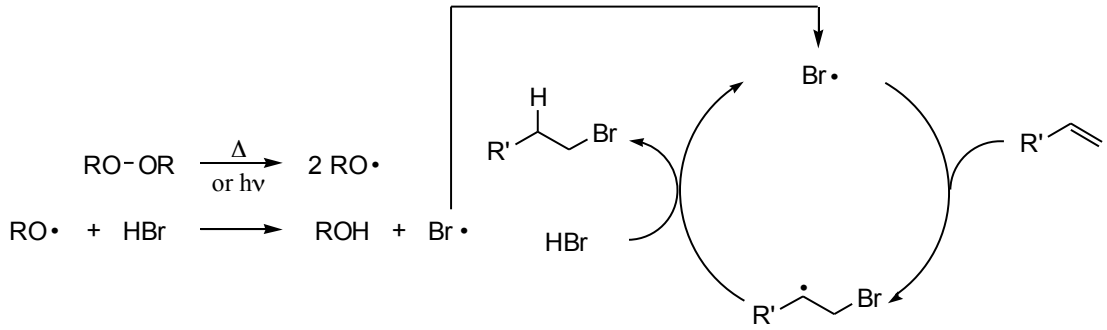

Scheme 10. Anti-Markovnikov radical addition of HBr to olefins.

Addition to carbonyl compounds is generally unfavourable, since the C=O π–bond is stronger than the alkene double bond by ca. 80 kJ mol^{-1}; therefore, most of the reported cases involve intramolecular examples. Carbon-centred radicals, especially the nucleophilic ones, show a certain propensity to attack electrophilic carbonyl carbons in a reversible fashion, whereas heteroatom-centred radicals like stannyls and silyls prefer to add to the carbonyl oxygen, due to alternative formation of a stronger metal–oxygen σ–bond. Very useful reactions, but largely confined to intramolecular examples, are those involving addition of nucleophilic radicals to the electrophilic carbon of nitriles, oximes, and hydrazones: these reactions are usually very fast and substantially irreversible, since fairly stable radical adducts are formed and in such cases there is no efficient driving force for the reverse reaction to compete.

Radical addition to aromatic groups is rather slow, due to the great stability of the aromatic π–system. The resulting cyclohexadienyl radicals can either

revert to the starting reactants or be oxidized, by formal loss of a hydrogen atom, to give substitution products in a process comparable to the electrophilic aromatic substitution. The addition rate strongly depends again on polar factors, hence nucleophilic and electrophilic radicals will react preferentially with electron-poor and electron-rich aromatics, respectively. The addition is often regioselective, since radicals prefer to attack the ring positions that give rise to cyclohexadienyls more stabilized by conjugative and/or inductive effects.

Radical Cyclisations as a powerful synthetic tool

Among the great number of useful radical transformations, ring closures reactions play undoubtedly a pivotal role in organic synthesis. Radical cyclisations can occur in sequence (tandem cyclisations) and can show high levels of regio- and even stereoselectivity, being probably the most popular, distinctive contribute of free-radical chemistry to the world of synthesis.

According to Baldwin's rule[52], radical (and also non-radical) cyclisations can be classified into exo and endo modes, depending on whether ring closure occurs on either the inside or the outside of the unsaturated moiety, respectively. In other words, exo- or endo-cyclisations are those leading to new radicals that are exocyclic or endocyclic with respect to the newly-formed rings. The exo or endo term is usually preceded by a number indicating the ring size and followed by an additional term representative of the hybridisation of the (carbon) atom at the reaction site. Hence, cyclisations are called tet, trig, or dig when the reaction sites are tetrahedral sp^3, trigonal sp^2, or digonal sp carbons, respectively (Scheme 10). As an example, a "5-exo-trig" cyclisation (one of the most common radical ring-forming reactions) is a ring-closure reaction that gives rise to a 5-membered ring through attack of the starting radical to the inner carbon atom of an alkene moiety, with consequent formation of a new exocyclic radical.

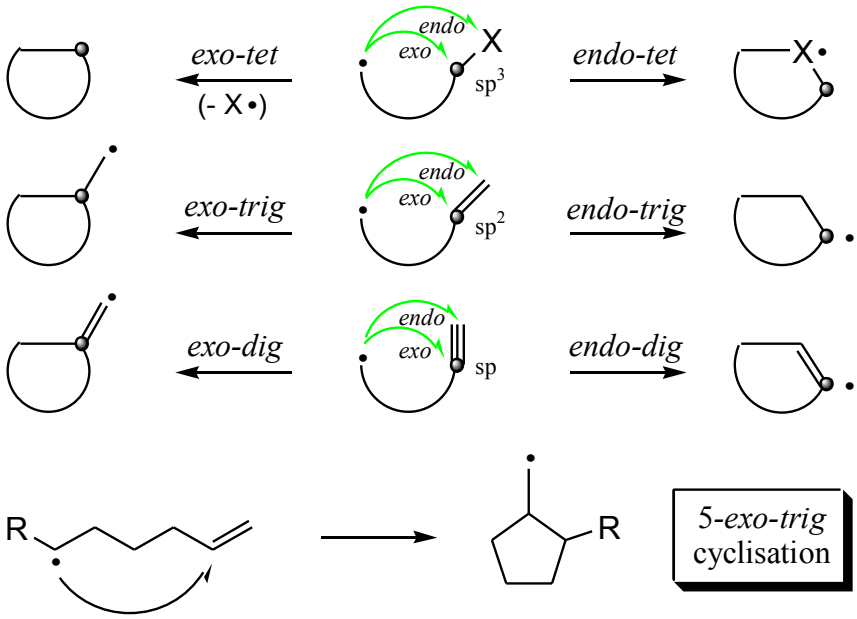

Scheme 11. Baldwin's rule for radical cyclisations.

At this stage it is worth noting that most useful radical reactions are exothermic processes. According to Hammond Postulate, the transition states of exothermic reactions – and thence of the radical reactions – are generally reagent-like (Figure 6).

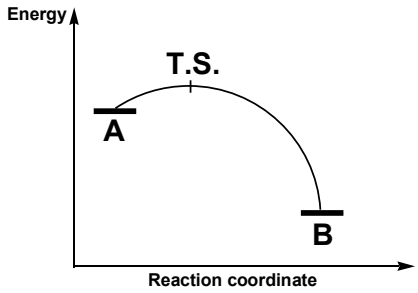

Figure 6. Generalized reaction profile for an exothermic reaction: the transition state (T.S.) is closer to the reagent (A) than to the products (B) along both coordinate axes.

In light of Hammond Postulate for two similar exothermic processes it is possible to envision a reaction profile like that shown in Figure 7, termed "crossing", where the process thermodynamically less favored (A→B) has however a transition state of lower energy, and is therefore kinetically more favored.

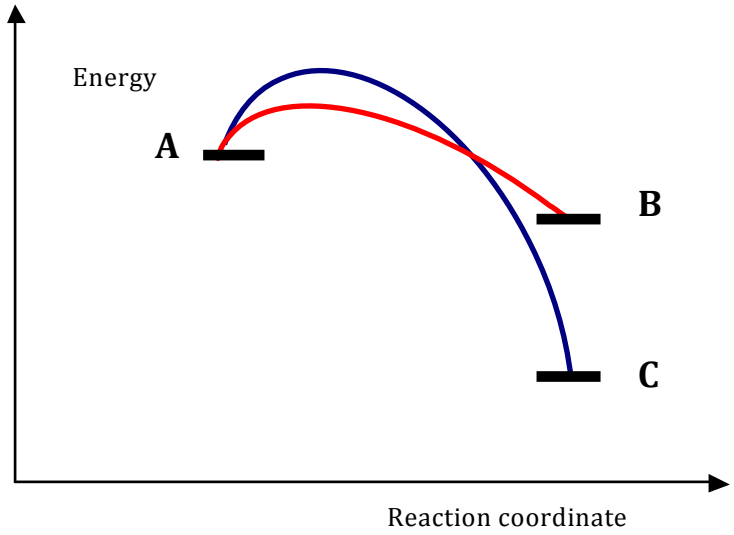

Figure 7. "Crossing" reaction profiles

The concepts just discussed can help to explain a very particular behaviour that occurs in the field of the radical cyclisations.

For radical reactions to be fast, the single occupied orbital (SOMO) of the reacting radical must overlap efficiently with a suitable orbital of the radicophilic partner. For intermolecular reactions this condition is easily fulfilled, since the reactants can rotate freely to ensure maximum overlap. On the other hand, intramolecular reactions, namely cyclisations, can be strongly affected by so-called "stereoelectronic effects", because not all the conformations are energetically favoured and the reaction could be kinetically controlled by the process triggered by the most favoured interaction. Cyclisation of the hex-5-en-1-yl radical is an emblematic example of this behaviour (Scheme 12).

For cyclisation of this radical, at 25 °C, the 5-exo mode (kexo = 2.3 × 105 s^{-1}) is about 60 times faster than the 6-endo competitive ring closure (kendo = 4.1 × 103 s^{-1}).[53]

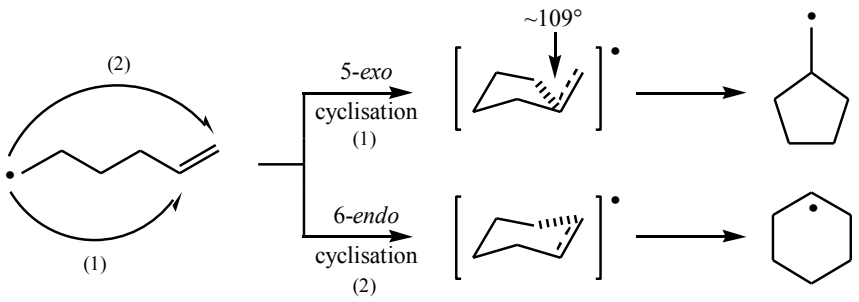

Scheme 12. Anti-Markovnikov radical addition of HBr to olefins.

At first sight, this fact is unexpected at least for two well-founded reasons: i) the cyclopentane ring is more strained than the cyclohexane ring, and ii) the radical arising from 5-membered cyclisation is a primary radical and should be therefore thermodynamically less stable than the secondary radical formed in the 6-membered ring closure. Nevertheless, at 25 °C, the 5-exo and 6-endo products are formed in a 98:2 ratio! Actually, stereo-electronic effects operate and the reaction is under kinetic rather then thermodynamic control. This is explained by the fact that the singly occupied orbital overlaps more favourably with the alkene π* orbital at the inner carbon atom, through a chair-like transition state (Beckwith model) that has been proved to be less strained and energetically favoured with respect to the 6-membered analogue: indeed, this overlap is characterised by an attack angle very close to 109 °C (i.e. the bond angle that is required in the product radical).

Since radicals are typically quite unstable, very reactive species, radical cyclisations are usually irreversible and kinetically controlled, and the product ratios (and even the stereochemistry!) strictly depend on stereo-electronic effects and can be often predicted on the basis of Beckwith models. However, if the cyclisation is reversible, due to the stability of the starting radical, the reaction can afford the thermodynamically favoured product, since ring opening of the less stable radical product can be faster than, for example, the hydrogen abstraction process involved in the reaction of Scheme 13.[54]

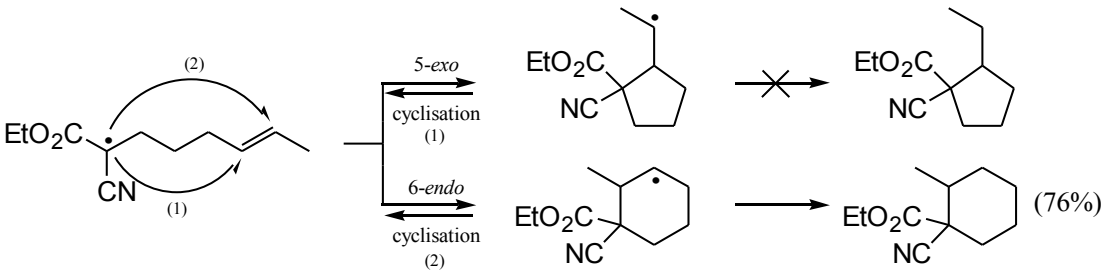

Scheme 13. Termodinamically controlled reaction due to reversible cyclisation

Radical Termination

The termination reactions are processes in which radical intermediates are destroyed as a result of coupling (or dimerisation), disproportionation, or one-electron exchanges.

Coupling or dimerisation (heterocoupling or homocoupling) reactions[55] involve combination of two radical species to yield a non-radical molecule as a result of the formation of a covalent bond (Scheme 14). These reaction are very fast and essentially diffusion controlled. Coupling products are though usually observed in very small amounts, since their formation requires fairly high radical concentrations, a condition rarely achieved due to the very short radical lifetimes.

Disproportionation entails transfer of a β–hydrogen between two carbon radicals with formation of a C=C π–bond and a C–H σ–bond. Also these reactions are very fast and the greater the number of β–hydrogens and the bulkier the radical centre, the more likely it is that a disproportionation will occur.

Electron transfer reactions convert radical species into anions and cations by one-electron reduction and oxidation processes, respectively. The 'redox reagent', as in the case of radical generation, can be a transition metal ion or an electrode. The reaction rate depends of course on the redox potential of the radicals: tertiary alkyl radicals are easily oxidized to carbocations, due to the stabilising +I inductive effect of the alkyl groups. Other less substituted carbon radicals can also be readily oxidized when bearing electron donating groups like OR and NR2 which can play an important role in cation stabilisation. On the contrary, primary alkyls prefer reduction to carbanions, and the process is

strongly favoured by electron-withdrawing groups (e.g. NO2, COOR), which can stabilise the resulting negative charge by –M mesomeric effect (Scheme 14).

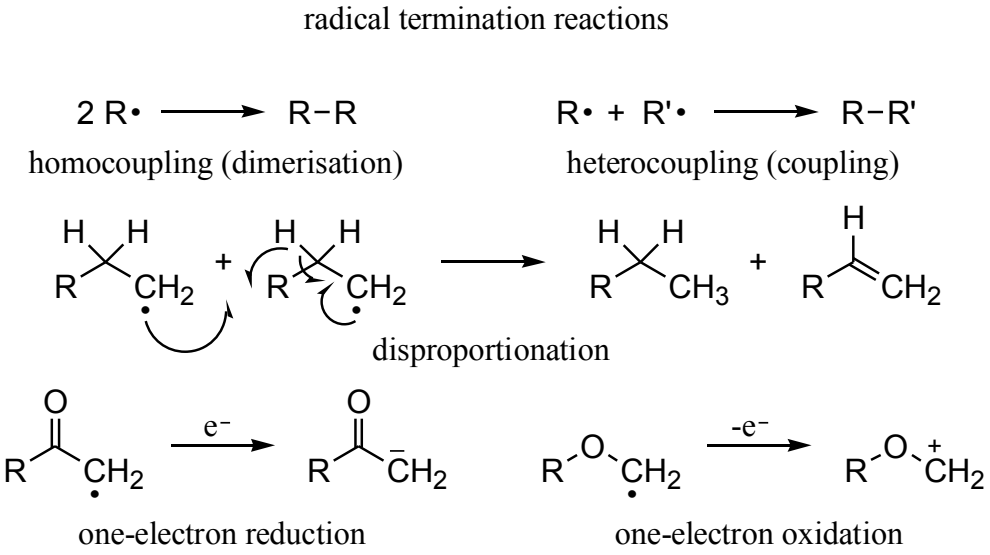

Scheme 14. Radical termination reactions

Starting from these bases, we can now penetrate in the 'world' of the radicals and explore their use in synthetic organic chemistry.

1.3 Thiol radical coupling

Growing interest has been devoted to the use of quick reactions that meet the main criteria of Click and Green Chemistry for an ideal synthesis, namely efficiency, versatility, and selectivity. The existing click reactions, like those discussed above, can offer many interesting applications, but, however, they present several intrinsic drawbacks such as, for example, removal of toxic heavy metal impurities from the final products, explosive nature of azido compounds, limited reactivity of Diels-Alder reagents and retro cycloaddition reactions at high temperatures.[56] In the past years Thiol–Ene coupling (TEC, Eq. 1), and, more recently, Thiol-Yne coupling (TYC, Eq. 2) have encountered renewed interest, after the original patent gained by Charles Goodyear at the beginning of the last century for his process concerning vulcanization of natural rubber by sulphur[57]. Those coupling reactions have been shown to be very versatile, and in fact have found valuable use in the production and modification of (bioconjugated) polymers,[58,59,60] and surfaces,[61] synthesis of star polymers, dendrimers[62] and disaccharides.[63]

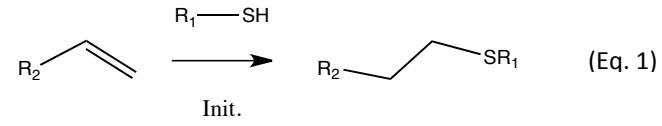

(Eq. 1)

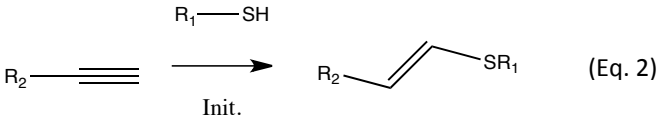

(Eq. 2)

TEC/TYC can actually proceed under a variety of conditions through radical processes or nonradical processes mediated by nucleophiles, acids, bases,[64] in the apparent absence of an added catalyst in highly polar solvents, such as water or DMF.[65]

We focused our attention to the radical thiol-click reactions owing to long interest of our group in free radical chemistry and, more importantly, to the fact that the radical thiol-click reactions, besides being modular, occur at room temperature with high efficiency and fast kinetics even in the presence of oxygen or water; moreover, they do not require any (toxic) catalyst, and are highly tolerant of a wide range of functional groups. Additionally, thiol-click reactions

are orthogonal to a wide range of chemistries.[9A] Like any radical thiol addition, the radical thiol-click reactions entail tree steps including initiation, propagation and termination.

Generation of thiyl radical (RS·) is the initiation of the process. There are different way to generate the radical:

-Homolytic cleavage of the S–S bond in their corresponding disulfides using photolysis (Eq. 3);

-H-atom abstraction from their thiols RSH (Eq. 4);

-Autoxidation of RSH with oxygen, very slow;

-Anodic oxidation, of thiols, in which cases where thiyl radicals are formed as intermediate.

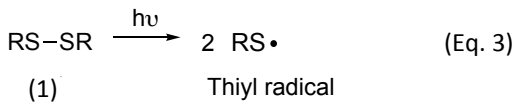

(Eq. 3)

(Eq. 4)

The S–S bond dissociation energy (BDE) in diphenyl disulfide (PhSSPh), 214.2 kJ/mol, is considerably lower than that of dialkyl disulfides (RSSR), which are reported to be in the range of 277 – 301 kJ/mol.[66] In fact, homolysis of the S-S bond is much more feasible with PhSSPh than with dialkyl disulfides (RSSR); owing to resonance-stabilization of ensuing phenylsulfanyl radicals.

A more useful method for RS· generation entails hydrogen-abstraction from corresponding thiols in the presence of radical initiators including photoinitiators like (2,4,6-trimethylbenzoyl)diphenylphosphine oxide (TMDPO), 2,2-dimethoxy-2-phenyl acetophenone (DMPA), benzophenone (BP), thioxanthone (TX), and camphorquinone (CQ), or typical thermal initiators like azobis(isobutyronitrile) (AIBN) at 80 °C.

H-abstraction from thiols in the presence of thermal/photochemical initiators provides a general method for sulfanyl radical production, but recent studies have established that the use of photoinitiators is especially effective to promote certain polymerization processes mediated by sulfanyl radicals.[67]

Thiol-ene coupling(TEC)

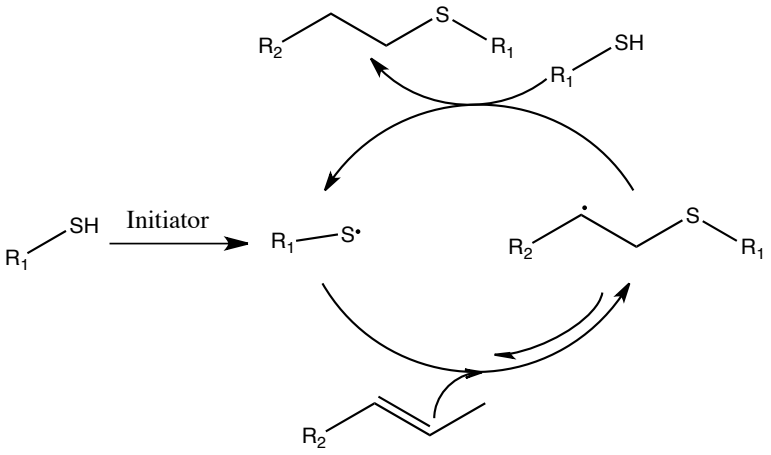

Scheme 15. The mechanism for the hydrothiolation of a C=C bond

Radical thiol additions to alkenes are generally very fast, even at ambient temperature and pressure, are tolerant of the presence of oxygen/air, and give rise to nearly quantitative formation of thio-ether products often in a regioselective fashion.

After the initial formation of a thiyl radical, RS·, the overal addition process takes place through two distinct steps (Scheme 15): primary addition of the thiyl radical to either carbon of the alkene double bond yielding an intermediate carbon-centered radical and subsequent H-transfer from the thiol reagent to the derived carbon radical with concomitant regeneration of a thiyl radical for chain propagation.

Generally, terminal alkenes are significantly more reactive towards radical hydrothiolation than internal alkenes and give rise to sulfide adducts in strictly regioselective anti Markovnikov fashion. Hoyle at al. reported that 1-hexene is eight-fold more reactive than trans-2-hexene and 18-fold more reactive than trans-3-hexene in radical hydrothiolations, thus discovering that steric effects play a significant role in affecting the radical alkene reactivity with thiols. However, it is worth note that an additional role can be played by usual reversibility of the primary addition of sulfanyl radical to the double bond.

Thiol-Yne coupling(TYC)

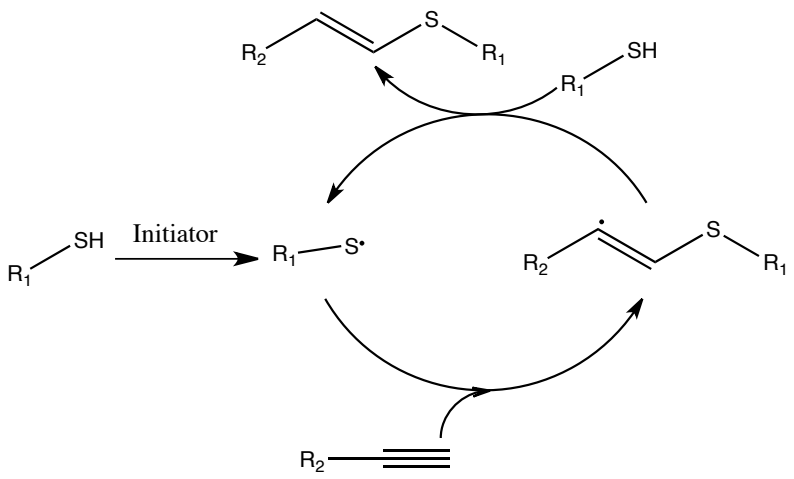

Scheme 16 The mechanism for the hydrothiolation of a C≡C bond

The radical thiol-yne processes (TYC) (Scheme 16) occur in analogous conditions to those of TECs and also involve two analogous radical steps. Indeed, an initially-formed thiyl radical, RS·, adds to either carbon of the alkyne triple bond yielding an intermediate β-sulfanyl-substituted vinyl radical, which then undergoes H-abstraction reaction with the thiol present to give the appropriate vinyl sulfide adduct with concomitant regeneration of a thiyl radical.

The whole hydrothiolation process, though being regioselective, at least with the terminal alkynes, is usually scarcely stereoselective, since the vinyl sulfide adducts are often formed as mixtures of E/Z geometrical isomers. As a consequence, TYC reactions often fail to fulfill one of the major requirements of click-reactions, i.e. stereoselectivity. TYCs are usually more effective with terminal than internal alkynes owing to lesser steric constraints; moreover, they are also more effective with electron-rich alkynes since these encourage primary addition of sulfanyl radicals known to possess somewhat electrophilic character.

Stereoselectivity and Regioselectivity

Thiyl radical addition to C=C bonds generally occurs in a reversible fashion[68] and is often accompanied by some isomerization process: in fact, thiyl radicals are usefully employed to bring about cis/trans isomerization of alkenes (Scheme 16 and Eq. 5).[69] Although the β-scission rate constants for β sulfanylvinyl radicals (k_{-2}) have not been actually determined, the reversibility

of RS· addition to alkyne C≡C triple bonds has been clearly proved (Eq. 6). The rate constants for sulfanyl radical additions to alkenes and alkynes, k_1 and k_2, are in the range of 10^3–10^8 $M^{-1}s^{-1}$ and 10^3–10^6 $M^{-1}s^{-1}$ at at ambient temperature: such rate constants normally exhibit a high dependence on the nature of substituents attached to the vinylic or ethynylic carbons.

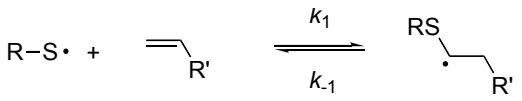

(Eq. 5)

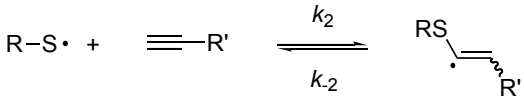

(Eq. 6)

During an addition if the R is an aryl[70] group, thiyl radical addition generally has a greater reversibility than for an alkyl group.[71] Cramer et al, postulate that the ratio of propagation to chain transfer kinetic parameters (kp/ kCT it is the same to say k_1/K_{-1}) and polymerization rates are correlated to the electron density of the vinyl groups and the carbon radical stability.[72] The rate constant as a consequence depends by all components of our reaction, thiyl radical group, substituent, electron density of vinyl group and the radical stability.

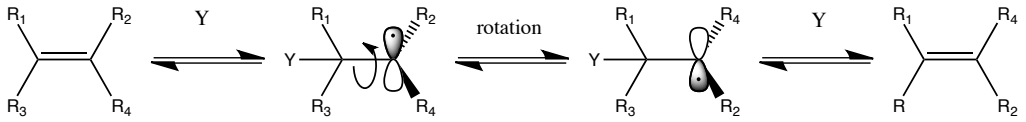

Scheme 17. Reversible step of C=C bond hydrothiolation. Cis Trans isomerization

In consequence to all point discussed before, result understandable why it is necessary an excess of one reagents.[73] To complete our reagent we have to shift the equilibrium towards the sulfide product. It be in contrast with the idea of Click Chemistry.

The addition of a sulphanyl radical to an alkyne gives rise to a vinylic carbon radical. This intermediate can be "σ-bent", in which case the unpaired electron is located in an sp2 orbital, or "π-linear" with the unpaired electron placed in a p-orbital (Scheme 17). π-Linear vinyl radicals usually occur when the R2 α-substituent is sterically bulky (e.g. t-Bu) or when this latter is able to

stabilize the unpaired electron through resonance delocalisation (e.g. Ph). The TYC rate constants (K_2)[74] are very sensitive to steric constrains and hence internal alkynes react more slowly than the terminal ones; moreover, electron-poor alkynes are less reactive than the electron-rich counterparts owing to the known fact sulfanyls are somewhat electrophilic species

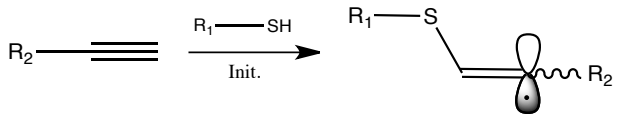

Scheme 18. π-linear vinyl radical

The σ-bent vinyl radicals can undergo fast inversion yielding syn/anti conformers in a fashion (highly) dependent on the bulkiness of the R2 α-substituent, (Scheme 19)

Interconversion is very slow when R_2 is a heteroatom.

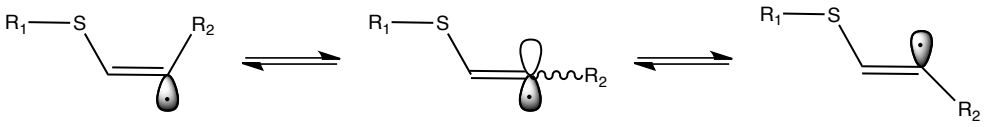

Scheme 19: σ-bent vinyl radical, fast inter-convention between Z-isomer to E-Isomer

With terminal alkynes radical hydrothiolation usually occurs in a regioselective anti-Markovnikov fashion. Indeed, with the aliphatic alkynes sulfanyl radical attack preferentially occurs at the terminal carbon since this is the site less sterically hindered; with the aromatic ones sulfanyl radical attack at the terminal carbon is even more preferred owing to resonance stabilization of ensuing vinyl radical by the attached aromatic ring.

Thiol-Yne / Thiol- Ene Reactions (TYC-TEC)

Using appropriate alkyne substrates and thiol reagents tandem adoption of TYC and TEC chemistry can enable successful achievement of a broad range of simple/complex bis-sulfide bis-adducts which are of significant interest in polymer or material chemistry (Scheme 20).

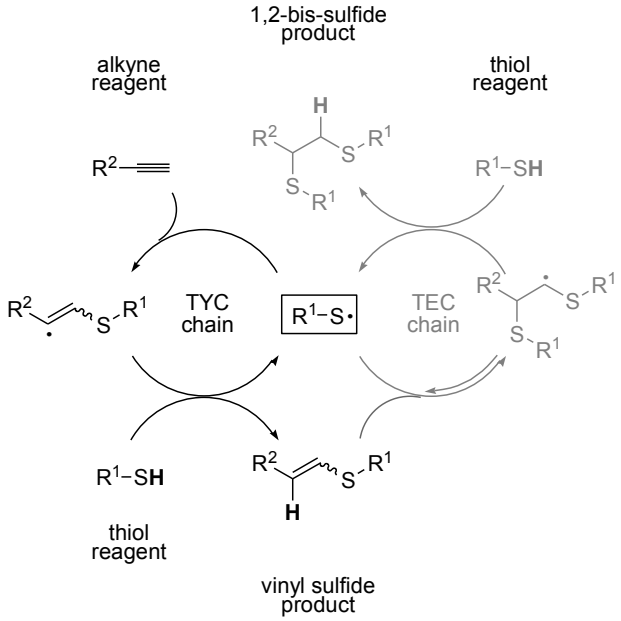

Scheme 20. Mechanism of TYC and TEC radical chains.

Patton et al. have demonstrated thiol-yne chemistry as a modular platform for rapid and practical fabrication of highly functional, multicomponent surfaces,[75] and recently a versatile post-polymerization modification strategy to synthesize multifunctional polymer brush surfaces via combination of surface-initiated photopolymerization and orthogonal thiol-click reactions[76] (Figure 8). This approach has demonstrate very interesting for material with model and commercially available thiols. The main idea will be extended to fabrication of multiplexed biomolecule.

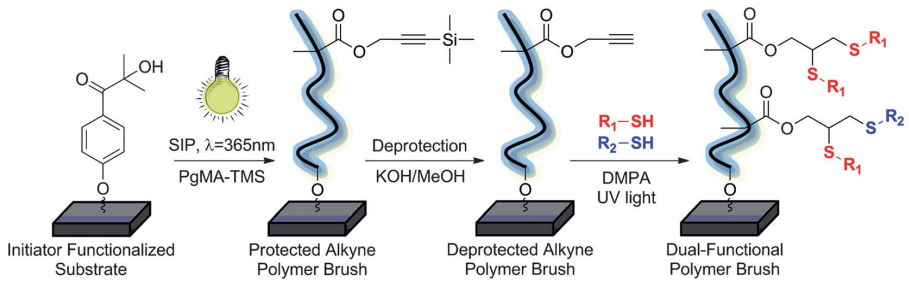

Figure 8 General schematic for dual-functional polymer brushes by one-pot thiol-yne co-click reactions from PgMA brushes (DMPA 1⁄4 2,2- Dimethoxy-2-phenylacetophenone). Based on similar thiol reactivities, the thiol-yne co-click reaction yields a distribution of 1,2-homo and 1,2-hetero dithioether adducts within the brush surface.[77]

The most important applications of TEC and/or TYC chemistry appeared in the past few years are covered by Nanni and Massi in a comprehensive monograph which is being published in Organic & Biomolecular Chemistry.[77]

1.4 Theoretical approach

In recent years, significant progress has been made in understanding at the molecular level the structures, functions and processes involved in many natural and artificial chemical systems thanks to instruments like EPR and LFP and their related analytical methods. Along with these advancements, quantum chemical methods have almost reached a speed and accuracy that make them a valuable tool for this kind of studies.

Today we can choose among various Quantum chemical approaches (see below).

Ab-initio[78]: the computation comes directly from theoretical principles, with no use of experimental data. The most common method in ab-initio calculations is Hartree Fock (**HF**)[79]; The most accurate methods based on an with HF approach is the Quantum Monte Carlo one[80].

Another opportunity for an ab-initio approach is a newer ab initio method, the Density Functional Theory (**DFT**)[81], in which the total energy is expressed in terms of the total electron density, instead of the wavefunction. In DFT calculations there is an approximate Hamiltonian and an approximate expression for the total electron density. The accuracy of results from DFT calculations can be poor to fairly good, depending on the choice of basis set and density function.

Broadly speaking, ab initio calculations give very good qualitative results and can yield increasingly accurate quantitative results as the involved molecules become smaller. The advantage of ab initio methods is that they eventually converge to the exact solution once all the approximations are made sufficiently small in magnitude.

However, this convergence is not monotonic. Sometimes, the smallest calculation gives a very accurate result for a given property. There are four sources of errors in ab initio calculations: the Born-Oppenheimer approximation, the use of an incomplete basis set, incomplete correlation, the omission of relativistic effects.

The disadvantage of ab initio methods is that they are expensive. These methods often take enormous amounts of computer CPU time, memory, and disk space

Semiempirical[82] semi-empirical quantum-mechanical methods developed by Dewar and coworkers[83] have successfully reproduced and interpreted molecular energies, molecular structures and chemical reactions[84]. . Semiempirical methods are much faster than ab initio calculations. The disadvantage of semiempirical calculations is that the results can be erratic and fewer properties can be reliably predicted They have been successfully applied in organic chemistry, wherethey can provide results accurate enough to be useful, since there are only few elements used extensively and the molecules are of moderate size.

These methods are generally good for predicting molecular geometry and energetics. This can be used for predicting vibrational modes and transition structures, but in a less reliable way than ab initio methods. Semiempirical calculations generally give poor results for van der Waals and dispersion intermolecular forces, due to the lack of diffuse basis. Initially, semiempirical methods have been devised specifically for the description of inorganic chemistry.

Molecular mechanics[85] are the calculation methods that it allows the modeling of enormous molecules, such as proteins and segments of DNA.

Molecular dynamic[86] examine the time dependent behavior of a molecule.. The application of molecular dynamics to solvent/solute systems allows the computation of properties such as diffusion coefficients or radial distribution functions for subsequent statistical mechanical analysis.

The favorable scaling (i.e. the computational effort required for a certain system size) of DFT compared to ab initio methods allows the analysis of far larger systems, and thus it encouraged much wider applications than ever before. Of course, the nearly exponential development in computer power has also had a major impact on this field of studies. Quantum chemistry has gone from being a quite expensive branch of science to quite a cheap one, where many problems can be addressed using a few ordinary personal computers.

In any quantum chemical studies, it is essential to choose the models to accurately represent the chemical situation.

Free-radical polymerization is an important and well-established process for the production of polyethylene. Reyniers et al. applied DFT ab initio density functional theory at the B3LYP/6-31g(d) level to study this process. The applied basis set took into account the high degree of conformational flexibility and internal rotations during the growing of the radical alkyl chains[87]

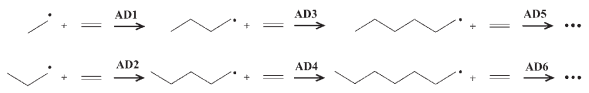

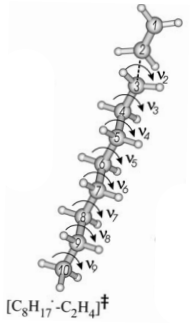

Figure 9. Addition reactions ADn : Cn + 1H2n + 3C + C_2H_4 !Cn + 3H2n + 7C. Distinction is made between propagation series with even and odd numbers of carbon atoms in the radical backbone.

It turned out to be a good approach to radical addition of alkyl radical to electro reach group and the polymerization trends are qualitatively well reproduced[88]. B3LYP/6-31+G(d) level of theory whereas single point calculations were performed with the new hybrid density functional BMK. BMK performs better for some types of calculations, like the barrier heights. This calculation was made with two-component method BMK/6-311+G(3df,2p)// B3LYP/6- 31+G(d) for geometry and single point optimization.

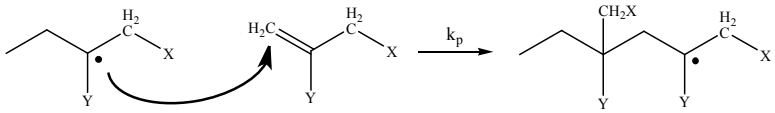

Figure 10. Radical addition to a substituted alkene (propagation). Other steps are: initiation, the chain transfer, and the termination (by disproportionation or by coupling)

The application of quantum-chemical methods to radical polymerization processes necessarily involves a compromise in which small model systems are used to mimic the reactions of their polymeric counterparts so that high levels of theory may be used. The development of computationally efficient quantum chemistry methods for the study of larger molecules, coupled with a quick and

non-stop increase to computer power, has now made possible to study the chemically controlled reactions in free-radical polymerization with chemical accuracy. Cote recently did an exhaustive study about this topic [89].

About radical addition, it is relatively simple to find papers about polymerisation. Reyniers et al topic[90], recently calculated thermochemical data of numerous organosulfur compounds and their radicals. They used CBS-QB3 level theory which proven to be able to yield accurate electronic energies for both hydrocarbons[91] and organosulphur[92], substrates present in our context. For small organosulphur compound recent works are not so numerous, since the attention in the latest years is more focused on the numerous biological precursors present in living systems.[93]

Alvarez-Idaboy et al.[94] calculated that reaction with SH· is about four times faster than with OH. The study was focused on analyzing atmospheric consequences in areas in which the H_2S concentration was significant. The energy calculations were performed with unrestricted ab initio methods. Two different approaches were used to optimize the geometries: density functional methods (DFT) and Moller–Plesset perturbation theory. The calculation showed an excellent agreement with experimental data using the BHandHLYP method. To avoid problems deriving from the basis set superposition error the energy profiles were recalculated using the complete basis set extrapolation CBS-QB3 approach, MP2/6-311++G(d,p).

All the calculations were performed with DFT ab initio. No theoretical work on the RS· radical addition to double/triple bonds has been published. Molecular dynamics approach hasn't been used for radical addition on small system yet. The method is very CPU expensive, thus usually it is used for big system, DNA[95], protein, chemical adsorption[96], or solvatation[97]. MD allows to observe the pathway during all the calculations, in particular, for solvated reactions, it allows to study the disposition of molecules depending on the different solvents.

Bibliography

[1] Anastas P. T. and Warner J. C., Green Chemistry Theory and Practice, Oxford University Press, New York, 1998.

[2] A) Trost BM (1991) The atom economy: A search for synthetic efficiency. Science 254:1471–1477. B) Trost BM (1995) Atom economy-A challenge for organic synthesis: Homogeneous catalysis leads the way.

3 Argyropoulos DS, eds (2007) Materials, Chemicals and Energy from Forest Biomass, ACS Symposium Series 954(American Chemical Society, Washington, DC).

4 A) Jimenez-Gonzales, C.; Curzons, A. D.; Constable, D. J. C.; Cunningham, V. L. Int J. LCA 2004, 114. B) Eissen, M.; Hungerbuhler, K.; Dirks, S.; Metzger, J. Green Chem. 2003, G25

5 DeSimone J. M., Science 297, 799 (2002).

6 Tanaka K., Kaupp G., Solvent-Free organic synthesis, Wiley-VCH, 2009

7 Acc. Chem. Res., 2007, 40(11), special issue on ionic liquids, ed. Robin D. Rogers and Gregory A. Voth.

8 A) Tumas W., DeSimone J.M . Green Chemistry Using Liquid and Supercritical Carbon Dioxide, Oxford University Press, New York, 2003; B) Chemical Synthesis Using Supercritical Fluids, ed. P.G. Jessop and W. Leitner, VCH/Wiley, Weinheim, 1999.

9 C.-J. Li, Chem. Rev., 2005, 105, 3095; C.-J. Li and T.-H. Chan, Comprehensive Organic Reactions in Aqueous Media, Wiley & Sons, New York 2007; Organic Reactions in Water, ed. U. M. Lindstrom, Blackwell, 2007.

10 S. G. Kazarian, B. J. Briscoe, T. Welton, Chem. Com-mun., 2047 (2000).

11 P. G. Jessop, W. Leitner, Eds., Chemical Synthesis Using Supercritical Fluid (Wiley-VCH, Weinheim, Germany, 1999).

12 Darr J. A., Poliakoff M., Chem. Rev. 99, 495 (1999).

13 12. E. Lack and H. Seidlitz. In Extraction of Natural Products using Near-Critical Solvents, M. B. King and T. R. Bott. (Eds.), pp. 101–139, Blackie, Glasgow (1993).

14 Stewart, Gina (2003), DeSimone J. M. and Tumas W., ed., "Dry Cleaning with Liquid Carbon Dioxide", Green chemistry using liquid and supercritical carbon dioxide (USA: Oxford University Press): 215–227

15 .K.L. Hoy and K.A. Nielsen, “Methods for Cleaning Apparatus Using Compressed Fluids”, US Patent No. 5,306,350 (1994).

16 J.J. Watkins and T.J. McCarthy, “Polymer/Metal Nanocomposite Synthesis in Supercritical CO2

17 Leitner W., Jessop P. G. (Eds), Supercritical Fluids, Vol. 4 of the Handbook of Green Chemistry, Paul Anastas (series editor), Wiley-VCH, 2010. B) P. G. Jessop, "Homogeneous Catalysis using Supercritical Fluids: Recent Trends and Systems Studied," J. Supercrit. Fluids, 2006, 38, 211-231.

18 A) Wasserscheid P, Welton T (2002) Ionic Liquids in Synthesis (Wiley-VCH, Weinheim, Germany). B) Sheldon, R. A.; Lau, R. M.; Sorgedrager, M. J.; Rantwijk, F. v.; Seddon, K. R. Biocatalysis in Ionic Liquids. Green Chem. 2002, 4, 147-151

19 Martínez-Palou R., Microwave-assisted synthesis using ionic liquids,Mol Divers (2010) 14:3–25 DOI 10.1007/s11030-009-9159-3

20 M. E. Zakrzewska, E. Bogel-Łukasik and R. Bogel-Łukasik Solubility of Carbohydrates in Ionic Liquids, Energy & Fuels, 2010 24 (2), 737-745

21 N. Winterton, Solubilization of polymers by ionic liquids, J. Mater. Chem., 2006, 16, 4281-4293

22 A)Roger RD, Seddon KR, Volkov S (eds) (2002) Green indus- trial applications of ionic liquids. NATO Science Series. Kluwer, Dordrecht. B) Rogers RD, Seddon KR (eds) (2002) Ionic liquids: industrial applications of green chemistry. ACS, Washington, DC

23 Wasserscheid P, Welton T (2002) Ionic Liquids in Synthesis (Wiley-VCH, Weinheim, Germany)

24 van Rantwijk F, Sheldon RA (2007) Biocatalysis in ionic liquids. Chem Rev 107:2757–2785. doi: 10.1021/cr050946x

25 Narayan, S.; Muldoon, J.; Finn, M. G.; Fokin, V. V.; Kolb, H. C.;Sharpless, K. B. Angew. Chem., Int. Ed. 2005, 44, 3275.

26 Itami K., Yoshida, J.-I. (2003), The Use of Hydrophilic Groups in Aqueous Organic Reactions. ChemInform, 34: no. doi: 10.1002/chin.200327272

27 A) Y. Hayashi,In Water or in the Presence of Water?, Angew. Chem. Int. Ed. 2006, 45, 8103 – 8104. B) Brogan, A. P.; Dickerson, T. J.; Janda, K. D., Enamine-Based Aldol Organocatalysis in Water: Are They Really “All Wet”, Angew. Chem., Int. Ed. 2006, 45, 8100.

28 H. C. Kolb, M. G. Finn, K. B. Sharpless, Angew. Chem. 2001, 113, 2056 – 2075 ; Angew. Chem. Int. Ed. 2001, 40, 2004 – 2021.

29 A) Tome, A. C. In Science of Synthesis; Storr, R. C., Gilchrist, T. L., Eds.; Thieme: Stuttgart, New York 2004; Vol. 13, pp 415. B) 1,3-Dipolar cycloaddition chemistry; Padwa, A., Ed.; Wiley: New York, 1984.

30 R. Huisgen, Angew. Chem. Int. Ed. 1963, 75, 604.

31 V. V. Rostovtsev, L. G. Green, V. V. Fokin, K. B. Sharpless, Angew. Chem. Int. Ed. 2002, 41, 2596.

32 C. W. Tornoe, C. Christensen, M. Meldal, J. Org. Chem. 2002, 67, 3057.

33 Lutz,J.F.(2008)Copper-freeazide-alkynecycloadditions:New insights and perspectives. Angew. Chem., Int. Ed. 47, 2182–4.

34 Zhang, L., Chen, X. G., Xue, P., Sun, H. H. Y., Williams, I. D., Sharpless, K. B., Fokin, V. V., and Jia, G. C. (2005) Ruthenium-catalyzed cycloaddition of alkynes and organic azides. J. Am. Chem. Soc. 127, 15998–9.

35 O. Diels, K. Alder, Liebigs Ann. 1928, 460, 98 – 122.

36 J. H. Kim, S. V. Lindeman, J. K. Kochi, J. Am. Chem. Soc. 2001, 123, 4951 – 4959.

37 Mark ‘Radical Chemistry’, M. John Perkins, Ellis Horwood Limited, 1994.

38 D. Nanni, "Radicals in Organic Synthesis: a Century (Actually much less!) of Playing with Unpaired Electrons", published in Seminars in Organic Synthesis [Monographs of the "A. Corbella" Summer School of Organic Chemistry (Gargnano, Italy), XXXII Edition], E. Licandro, R. Ballini, L. Banfi, M. V. D’Auria, M. Maggini, and C. Morelli, Ed.s; Società Chimica Italiana, Rome, 2007, pgg. 159-182

[39] Mark The real importance of the captodative effect is however still debated. For a recent review, see: Stella, L.; Harvey, J. N. in Radicals in Organic Synthesis, Renaud, P. and Sibi, M. P., Eds.; Wiley-VCH: Weinheim, 2001, Vol. 1, p. 360. See also: Viehe, H. –G.; Janousek, Z.; Merényi, R.; Stella, L. Acc. Chem. Res. 1985, 18, 148.

[40] It should also be underlined that the term "unstable" is inappropriate for many short-lived radicals. It is more usually used in the sense of unimolecular instability. In fact, in the vacuum methyl radical 4 would be long-lived!

[41] a) For a discussion on the persistent radical effect, see: Fischer, H. J. Am. Chem. Soc. 1986, 108, 3925 and Fischer, H. Chem. Rev. 2001, 101, 3581. For the use of nitroxides (such as TEMPO) in organic synthesis, see: b) Braslau, R.; Anderson, M. O. in Radicals in Organic Synthesis, Renaud, P. and Sibi, M. P., Eds.; Wiley-VCH: Weinheim, 2001, Vol. 2, p. 127 and c) Studer, A. Angew. Chem. Int. Ed. Engl. 2000, 39, 1108. d) For living-radical polymerisation, see Ref. 4b and: Georges, M. ibid., Vol. 1, p. 479.

[42] Mark For comprehensive, recent insights into the world of radical reactions and their applications to organic synthesis, see: a) Crich, D.; Motherwell, W. B. Free Radical Chain Reactions in Organic Synthesis; Academic Press: London, 1991. b) Perkins, M. J. Radical Chemistry; Ellis Horwood: London, 1994. c) Parsons, A. F. An Introduction to Free Radical Chemistry; Blackwell Science: Oxford, 2000. d) Radicals in Organic Synthesis, Vols. 1 and 2, Renaud, P. and Sibi, M. P., Eds.; Wiley-VCH: Weinheim, 2001. e) Togo, H. Advanced Free Radical Reactions for Organic Synthesis; Elsevier; Amsterdam, 2004.

[43] Deepened discussions on this subject can be found on the books reported in Ref.s 2 as well as in: Giese, B. Radicals in Organic Synthesis: Formation of Carbon-Carbon Bonds; Pergamon Press: Oxford, 1986, Chp. 2.

[44] In the brought example, the initiator is also a starting reagent (Cl2), but it is always not this way.

[45] A chain can also finish through processes of electron transfer that oxidizes or reduces the radical to the corresponding ion.

[46] Mark Additional, but not very used, radical sources include also radiolysis (with X– or γ–radiation) and sonolysis (with ultrasounds).

[47] Mark Porter, N. A. Acc. Chem. Res. 1986, 19, 262.

[48] For excellent reviews on these subjects, see, for example: a) Iqbal, J.; Bhatia, B.; Nayyar, N. K. Chem. Rev. 1994, 94, 519. b) Snider, B. B. Chem. Rev. 1996, 96, 339.

[49] The reactions reported below in this section are the key processes that characterise the whole radical reactivity. Many famous radical reactions (e.g. the Sandmeyer reaction, the neophyl rearrangement, the Kolbe decarboxylation, the Barton-McCombie reaction, or even the Toray process for cyclohexanone oxime) can simply be regarded as sequences of these key steps.

[50] In reversible processes one can isolate products derived from a rearranged, less stable radical if this reacts very fast with a radical trap.

[51] Due to their importance in organic synthesis, radical cyclisations will be discussed more thoroughly in the subsequent section.

[52] Mark Baldwin, J. E. J. Chem. Soc., Chem. Commun. 1976, 734.

[53] Beckwith, A. L. J.; Schiesser, C. H. Tetrahedron 1985, 41, 3925. The whole Volume 41 of Tetrahedron is concerned with selectivity and synthetic applications of radical reactions.
Mark Julia, M. Acc. Chem. Res. 1971, 386

[54] Julia, M. Acc. Chem. Res. 1971, 386.

[55] "Dimerisation" (or homocoupling) usually refers to coupling between two identical radical species, whereas "coupling" (or heterocoupling) entails combination of two different radicals.

[56] B. R. Pool, J. M. White, Org. Lett. 2000, 2, 3505.

[57] United States Patent Office, patent number 3633, June 15, 1844

[58] G. J. Chen, S. Amajjahe, M. H. Stenzel, Chem. Commun. 2009, 1198.

[59] R. J. Pounder, M. J. Stanford, P. Brooks, S. P. Richards, A. P. Dove, Chem. Commun. 2008, 5158.

[60] A) C. N. Bowman and C. E. Hoyle, Thiol–Ene Click Chemistry, Angew. Chem. Int. Ed. 2010, 49, 1540 – 1573 B) Lowe A. B, Thiol-ene "click" reactions and recent applications in polymer and materials synthesis, Polym. Chem., 2010, 1, 17-36 C) A. Dondoni, Angew. Chem. 2008, 120, 9133–9135; Angew. Chem. Int. Ed. 2008, 47, 8995 – 8997.

[61] L. A. Connal, C. R. Kinnane, A. N. Zelikin, F. Caruso, Chem. Mater. 2009, 21, 576.

[62] J. W. Chan, B. Yu, C. E. Hoyle, A. B. Lowe, Chem. Commun. 2008, 4959.

[63] K. L. Killops, L. M. Campos, C. J. Hawker, J. Am. Chem. Soc. 2008, 130, 5062.

[64] A) J. W. Chan, C. E. Hoyle and A. B. Lowe, J. Am. Chem. Soc., 2009, 131, 5751–5753 B) J. W. Chan, B. Yu, C. E. Hoyle and A. B. Lowe, Chem. Commun., 2008, 4959–4961.

[65] H. Kakwere and S. Perrier, J. Am. Chem. Soc., 2009, 131, 1889–1895.

[66] Luo, Y.-R. Handbook of Bond Dissociation Energies in Organic Compounds CRC Press: Boca Raton, London, New York, Washington D.C., 2003.

[67] M. Uygun, M. A. Tasdelen, Y. Yagci, Macromol. Chem. Phys. 2010, 211, 103–110

[68] A) C. Walling and W. Helmreich, J. Am. Chem. Soc., 1959, 81, 1144– 1148. B) C. Chatgilialoglu, A. Altieri and H. Fischer, J. Am. Chem. Soc., 2002, 124, 12816–12823. C) C. Ferreri, A. Samadi, F. Sassatelli, L. Landi and C. Chatgilialoglu,J. Am. Chem. Soc., 2004, 126, 1063–1072.

[69] A) Benson S.W., Egger K.W., Golden D.M. (1965) J Am Chem Soc 87:468 B) Golden D. M., Furuyama S., Benson S. W.,Int. J. Chem. Kinet, 1, 57 (1969).

[70] Benati, L.; Montevecchi, P. C.; Spagnolo, P. J. Chem. Soc., Perkin Trans. 1 1991, 2103-2109.

[71] Melandri, D.; Montevecchi, P. C.; Navacchia, M. L. Tetrahedron 1999, 55, 12227-12236.

[72] Cramer N. B., Reddy S. K., O'Brien A.K., Bowman N. C., Thiol-Ene Photopolymerization Mechanism and Rate Limiting Step Changes for Various Vinyl Functional Group Chemistries, Macromolecules 2003, 36, 7964-7969

[73] A) Griesbaum, K. Problems and possibilities of the free-radical addition of thiols to unsaturated compounds Angew. Chem. Int. Ed., 1970, 9, 273; B) Jarvis, B. B. Free-radical additions to dibenzotricyclo[3.3.0.02,8]-3,6-octadiene J. Org. Chem., 1970, 35, 924; C) Brown, H. C.; Kawakami, J. H.; Liu, K.-T. Additions to bicyclic olefins. V. Effect of 7,7-17dimethyl substituents on the stereochemistry and rates of cyclic additions to norbornenes J. Am. Chem. Soc., 1973, 95, 2209.

[74] A) P. C. Montevecchi and M. L. Navacchia, J. Org. Chem., 1997, 62, 5600-5607; B) D. Melandri, P. C. Montevecchi and M. L. Navacchia, Tetrahedron, 1999, 55, 12227-12236. C) B. D. Fairbanks, E. A. Sims, K. S. Anseth and C. N. Bowman, Macromolecules, 2010, 43, 4113-4119.

[75] Hensarling R. M., Doughty V. A., Chan J. C., Patton D. L. "Clicking" Polymer Brushes with Thiol-yne Chemistry: Indoors and Out, J. AM. CHEM. SOC. 2009, 131, 14673–14675

[76] Rahane S. B., Hensarling R. M., Sparks B. J., Staffordb C. M. and Patton D. L., Synthesis of multifunctional polymer brush surfaces via sequential and orthogonal thiol-click reactions, J. Mater. Chem., 2012, 22, 932–943

[77] Massi A., Nanni D., Thiol-yne coupling: revisiting old concepts as a breakthrough for up-to-date applications. Advanced article 2012

[78] F. Jensen, Introduction to Computational Chemistry John Wiley & Sons, New York (1999).

[79] P. Jùrgensen, Ann. Rev. Phys. Chem. 26, 359 (1975).

[80] J. B. Anderson, Rev. Comput. Chem. 13, 132 (1999).

[81] M. Ernzerhof, J. P Perdew, K. burke, D. J. W. Geldart, A. Holas, N. H. March, R. van Leeuwen, O. V. Gritsenko, E. J. Baerends, E. V. LudenÄa, R. LoÂpez-Boada, Density Functional Theory I Springer, Berlin (1996).

[82] J. Sadlej, Semi-Empirical Methods of Quantum Chemistry Ellis Harwood, Chichester (1985).

[83] Bingham, R. C., M. J. S. Dewar and D. H. Lo, J. Am. Chem. Soc., Vol. 97, pp. 1285-1293, 1975.

[84] Hirst, D. M. A., Computational Approach to Chemistry, Blackwell Scientific Publications, Oxford, 1990.

[85] F. Jensen, Introduction to Computational Chemistry John Wiley & Sons, New York (1999).

[86] D. C. Rapaport, The Art of Molecular Simulation Cambridge, Cambridge (1997).

[87] Van Cauter, K., Van Speybroeck, V., Vansteenkiste, P., Reyniers, M.-F. and Waroquier, M. (2006), Ab Initio Study of Free-Radical Polymerization: Polyethylene Propagation Kinetics. ChemPhysChem, 7, 131–140. doi: 10.1002/cphc.200500249

[88] Degirmenci I, A computational approach to the free radical polymerization of acrylates and methacrylates, Ghent University. Faculty of Engineering, 2010

[89] Coote M. L., Quantum-Chemical Modeling of Free-Radical Polymerization, Macromol. Theory Simul. 2009, 18, 388–400

[90] Vandeputte A. G., Maarten K. Sabbe, Reyniers M-F, and Marin G. B., Chem. Eur. J. 2011, 17, 7656 – 7673

[91] M. Saeys, M. F. Reyniers, G. B. Marin, V. Van Speybroeck, M. Waro- quier, J. Phys. Chem. A 2003, 107, 9147 – 9159.

[92] A) A. G. Vandeputte, M. F. Reyniers, G. B. Marin, Theor. Chem. Acc. 2009, 123, 391 – 412. B) A. G. Vandeputte, M. F. Reyniers, G. B. Marin, J. Phys. Chem. A 2010, 114, 10531–10549.

[93] van Gastel M., Lubitz W., Lassmann G., Neese, J. Am. Chem. Soc. 2004, 126, 2237-2246

[94] Francisco-Màrquez M., Alvarez-Idaboy J. R., Galano A., Vivier-Bunge A., Quantum chemistry and TST study of the mechanism and kinetics of the butadiene and isoprene reactions with mercapto radicals, Chemical Physics 344 (2008) 273–280

[95] Perez A., Luque F. J., Orozco M.,Frontiers in Molecular Dynamics Simulations of DNA, Accounts of Chemical Research Article ASAP doi:10.1021/ar2001217

[96] Malek K., Sahimi S., J. Chem. Phys. 132, 014310 (2010); doi:10.1063/1.3284542

[97] Pabis A., Szala-Bilnik J., and Swiatla-Wojcik D., Phys. Chem. Chem. Phys., 2011, 13, 9458–9468

CHAPTER 2

Radical Additions of Thiols to Alkenes and Alkynes in Ionic Liquids[1]

2.1 Introduction

Has been focused the concepts of the new approach to chemistry. Particular attention has been dedicated to make radical reactions enter the realm of sustainable and 'green' chemistry, exploring the possibilities to carry out radical processes either/both in environmentally friendly solvents or/and under 'green' conditions that could avoid the use of typical (but often highly toxic) radical reagents such as stannanes and metal-based oxidants/reductants.[2]

Among unconventional solvents, over the last decade ionic liquids have achieved the status of an efficient alternative to conventional volatile organic solvents. They have already proved to be no longer an exotic medium, but instead a valuable, benign vehicle that can improve the outcome of many organic syntheses, both by enhancing separation processes (and safety) and, in many cases, by improving reactions rate and selectivity[3]. Surprisingly, with the exception of radical polymerization[4], which has been quite extensively studied, the number of reported examples of radical synthetic procedures carried out in ionic liquids is extremely low[5]: the investigated reactions include formation of carbon-carbon bonds through manganese(III) acetate[5a] and CAN- mediated[5c] oxidations of 1,3-dicarbonyl precursors, triethyl borane-induced addition (or cyclization)/reduction sequences or atom-transfer cascade reactions[5b], and three-component photo-induced atom-transfer carbonylations[5d].

On this ground, we were prompted to study the feasibility in ionic liquids of a long-known radical reaction, i.e. the addition of thiols to double (or triple) carbon-carbon bonds. Although reported long time ago[6], more recently this reaction has moved to the forefront of free-radical research both for its applications in the field of tin-free generation of radical intermediates[7,3b,c,e] and its relevance in the "click-chemistry" domain: in the latter area, the addition of thiols to alkenes is indeed known as the "thiol-ene" coupling (TEC) reaction and it is widely employed in polymer chemistry, in synthesis of biomaterials, dendrimers, and, in general, molecules of bioorganic interest (glycopeptides, alkylated aminoacids, etc.)[8]. Here we report some results on the radical addition

of a few thiols to double and triple carbon-carbon bonds in ionic liquids under various experimental conditions and radical generation methods.

2.2 Result and discussion

The radical addition of thiols to alkenes was initially tested by reacting equimolar amounts (1 mmol) of benzenethiol (**2A**) and aliphatic (**1a,e**) or aromatic (**1b-d**) alkenes in [bmim][PF6] (1 mL) at various temperatures in the presence of suitable radical initiators (triethylborane [Et_3B] for T ≤ 40 °C, 1,1'-azo-bis-iso-butyronitrile [AIBN] for T = 80 °C) (Scheme 1 and Table 1). The expected anti- Markovnikov reaction products (**3**) were recovered by centrifuge-mediated extraction with diethyl ether; the ionic liquid was usually recycled up to 3 times without any significant change in yields and byproducts. The overall results, while being strictly comparable with those previously reported in usual solvents (e.g. benzene)[9], sometimes reveal slightly improved yields at enhanced temperatures (e.g. for **3cA** and **3dA**). It is worth noting that yields are generally far from being quantitative, but this is the common case for radical addition of (electrophilic) thiols to non- activated alkenes: this reaction is indeed known to be a reversible process explained before[10] and, to attain the best results, it typically requires high thiol concentrations and/or excess of alkene to shift the equilibrium towards the addition products. Back fragmentation to the starting alkene seems particularly favored in the case of 1,1-disubstituted alkenes such as methylenecyclohexane (**1e**), which gave a notably low yield of hydrothiolation product (**3eA**).

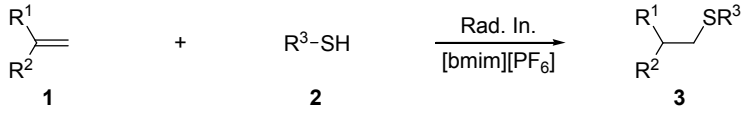

a: R^1 = *n*-C_6H_{13}, R^2 = H
b: R^1 = Ph, R^2 = H
c: R^1 = *p*-Cl-C_6H_4, R^2 = H
d: R^1 = *p*-MeO-C_6H_4, R^2 = H
e: R^1,R^2 = *c*-C_6H_{10}
f: R^1 = *n*-BuO, R^2 = H
g: R^1 = MeC(O)O, R^2 = H

A: R^3 = Ph
B: R^3 = MeO(CO)CH_2

Scheme 1. General scheme for radical addition of thiols to alkenes.

Comp.	Rad. In.	T/°C	Time/h	Yield/%
3aA	Et_3B	0	0.5	60
3aA	Et_3B	40	1	63
3bA	Et_3B	20	1	40
3bA	AIBN	80	1	50
3cA	Et_3B	20	0.5	70
3cA	AIBN	80	1	90
3dA	Et_3B	20	1	63
3dA	Et_3B	40	1	90
3dA	AIBN	80	1	90
3eA	Et_3B	0	1	38
3eA	Et_3B	40	1	25

Table 1. Results of radical addition of benzenethiol to alkenes in [bmim][PF_6].

The possible effect of benzene and [bmim][PF6] solvent in the radical thiol-ene coupling reaction was next examined with two thiols, i.e. benzenethiol **2A** and methyl thioglycolate **2B**, and two activated olefins, i.e. n-butyl vinyl ether **1f** and vinyl acetate **1g**. The reactions were carried out at r.t. with equimolar amounts of reagents and Et_3B as the radical initiator either in benzene or [bmim][PF6] at different reagents concentrations. Under 1 M conditions, both solvents afforded the same results, giving the corresponding adducts (**3fA**, **3fB**, **3gA**, and **3gB**) in almost quantitative yields. When the reactions were instead carried out under more diluted conditions (0.1 M), benzene gave only trace amounts of the

addition products, whereas [bmim][PF6] afforded much more interesting results, producing the aimed sulfides in 60-70% yields. This outcome clearly shows that the radical hydrothiolation of alkenes can be favored by the ionic liquid, a feature that should not be surprising, at least taking the second reaction step into consideration. Indeed, hydrogen transfer reactions are known to be highly affected by polar factors and substituents capable of stabilizing a partial charge separation in the transition state are generally established to increase the reaction rate(will be treat with a theoretical approach in Chaper 4).[11] The same effect would be achieved by carrying out the reaction in a polar medium such as an ionic liquid, which could stabilize charge separation, hence lowering the activation energy of H-atom donation from the (electrophilic) thiol to the intermediate (nucleophilic) β-sulfanyl-substituted alkyl radical. Such kind of effect has already been suggested with ionic liquids not only in radical reactions involving metal ions[5a,c] or radical/polar crossover synthetic sequences[5d], but also in typical radical reactions such as chain intermolecular halogen atom transfers[5b,12]. However cannot be exclude the high cohesive energy density of the ionic liquid, forcing a decrease in the volume of the reactants in analogy with what happens in water[1e], could play an additional role by lowering the rate of back fragmentation of β-sulfanyl- substituted alkyl radicals: this effect would facilitate the subsequent hydrogen transfer, hence favoring the formation of the final hydrothiolation product.[4a]

It is worth noting that the hydrothiolation reaction can be performed in [bmim][PF6] even using other radical conditions, i.e. at r.t. under UV irradiation (λ 310-400 nm) in the presence of either AIBN (15%)[13] or 2,2-dimethoxy-2-phenylacetophenone (DMPA, 15%) as a photoinitiator[14]. Electron-rich alkenes such as **1f,g** are not suitable for these conditions, since they give rise to extensive polymerization and very complicate reaction mixtures, but non-activated olefins can be efficiently employed: for example, 1-octene 1a underwent photochemical reactions with both thiols **2A,B** to give almost quantitative yields of the corresponding adducts **3a,A** and **3a,B**. Under these conditions the only identifiable byproducts were trace amounts of disulfides and (probably) sulfoxides of adducts **3**. The ionic liquid remained substantially

unchanged under photolytical conditions: a darkening of its color did not affect the reaction outcome and the ionic liquid was recycled up to 3 times without any significant problem.

We subsequently investigated the radical addition of benzenethiol to alkynes in ionic liquids, in view of the known synthetic potential of the expected vinyl sulfide products [18]. Reactions were carried out for ca. 3 h with equimolar amounts (0.1 mmol) of benzenethiol **2A** and various alkynes **4a-d**, both at r.t. and at 100 °C, in three different ionic liquids (1 mL), i.e. [bmim][PF6], [bmim][Tf2N], and [bmim][BF4].

Radical initiation was attained with either Et_3B or 1,1'-azo-bis-cyclohexanecarbonitrile (VAZO®), depending on the reaction temperature. In almost all cases, after usual workup, nearly quantitative yields of vinyl sulfides **5** were obtained as mixtures of E- and Z-isomers (Scheme 2 and Table 2).

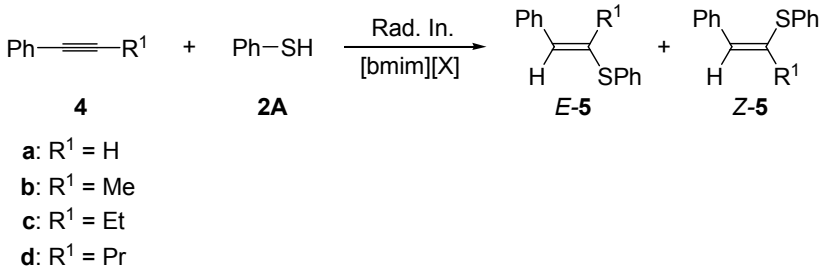

Scheme 2. Radical addition of benzenethiol to alkynes.

Comp	Rad. In.	T/°C	Solvent	Yeld% (E/Z ratio)
5aA	Et_3B	20	[bimim][PF_6]	>95(27:73)
5aA	VAZO®	100	[bimim][PF_6]	>95(84:16)
5aA	Et_3B	20	[bimim][Tf_2N]	>95(25:75)
5aA	Et_3B	20	[bimim][BF_4]	>95(53:47)
5bA	Et_3B	20	[bimim][PF_6]	>95(25:75)
5bA	VAZO®	100	[bimim][PF_6]	>95(57:43)
5bA	Et_3B	20	[bimim][Tf_2N]	>95(52:48)
5bA	Et_3B	20	[bimim][BF_4]	>95(53:47)
5cA	Et_3B	20	[bimim][PF_6]	80 (16:84)
5cA	VAZO®	100	[bimim][PF_6]	>95(40:60)
5cA	Et_3B	20	[bimim][Tf_2N]	>95(27:73)
5cA	Et_3B	20	[bimim][BF_4]	70 (37:63)
5dA	Et_3B	20	[bimim][PF_6]	>95(25:75)
5dA	VAZO®	100	[bimim][PF_6]	>95(37:63)
5dA	Et_3B	20	[bimim][Tf_2N]	70 (41:59)
5dA	Et_3B	20	[bimim][BF_4]	>95(32:68)

Table 2. Results of radical addition of benzenethiol to alkynes in various ionic liquids.

As expected on the basis of a free-radical mechanism, all of the vinyl sulfide products **5aA-dA** derived from anti-Markovnikov addition of benzenethiol to the respective alkyne; vinyl sulfides **5bA-dA**, in particular, derived from regioselective addition of benzenesulfanyl radicals to the alkyl end of the alkyne triple bond, a result that is consistent with the intermediacy of α-phenyl-substituted vinyl radicals, which are more stable than the alternative, isomeric α-alkyl-substituted counterparts.[15]

The observed significant (often predominant) formation of the Z-isomers was not unexpected. Indeed, α-phenyl-β-(arylsulfanyl)vinyl radicals, to minimize steric hindrance, are known to approach hydrogen donors from the side trans to the sulfanyl moiety, yielding the corresponding vinyl sulfides in kinetically controlled 1:9 E/Z ratio when the reactions are carried out at 100 °C

in neat alkyne[15]. At the same temperature, as a result of thermodynamic control attained through the use of equimolar amounts of reagents in 0.1 M benzene solutions[15] (i.e. concentrations identical to those we presently used in ionic liquids), alkynes **4a-d** have been reported to give the corresponding adducts **5aA-dA**, at 100 °C, in 9:1, 9:1, 5:5, and 4:6 E/Z ratio, respectively. If we compare these results with those obtained in ionic liquids at the same temperature, it can be seen that [bmim][PF_6] favors formation of the Z-isomer to a small extent: this is particularly notable for adduct **5bA**. This outcome suggests that hydrothiolation of alkynes is somewhat faster in ionic liquids with respect to aromatic solvents, in line with what suggested above for hydrothiolation of alkenes. Under radical conditions, Z/E isomerization of vinyl sulfides occurs by reversible addition (discussed before in Thiol radical coupling, Chapter 1) of sulfanyl radicals to the carbon-carbon double bond: as a consequence, the more efficient is the hydrothiolation reaction, the lower will be the concentration of sulfanyl radicals and hence the slower the isomerization. Of course, formation of the kinetic product is favored at lower temperatures, although kinetic control was never attained in any ionic liquid. By comparing the various results obtained at r.t., it seems that [bmim][PF_6] would be the best solvent for promoting formation of the Z-isomer, and hence the medium in which hydrothiolation of alkynes is faster.

Finally, we briefly examined the possible use of ionic liquid solvents in click-chemistry reactions leading to biologically interesting molecules. Our preliminary results include addition of **8** L-N-Fmoc-cysteine tert-butyl ester to 1-hexadecene and to an O-allyl glucoside, and hydrothiolation of phenylacetylene with L-cysteine ethyl ester hydrochloride (Scheme 3).

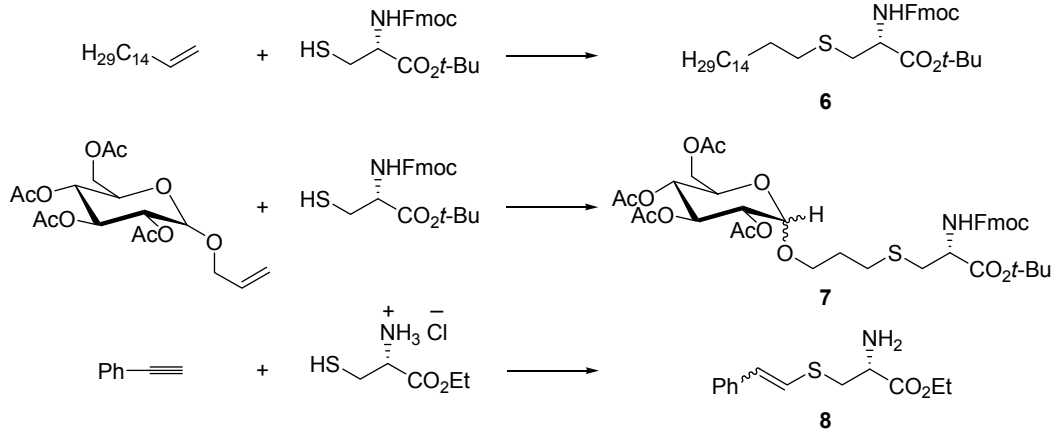

Scheme 3. Hydrothiolation as a tool for the synthesis of biologically interesting compounds.

The first adduct (**6**), which has been recently synthesized in 42% yield by Brunsveld and Waldmann through a radical thiol-ene, racemization-free procedure using thermal conditions, was chosed as a target compound for the recent interest in accessing hydrolysis-resistant non-natural *S*-alkylated cysteine derivatives[13]. Our present reaction was carried out in [bmim][PF_6] under DMPA-promoted photolysis conditions with 3 equiv of 1-hexadecene for 5 h and, after usual workup followed by chromatography, similarly gave adduct **6** but in somewhat lower yield (30%).

The second sulfide (**7**) was selected in view of the ever growing importance of O-linked glycosides and their use for preparation of glyco- and/or peptidomimetics[16]. Also in this case the reaction was performed by DMPA-promoted photolysis of the peracetylated O-allyl glucoside (ca. 1:1 α/β mixture) in [bmim][PF_6] in the presence of orthogonally-protected L-N-Fmoc-cysteine tert-butyl ester (1 equiv). After workup and chromatography, the target compound **7** was obtained in 50% yield.

The third reaction was simply a trial experiment to see whether mercapto-substituted aminoacids can add efficiently to an alkyne to give **8**-like vinyl sulfide adducts. The reaction between phenylacetylene and L-cysteine ethyl ester hydrochloride was carried out in [bmim][PF_6] by DMPA-promoted photolysis and yielded vinyl sulfide **8** in 78% yield (55:45 E/Z ratio). It is worth noting that this reaction gave **8** only to a slightly higher extent (86%) (55:45 E/Z ratio) when was repeated in a traditional solvent such as DMF. The use of

cysteine ethyl ester hydrochloride is strictly necessary, since the reaction carried out with 'free' cysteine ethyl ester gave only tars.

2.3 Conclusions

This report shows that radical hydrothiolation of alkenes and alkynes can occur in ionic liquids with at least as the same efficiency as in traditional solvents. The ionic liquids are compatible with the use of different radical initiation conditions, i.e. thermal decomposition of azo-initiators (80-100 °C), reaction of triethylborane with dioxygen (r.t.), and UV-photolysis at r.t. in the presence of either an azo-initiator (AIBN) or a photosensitizer (DMPA). The reaction products can be efficiently isolated from the ionic liquid by centrifuge-mediated extraction with diethyl ether, and the ionic liquid can be usually recycled up to 3 times without any significant change in yields and byproducts under any reaction conditions. Some results show that the ionic liquids, if compared with traditional solvents, seem to favor the hydrothiolation reaction, probably through stabilization of the transition state for hydrogen transfer from the starting thiol to the intermediate alkyl or vinyl radical. Although the results are merely preliminary and yields are not optimized, it seems that this protocol could be successfully applied to the synthesis of biologically interesting molecules through click-chemistry procedures carried out in ionic liquids.

2.4 Experimental Section

General Remarks. IR spectra were recorded on a FT-IR Perkin Elmer Spectrum RXI instrument in $CHCl_3$ solutions. ^1H- and ^{13}C-NMR spectra were recorded in $CDCl_3$ solutions on a Varian Mercury Plus 400 MHz (^1H: 400 MHz, ^{13}C: 100 MHz, internal ref. for ^1H-NMR spectra, δ 7.26 ppm for $CHCl_3$, internal ref. for ^{13}C-NMR spectra, δ 77.0 for $CHCl_3$). In reporting spectral data, the following abbreviations were used: d = doublet, t = triplet, q = quartet, m = multiplet, br s = broad singlet, br t = broad triplet. J values are reported in Hz. Electron spray ionization (ESI)mass spectra were recorded in acetonitrile solution with a Waters – Micromass ZQ4000 instrument. GC-MS analyses were performed using a ThermoFisher – Focus DSQ system. Column chromatography was carried out on ICN silica gel (63–200, 60 Å) by gradual elution with hexane/diethyl ether. Benzenethiol **2A**, methyl thioglycolate **2B**, L-cysteine ethyl ester hydrochloride,

L-cystine, 1-octene **1a**, styrene **1b**, p-chlorostyrene **1c**, p-methoxystyrene **1d**, methylenecyclohexane **1e**, butyl vinyl ether **1f**, vinyl acetate **1g**, phenylacetylene **4a**, 1- phenylpropyne **4b**, 1-phenylbutyne **4c**, 1-phenylpentyne **4d**, 1-hexadecene, [bmim][PF_6], [bmim][Tf2N], [bmim][BF_4], DMPA, and AIBN were commercially available (AIBN was recrystallized at r.t. from chloroform/ methanol); VAZO® and triethylborane (1.0 M solution in hexane) were commercially available as well and were used as received. L-N-Fmoc-cysteine-tert- butyl ester[17] and tetraacetyl O-allyl glucoside (1:1 α/β mixture)[18] were prepared according to reported literature procedures.

General Procedure for the Addition of Thiols to Alkenes.

For the reactions at 0-40 °C, a solution of alkene (1 mmol), thiol (1 mmol), and Et_3B (100 μl) in [bmim][PF_6] (1 mL) was kept under stirring for 0.5-1 h; the reactions at 80 °C were carried out by replacing Et_3B with VAZO® (10%) and by keeping the resulting solutions at 80 °C for 0.5-1 h; photolysis were performed by keeping the above stirred solutions at ca. 2.5 cm from the UV source (4 bulb-lamp, 15 W each, type 3, λ 310-400 nm) in the presence of either azo-bis-iso-butyronitrile (AIBN, 15%) or 2,2-dimethoxy- 2-phenylacetophenone (DMPA, 15%) as a photoinitiator. Workup was performed by adding diethyl ether (3 × 2 mL) and centrifuging the resulting mixture for 2 min at 2000 rpm; the ether layer was separated, the solvent evaporated and the residue analyzed by GC-MS/NMR. Addition products **3aA-eA**, **3gA**, **3aB**, **3fB**, and **3gB** were identified by comparison with authentic samples[19]; spectral data of compound **3fA** were as follows: ^{1}H-NMR (400 MHz) δ 0.91 (3 H, t, J = 7.4), 1.32- 1.40 (4 H, m), 3.11 (2 H, t, J = 7.0), 3.44 (2 H, t, J = 6.7), 3.61 (2 H, t, J = 7.0), 7.17-7.20 (1 H, m), 7.27-7.31 (2 H, m), 7.35-7.38 (2 H, m); ^{13}C-NMR (100 MHz) δ 13.9, 19.2 (CH2), 31.7 (CH2), 33.2 (CH2), 69.4 (CH2), 71.0 (CH2), 126.0, 128.9, 129.3, 129.8 (C); GC-MS m/z (rel. inten.) 210 (M+,34), 154 (36), 123 (77), 110 (86), 109 (44), 57 (100). Anal. Calcd. for C12H18OS: C, 68.52; H, 8.63. Found: C, 68.70; H, 8.67. Yields are reported in Table 1 and in the text.

General Procedure for the Addition of Thiols to Alkynes.

For the reactions at r.t., a solution of alkyne (1 mmol), benzenethiol (1 mmol), and Et_3B (100 μl) in the suitable ionic liquid (1 mL) was kept under stirring for 3 h; the reactions at 100 °C were carried out by replacing Et_3B with VAZO® (10%) and by keeping the resulting solutions at 100 °C for 3 h. Workup was performed by adding diethyl ether (3 × 2 mL) and centrifuging the resulting mixture for 2 min at 2000 rpm; the ether layer was separated, the solvent evaporated and the residue analyzed by GC-MS/NMR. Addition products **5aA-dA** were identified by comparison with authentic samples[15a]. Yields and E/Z ratios are reported in Table 2.

Reaction of L-N-Fmoc-Cysteine tert-Butyl Ester with 1-Hexadecene.

A mixture of 1- hexadecene (0.9 mmol), aminoacid (0.3 mmol), and DMPA (50%) in [bmim][PF_6] (3 mL) was kept under stirring at ca. 2.5 cm from the UV source (4 bulb-lamp, 15 W each, type 3, λ 310-400 nm) for 5 h. Workup was performed by adding diethyl ether (3 × 2 mL) and centrifuging the resulting mixture for 2 min at 2000 rpm; the ether layer was separated, the solvent evaporated and the residue chromatographed to give adduct 6 (30% yield), which was identified by comparison with an authentic sample[13].

Reaction of L-N-Fmoc-Cysteine tert-Butyl Ester with Tetraacetyl O-Allyl Glucoside.

A mixture of tetraacetyl O-allyl glucoside (1:1 α/β mixture, 30 mg, 0.077 mmol), Fmoc-Cys-OtBu (31 mg, 0.077 mmol), and DMPA (2 mg, 7.70 μmol) in [bmim][PF_6] (0.5 mL) was irradiated at room temperature for 1 h as described above. After usual workup, the resulting residue was eluted from a column of silica gel with 1:1 cyclohexane/ethyl acetate to give sulfide 7 (30 mg, 50%, ~ 1:1 anomeric mixture), slightly contaminated by the starting alkene; ^1H NMR (selected data) δ 7.80 (2 H, d, J = 7.4, Ar), 7.64 (2 H, d, J = 7.4, Ar), 7.50-7.20 (4 H, m, Ar), 5.76 (0.5 H, d, J = 8.0, NH), 5.74 (0.5 H, d, J = 8.0, NH), 5.20 (0.5 H, d, J = 4.0, H-1α), 4.60 (0.5 H, d, J = 9.5, H-1β), 2.20-2.02(12 H, 8s, Me), 1.44 (4.5 H, s, t-Bu), 1.42 (4.5 H, s, t-Bu); ESI MS (787.87): 788.8 ($M + H^+$), 805.5 ($M + NH_4^+$).

Reaction of L-Cysteine Ethyl Ester Hydrochloride with Phenylacetylene.

A solution of phenylacetylene (1 mmol), aminoacid (1 mmol), and DMPA (5%) in [bmim][PF_6] (1 mL) was kept under stirring at ca. 2.5 cm from the UV source (4 bulb-lamp, 15 W each, type 3, λ 310-400 nm) for 1h. Workup was performed by adding first an aqueous solution of sodium carbonate, then diethyl ether, and finally centrifuging the resulting mixture for 2 min at 2000 rpm; the ether layer was separated, the solvent evaporated and the residue chromatographed to give vinyl sulfide **8** (78% yield, 55:45 E/Z ratio): IR νmax 1188, 1598, 1735, 2934, 3011, 3305, 3376 cm^{-1}; ^{1}H-NMR (400 MHz) δ 1.26 (6 H, br t, J = 7.1, both isomers), 2.08 (4 H, br s, both isomers), 2.99-3.09 (2 H, m), 3.13-3.23 (2 H, m), 3.69-3.75 (2 H, m), 4.16 (2 H, q, J = 7.1), 4.18 (2 H, q, J = 7.1), 6.23 (1 H, d, J = 10.8, Z-isomer), 6.45 (1 H, d, J = 10.8, Z-isomer), 6.57 (1 H, d, J = 15.6, E-isomer), 6.68 (1 H, d, J = 15.6, E-isomer), 7.16-7.38 (8 H, m, both isomers), 7.44-7.48 (2 H, m, both isomers); ^{13}C-NMR (100 MHz) δ 14.0, 37.9 (CH_2), 40.7 (CH_2), 54.1, 54.6, 61.2 (CH_2), 61.3 (CH_2), 123.9, 125.5, 126.3, 126.4, 126.7, 127.1, 128.1, 128.4, 129.5, 128.9, 136.4 (C), 136.5 (C), 173.3 (C), 173.5 (C); GC-MS m/z (rel. inten.) 251 (M+, 55), 178 (41), 150 (100), 149 (43), 135 (67), 134 (36), 116 (32), 115 (53), 102 (48), 91 (50), 74 (49). A control experiment performed in DMF for 1 h with the same reagents in the same amounts afforded, after basic aqueous workup, extraction with diethyl ether, and chromatography, vinyl sulfide 8 in 86% yield (55:45 E/Z ratio).

2.5 Bibliography

[1] T. Lanza, M. Minozzi, A. Monesi, D. Nanni, P. Spagnolo and C. Chiappe, Curr. Org. Chem., 2009,13, pp. 1726 - 1732

[2] **a)** Walton, J. C. Linking borane with N-heterocyclic carbenes: effective hydrogen-atom donors for radical reactions Angew. Chem. Int. Ed., 2009, 48, 1726; **b)** Bencivenni, G.; Lanza, T.; Leardini, R.; Minozzi, M.; Nanni, D.; Spagnolo, P.; Zanardi, G. Tin-free generation of alkyl radicals from alkyl 4-pentynyl sulfides via homolytic substitution at the sulfur atom Org. Lett., 2008, 10, 1127; **c)** Benati, L.; Bencivenni, G.; Leardini, R.; Minozzi, M.; Nanni, D.; Scialpi, R.; Spagnolo, P.; Zanardi, G. Reaction of azides with dichloroindium hydride: very mild production of amines and pyrrolidin-2-imines through possible indium-aminyl radicals Org. Lett., 2006, 8, 2499; **d)** Healy, M. P.; Parsons, A. F.; Rawlinson, J. G. T. Consecutive approach to alkenes that combines radical addition of phosphorus hydrides with Horner−Wadsworth−Emmons-type reactions Org. Lett., 2005, 7, 1597; **e)** Benati, L.; Leardini, R.; Minozzi, M.; Nanni, D.; Scialpi, R.; Spagnolo, P.; Strazzari, S.; Zanardi, G. A novel tin-free procedure for alkyl radical reactions Angew. Chem. Int. Ed., 2004, 43, 3598; **f)** Studer, A.; Amrein, S. Tin hydride substitutes in reductive radical chain reactions Synthesis, 2002, 835. See also: Togo, H., Advanced Free Radical Reactions for Organic Synthesis, Elsevier: Amsterdam, 2004, chp. 12, p. 247.

[3]**a)** Ionic Liquids in Synthesis, Peter Wasserscheid and Tom Welton Ed.s; Wiley-VCH: Weinheim, 2008; **b)** Pârvulesku, V. I.; Hardacre, C. Catalysis in ionic lLiquids Chem. Rev., 2007, 107, 2615; **c)** Harper, J. B.; Kobrak, M. N. Understanding organic processes in ionic liquids: achievements so far and challenges remaining Mini-Rev. Org. Chem., 2006, 3, 253; **d)** Chiappe, C.; Malvaldi, M.; Pomelli, C. S. Ionic liquids: solvation ability and polarity Pure Appl. Chem., 2009, 81, 767.

[4] **a)** Carmichael, A. J.; Haddleton, D. M.; Bon, S. A. F.; Seddon, K. R. Copper(I) mediated living radical polymerisation in an ionic liquid Chem. Commun., 2000, 1237; **b)** Biedron, T.; Kubisa, P. Atom-transfer radical polymerization of acrylates in an ionic liquid Macromol. Rapid Commun., 2001, 22, 1237; **c)** Harrisson, S.; Mackenzie, S. R.; Haddleton, D. M.
16Unprecedented solvent-induced acceleration of free-radical propagation of methyl methacrylate in ionic liquids Chem. Commun., 2002, 2850; **d)** Biedron, T.; Kubisa, P. Atom transfer radical polymerization of acrylates in an ionic liquid: synthesis of block copolymers J. Polym. Sci. Part A, 2002, 40, 2799; **e)** Zhang, H.; Hong, K.; Jablonsky, M.; Mays, J. W. Statistical radical copolymerization of styrene and methyl methacrylate in a room temperature ionic liquid Chem. Commun., 2003, 1356; **f)** Thurecht, K. J.; Gooden, P. N.; Goel, S.; Tuck, C.; Licence, P.; Irvine, D. J. Free-radical polymerization in ionic liquids: the case for a protected radical Macromolecules, 2008, 41, 2814 and references therein. See also Ref. 4a, chp. 7, p. 619.

[5] **a)** Bar, G.; Parsons, A. F.; Thomas, C. B. Manganese(III) acetate mediated radical reactions in the presence of an ionic liquid Chem. Commun., 2001, 1350; **b)** Yorimitsu, H.; Oshima, K. Triethylborane-induced radical reactions in ionic liquids Bull. Chem. Soc. Jpn., 2002, 75, 853; **c)** Bar, G.; Bini, F.; Parsons, A. F. CAN-Mediated oxidative free radical reactions in an ionic liquid Synth. Commun., 2003, 33, 213; **d)** Fukuyama, T.; Inouye, T.; Ryu, I. Atom transfer carbonylation using ionic liquids as reaction media J. Organomet. Chem., 2007, 692, 685. For other examples concerning the behavior of radical intermediates in ionic liquids, see: **e)** Grodkowski, J.; Neta, P. Reaction kinetics in the ionic liquid methyltributylammonium bis(trifluoromethylsulfonyl)imide. Pulse radiolysis study of •CF3 radical reactions J. Phys. Chem. A, 2002, 106, 5468; **f)** Zhao, D.; Wang, J.; Zhou, E. Oxidative desulfurization of diesel fuel using a Brønsted acid room temperature ionic liquid in the presence of H2O2 Green Chem., 2007, 9, 1219; **g)** Baj, S.; Chrobok, A. Autooxidation of hydrocarbons with oxygen in ionic liquids as solvents Int. J. Chem. Kin., 2008, 40, 287.

[6] **a)** Griesbaum, K. Problems and possibilities of the free-radical addition of thiols to unsaturated compounds Angew. Chem. Int. Ed., 1970, 9, 273; **b)** Jarvis, B. B. Free-radical additions to dibenzotricyclo[3.3.0.02,8]-3,6-octadiene J. Org. Chem., 1970, 35, 924; **c)** Brown, H. C.; Kawakami, J. H.; Liu, K.-T. Additions to bicyclic olefins. V. Effect of 7,7-
17dimethyl substituents on the stereochemistry and rates of cyclic additions to norbornenes J. Am. Chem. Soc., 1973, 95, 2209.

[7] **a)** Benati, L.; Bencivenni, G.; Leardini, R.; Minozzi, M.; Nanni, D.; Scialpi, R.; Spagnolo, P.; Zanardi, G. Generation and cyclization of unsaturated carbamoyl radicals derived from S-4- pentynyl carbamothioates under tin-free conditions J. Org. Chem., 2006, 71, 3192; **b)** Benati, L.; Leardini, R.; Minozzi, M.; Nanni, D.; Scialpi, R.; Spagnolo, P.; Zanardi, G. Radical chain reaction of benzenethiol with pentynylthiol esters: production of aldehydes under stannane/silane-free conditions Synlett, 2004, 987; **c)** Benati, L.; Calestani, G.; Leardini, R.; Minozzi, M.; Nanni, D.; Spagnolo, P.; Strazzari, S. Generation and intramolecular reactivity of acyl radicals from alkynylthiol esters under reducing tin-free conditions Org. Lett., 2003, 5, 1313; **d)** Bachi, M. D.; Korshin, E. E.; Ploypradith, P.; Cumming, J. N.; Xie, S.; Shapiro, T. A.; Posner, G. H. Synthesis and in vitro antimalarial activity of sulfone endoperoxides Bioorg. Med. Chem. Lett., 1998, 8, 903; **e)** Bilokin, Y. V.; Melman, A.; Niddam, V.; Benhamu, B.; Bachi, M. D. Synthesis of thiabicyclic heterocycles through free radical cyclization of β-thioacrylates Tetrahedron, 2000, 56, 3425; **f)** Korshin, E. E.; Hoos, R.; Szpilman, A. M.; Konstantinovski, L.; Posner, G. H.; Bachi, M. D. An efficient synthesis of bridged-bicyclic peroxides structurally related to antimalarial yingzhaosu A based on radical co-oxygenation of thiols and monoterpenes Tetrahedron 2002, 58, 2449; **g)** Majumdar, K. C.; Debnath, P. Thiol- mediated radical cyclizations Tetrahedron, 2008, 64, 9799; **h)** Majumdar, K. C.; Taher, A. Wittig olefination and thiol mediated 7-endo-trig radical cyclization: novel synthesis of oxepin derivatives Tetrahedron Lett., 2009, 50, 228; **i)** Carta, P.; Puljic, N.; Robert, C.; Dhimane, A.-L.; Fensterbank, L.; Lacôte, E.; Malacria, M. Generation of phosphorus-centered radicals via homolytic substitution at sulfur Org. Lett., 2007, 9, 1061. See also ref. 3b.

[8] For leading references, see: **a)** Dondoni, A. The emergence of thiol–ene coupling as a click process for materials and bioorganic chemistry Angew. Chem. Int. Ed., 2008, 47, 8995; **b)** Becer, C. R.; Hoogenboom, R.; Schubert, U. S. Click chemistry beyond metal-catalyzed
18cycloaddition Angew. Chem. Int. Ed., 2009, 48, 4900; **c)** Hoyle, C. E.; Lee, T. Y.; Roper, T. Thiol-enes: chemistry of the past with promise for the future J. Polym. Sci. Part A, 2004, 42, 5301, and references therein.

[9] The Chemistry of the Thiol Group, Patai, S., Ed.; Wiley: New York, 1974.

[10] **a)** Is treated before in Chapter 1 Thiol radical coupling, **b)** Kice, J. L. in Free Radicals, Jay K. Kochi, Ed.; Wiley: New York, 1973; Vol. II, p. 720.

[11] A thorough discussion on this subject can be found in: Giese, B., Radicals in Organic Synthesis: Formation of Carbon-Carbon Bonds; Pergamon Press: Oxford, 1986; Chp. 2.

[12] Morrow, T. I.; Maginn, E. J. Molecular dynamics study of the ionic liquid 1-n-butyl-3-methylimidazolium hexafluorophosphate J. Phys. Chem. B, 2002, 106, 12807; Jenner, G. Role of the medium in high pressure organic reactions. A review Mini-Rev. Org. Chem., 2004, 1, 9.

[13] Triola, G.; Brunsveld, L.; Waldmann, H. Racemization-free synthesis of S-alkylated cysteines via thiol-ene reaction J. Org. Chem., 2008, 73, 3646.

[14] Killops, K. L.; Campos, L. M.; Hawker, C. J. Robust, efficient, and orthogonal synthesis of dendrimers via thiol-ene “click” chemistry J. Am. Chem. Soc., 2008, 130, 5062.

[15] **a)** Benati, L.; Montevecchi, P. C.; Spagnolo, P. Free-radical reactions of benzenethiol and diphenyl disulphide with alkynes. Chemical reactivity of intermediate 2-(phenylthio)vinyl radicals J. Chem. Soc., Perkin Trans. 1, 1991, 2103 and references therein. For scavenging of β-sulfanyl-substituted vinyl radicals, see also: **b)** Leardini, R.; Nanni, D.; Zanardi, G. Radical addition to isonitriles: a route to polyfunctionalized alkenes through a novel three-component radical cascade reaction J. Org. Chem., 2000, 65, 2763.

[16] **a)** Jensen, K. J.; Brask, J. Carbohydrates in peptide and protein design Pept. Sci., 2005, 80, 747. For a recent example, see: **b)** Fauré, R.; Shiao, T. C.; Lagnoux, D.; Giguère, D.; Roy, R.
20En route to a carbohydrate-based vaccine against Burkholderia cepacia Org. Biomol. Chem.,2007, 5, 2704.

[17] This compound was prepared from commercially available L-cystine according to: Mustapa, M. F. M.; Harris, R.; Bulic-Subanovic, N.; Elliott, S. L.; Bregant, S.; Groussier, M. F. A.; Mould, J.; Schultz, D.; Chubb, N. A. L.; Gaffney, P. R. J.; Driscoll, P. C.; Tabor, A. B. Synthesis of orthogonally protected lanthionines J. Org. Chem., 2003, 68, 8185.

[18] Synthesis: Mandai, T.; Okumoto, H.; Oshitari, T.; Nakanishi, K.; Mikuni, K.; Hara, K.-J.; Hara, K.-Z. A practical synthetic method for α- and β-glycosyloxyacetic acids Heterocycles, 2000, 52, 129. Spectroscopic data for the β-anomer: Kishida, M.; Akita, H. Simple preparation of phenylpropenoid β-d-glucopyranoside congeners by Mizoroki–Heck type reaction using organoboron reagents Tetrahedron, 2005, 61, 10559. Spectroscopic data for the α-anomer: Roy, B.; Mukhopadhyay, B. Sulfuric acid immobilized on silica: an excellent catalyst for Fischer type glycosylation Tetrahedron Lett., 2007, 48, 3783.

[19] **3aA**: Fernandez-Rodriguez, M. A.; Shen, Q.; Hartwig, J. F. A general and long-lived catalyst for the palladium-catalyzed coupling of aryl halides with thiols J. Am. Chem. Soc., 2006, 128, 2180; **3bA**: Kumar, P.; Pandey, R. K.; Hegde, V. R. Anti-Markovnikov addition of thiols across double bonds catalyzed by H-Rho-zeolite Synlett, 1999, 12, 1921; **3cA**: Ranu, B. C.; Mandal, T. Indium(I) iodide promoted cleavage of dialkyl/diaryl disulfides and subsequent anti-Markovnikov addition to styrenes: a new route to linear thioethers Tetrahedron Lett., 2006, 47, 6911; **3dA**: Baciocchi, E.; Lanzalunga, O.; Pirozzi, B. Oxidations of benzyl and phenethyl phenyl sulfides. Implications for the mechanism of the microsomal and biomimetic oxidation of sulfides Tetrahedron, 1997, 53, 12287; **3eA**: Mirafzal, G. A.; Liu, J.; Bauld, N. L. Hole transfer promoted hydrogenation: one-electron oxidation as a strategy for selective reduction of .pi.-bonds J. Am. Chem. Soc., 1993, 115, 6072; **3gA**: Rosnati, V.; Di Vona, M. L.; Traldi, P. Neighboring-group participation. A quasi-SNi mechanism in the acetolysis and thioacetolysis of 1-(phenylthio)-2-[(p-tolylsulfonyl)oxy]ethane J. Org. Chem., 1989, 54, 761; **3aB**: Jones, P. B.; Parrish, N. M.; Houston, T. A.; Stapon, A.; Bansal, N. P.; Dick, J. D.; Townsend, C. A. A new class of antituberculosis agents J. Med. Chem., 2000, 43, 3304; **3fB**: Cadogan, J. I. G.; Sadler, I. H. Quantitative aspects of radical addition. Part IV. Rate-constant ratios for addition of trichloromethyl and thiyl radicals to olefins J. Chem. Soc. B, 1966, 1191; **3gB**: Gouault, S.; Pommelet, J. C.; Lequeux, T. First synthesis of 4,4-difluoro-1,3-oxathiolan- 5-one Synlett, 2002, 6, 996.

CHAPTER 3

Thiol/Yne Coupling for Peptide Glycosidation[1]

3.1 Introduction

Here, we report an explorative study on model substrates that aimed at getting more insight into the conditions affecting the coupling reaction outcome, particularly the ensuing mono- and bis-adduct ratio. Both classical organic solvents and water (or water/solvent mixtures) were taken into account for carrying out the reactions, since the aqueous medium would be crucial for applying Thiol-Yne Couplings as a ligation strategy, for instance, for peptide glycosylation, similarly to what has been done with TEC procedures.[2] In addition, we are going to confirm that, compared to alkylacetylenes, C-C triple bonds linked to aromatic substrates (arylacetylenes) work as a better trap toward sulfanyl radicals:[3] to the best of our knowledge, this enhanced behavior has been exploited neither in the domain of bioconjugation nor in that of material derivatization and could entail interesting consequences in both fields. Finally, some preliminary results will be reported showing that the data obtained from the explorative study could be successfully applied to some bioconjugation examples including glycosylation of the native form of glutathione and of an unmodified nonapeptide containing a cysteine residue.

3.2 Result and Discussion

Our long, earlier interest in the radical reactions of thiols with alkynes[4] led us to ascertain that, under thermal conditions (80-100 °C) and in hydrocarbon solvents (e.g., benzene or toluene), derived sulfanyl radicals usually lead to vinyl sulfide adducts only. Consistent with our original evidence, methyl thioglycolate **1** was presently found to react with equimolar amounts of 1-octyne **2** in toluene solution at 80 °C in the presence of AIBN as a radical initiator, affording vinyl sulfide **3** (62%) and disulfide **5** (28%) as the only identifiable reaction products (Table 1, entry 1). Nevertheless, the reaction outcomes alter to a considerable extent by changing conditions (i.e., solvent, temperature, concentration, and initiation method), as proved by a series of experiments (Tables 1-4) carried out between two thiols (methyl thioglycolate **1** and N-acetyl-L-cysteine methyl ester **10**) and two alkynes (1-octyne **2** and phenylacetylene **6**). The parallel behavior

of thiols with aromatic and aliphatic alkynes has never been addressed in the recently reported TYC studies, but in light of our previous investigations, we thought that this point should deserve adequate consideration. Different reaction solvents were chosen on the basis of their potential employment in bioconjugation procedures (water and 95:5 water/DMSO mixtures) or material derivatization (DMSO, DMF). All the reactions were carried out at room temperature(r.t.)[5] for 1-2 h by irradiation with UV-lamp (max 365 nm) using 2,2-dimethoxy-2-phenylacetophenone (DMPA, 10 mol %) as a radical initiator, that is, the conditions normally employed in this kind of radical couplings.[6] Thus, the model reaction of thiol **1** with alkyne **2** (1 equiv) in toluene (0.5 M) solution afforded, under these conditions, both mono- (**3**) and bis-adduct (**4**) in comparable amounts (45:55 ratio, 76% overall yield), together with very minor amounts (<5%) of disulfide **5** (Table 1, entry 2).

TABLE 1. Thiol−Yne Couplings of Methyl Thioglycolate 1 with 1-Octyne 2[a]

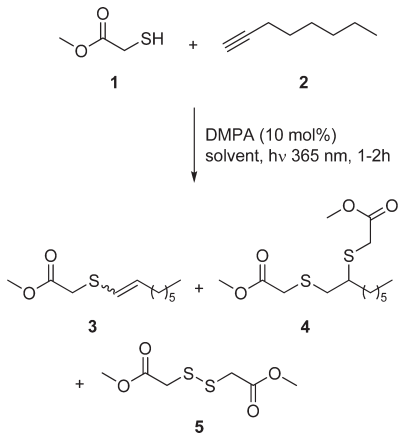

entry	**1**/**2**	solvent (*c* [M])	**3**/**4** [%][b,c]	yield **3** + **4** [%][d]
1	1:1	Toluene (0.5)[e]	100/−	62
2	1:1	Toluene (0.5)[f]	45/55	76
3	1:1	DMSO (0.02)	80/20	55
4	1:1	H_2O−DMSO (0.5)[g]	45/55	90
5	1:1	H_2O (0.5)	11/89	85
6	1:1	[bmim][PF_6]	25/75	52
7	2:1	DMSO (0.5)	−/100	75
8	2:1	H_2O−DMSO (0.5)[g]	−/100	90
9	2:1	H_2O (0.5)	−/100	89

[a]Photoinduced reactions were carried out at r.t. with a household UVA lamp apparatus at λ_{max} 365 nm (see the Experimental Section for equipment setup). Reactions performed with **1** normally gave the corresponding disulfide **5** in < 5% yield; only the reaction of entry 3 afforded **5** in ca. 10% yield. [b]Values are relative percentages and were determined by GC−MS and ^{1}H NMR analysis. [c]Adduct **3** was a 1.2:1 mixture of *E* and *Z* isomers. [d]Isolated yield calculated on the basis of the starting alkyne. [e]Reaction performed under thermal conditions (80 °C) with AIBN as the radical initiator. [f]Similar results were obtained in DMSO or DMF. [g]H_2O/DMSO 95:5.

As far as the 3/4 ratio is concerned, almost identical results were obtained by substituting toluene with DMSO or DMF, albeit with lower overall yields. It would therefore seem that temperature plays a pivotal role in affecting the outcoming sulfide-3/bis-sulfide-4 ratio (by comparison of entries 1 and 2), as an expected result of a faster or slower back fragmentation of the dithioalkyl radical precursor of the bis-adduct. Interestingly, unlike the aliphatic acetylene **2**, under the same conditions phenylacetylene **6** gave only vinyl sulfide **7** in 90% yield (Table 2, entry 1).[7]

Dilution of the reaction mixture from 0.5 to 0.02 M led, with 1-octyne in DMSO, to preferential formation of mono-adduct **3** (**3**/**4** ratio ca. 4:1; Table 1,

entry 3), whereas the reaction with alkyne **6** was not substantially affected, yielding again the mono adduct **7** (65%) as the only coupling product (Table 2, entry 2); both reactions also afforded disulfide **5** as a byproduct (ca. 10%). Since, in general, dilution was found to affect negatively the reaction outcome in terms of lower overall yields, formation of byproducts, and lower conversions, all the subsequent reactions were performed in 0.5 M solutions. When the reaction of 1 with 2 was carried out in water/DMSO 95:5, no change in product distribution was observed (Table 1, entry 4), whereas pure water[8] strongly favored occurrence of bis-adduct **4** over the mono adduct **3** (**3**/**4** ratio ca. 1:8; Table 1, entry 5). So strong seems this effect of water that with this solvent also phenyl acetylene **6** afforded small amounts (10%) of bis-adduct as a mixture of regioisomers **8** and **9** in a 2:1 ratio (Table 2, entry 4).The outcoming difference in the regiochemistry of the bis-sulfide adducts arising from octyne **2** and phenylacetylene **6** probably reflects the relative stability of the alkyl radicals R and à that could in principle arise from further addition of sulfanyl radical to the respective double bond of vinyl sulfides **3** and **7** (Scheme 2). With sulfide **3**, the sulfanyl would strictly prefer to form the more stable radical β, R = C_6H_{13}, owing to back-donation stabilization provided by the attached sulfur atom; with sulfide **7**, the formation of the corresponding radical β, R = Ph, would be discouraged to some

TABLE 2. Thiol−Yne Couplings of Methyl Thioglycolate 1 with Phenylacetylene 6[a]

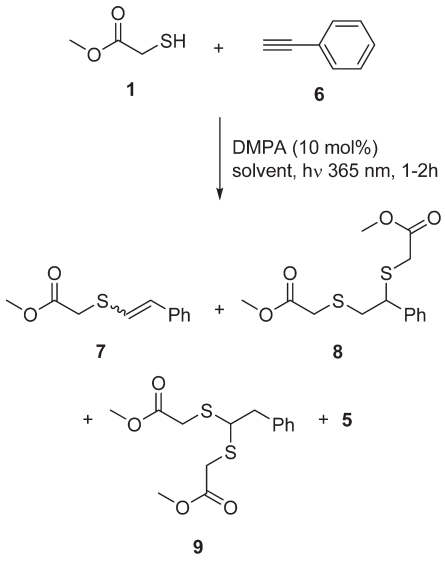

entry	**1**/**6**	solvent (*c* [M])	**7**/**8** + **9** [%][b,c]	yield **7** + **8** + **9** [%][d]
1	1:1	Toluene (0.5)[e]	100/−	90
2	1:1	DMSO (0.02)	100/−	65
3	1:1	H_2O−DMSO (0.5)[f]	100/−	87
4	1:1	H_2O (0.5)	90/10[g]	91
5	1:1	[bmim][PF_6]	90/10[g]	58
6	2:1	DMSO (0.5)	40/60[g]	69
7	2:1	H_2O−DMSO (0.5)[f]	22/78[g]	88
8	2:1	H_2O (0.5)	5/95[g]	91

[a]Photoinduced reactions were carried out at r.t. with a household UVA lamp apparatus at λ_{max} 365 nm (see the Experimental Section for equipment setup). Reactions performed with **1** normally gave the corresponding disulfide **5** in < 5% yield; only the reaction of entry 2 afforded **5** in ca. 10% yield. [b]Values are relative percentages and were determined by GC−MS and ^{1}H NMR analysis. [c]Adduct **7** was a 2:1 mixture of *Z* and *E* isomers. [d]Isolated yield calculated on the basis of the starting alkyne. [e]Similar results were obtained in DMSO or DMF. [f]H_2O/DMSO 95:5. [g]**8**/**9** ~2:1.

extent in favor of the resonance-stabilized benzylic radical α, R = Ph (Scheme 2).

SCHEME 2. Reaction Mechanism of Formation of Bis-Adducts 4, 8, and 9

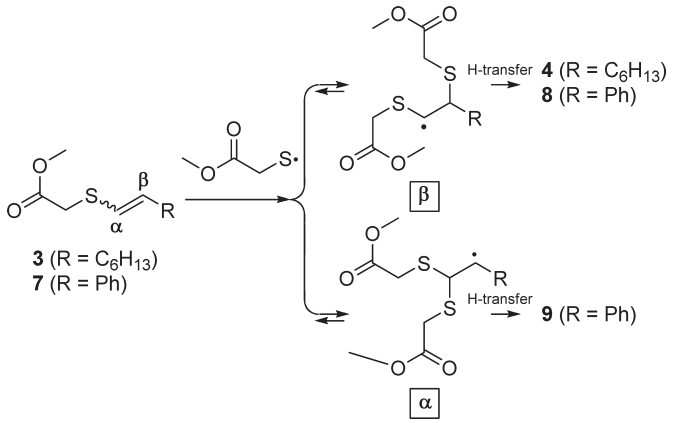

It is worth noting that an analogous effect in favor of bis-hydrothiolation was observed by changing water with an ionic liquid ([bmim][PF_6]): with this solvent, 1-octyne gave adducts **4** and **3** in a 3:1 ratio (Table 1, entry 6) and phenyl acetylene afforded again mono adduct **7** accompanied with minor amounts of bis-adducts **8** and **9**[9] (Table 2, entry 5). Preferential occurrence of bis-sulfide **4** at the expense of vinyl sulfide **3** would possibly entail especially fast H-transfer from thiol **1** to the intermediate dithioalkyl radical. Under these circumstances, in fact, that radical intermediate could be (seriously) discouraged to suffer usual β-elimination of sulfanyl radical yielding back vinyl sulfide **3** (see Scheme 1). Thus, our present findings with octyne **2** in the above ionic liquid seem to substantiate previous chemical evidence that thiols in ionic liquid solvents could act as very strong H-donors.[10] Moreover, the corresponding findings achieved in pure water first suggest that in such medium thiols should interestingly become even stronger H-donors. Whether the enhanced H-donor properties of thiol in ionic liquid and, especially, water would result from some solvent stabilization of the H-transfer transition state, as previously suggested,[10] or would just be a consequence of 'neat' reactions occurring inside organic droplets[11] is a debated question that will be dealt with in future studies.

Taking into account the overall results obtained with thiol **1** (Tables 1 and 2), we can infer that it is possible to modify properly the reaction outcome by tuning the reaction conditions. Starting from equivalent amounts of thiol and

alkyne,with 1-octyne **2** (Table 1), formation of monoadduct **3** is favored at higher temperatures (AIBN-initiated reaction in toluene) or diluted mixtures (0.02 M in DMSO), whereas formation of bis-adduct **4** is strongly favored in an ionic liquid such as [bmim][PF_6] and, particularly, in water. With phenyl-acetylene **6** (Table 2), the monoadduct **7** is always the exclusive product, with the exception of the small amounts of the regioisomeric bis-adducts **8** and **9** isolated in water or [bmim][PF_6]. If total production of bis-sulfide is desired, this can be readily achieved by using a 2-fold excess of thiol reagent. Indeed, the photolytically initiated reaction of alkyne 2 in the presence of 2 equiv of thiol **1** was found to afford virtually quantitative amounts of bis-sulfide 4 irrespective of the solvent employed (DMSO, H_2O/DMSO, or H_2O) (Table 1, entries 7-9). Even in the presence of the same excess of thiol **1**, the aromatic alkyne **6** behaved in a different fashion, since it could still afford significant amounts of monoadduct **7** both in DMSO and H_2O/DMSO (Table 2, entries 6 and 7). In pure water, however, **6** succeeded in forming virtually exclusive amounts of the bis-sulfides **8** and **9**, in line with the discovered effect of water solvent (Table 2, entry 8).

As far as the cysteine thiol **10** is concerned (Tables 3 and 4), its reactions appear slower than those of the congener **1** as a possible result of a higher steric hindrance.[12] This probably justifies the preferential formation of monoadduct **11**,[6d] which is the major product both in DMSO, water/DMSO, and pure water (Table 3, entries 1-3).

It is worth noting that highly selective production of the monoadduct **11** could be achieved by carrying out the reaction under diluted (0.02 M DMSO) conditions (35% yield of **11**, with only 50% conversion; not reported) or using a 2-fold excess of the alkyne **2** (**11**/**12** ratio ~19:1; Table 3, entry 4). Conversely, the use of a 2-fold excess of cysteine **10** allowed highly selective occurrence of the bis-sulfide **12** (**11**/**12** ratio >1:19 both in water/DMSO and water) in very good yield (>90%) (Table 3, entries 5 and 6). In parallel, the TYC of the same cysteine **10** with equimolar phenylacetylene **6** afforded the monoadduct **14** in a very selective fashion under all conditions employed (Table 4, entries 1-3). No evidence of formation of a bis-adduct was observed either with 2 equiv of thiol (entries 4 and 5).

TABLE 3. Thiol−Yne Couplings of *N*-Acetyl-L-cysteine Methyl Ester 10 with 1-Octyne 2[a]

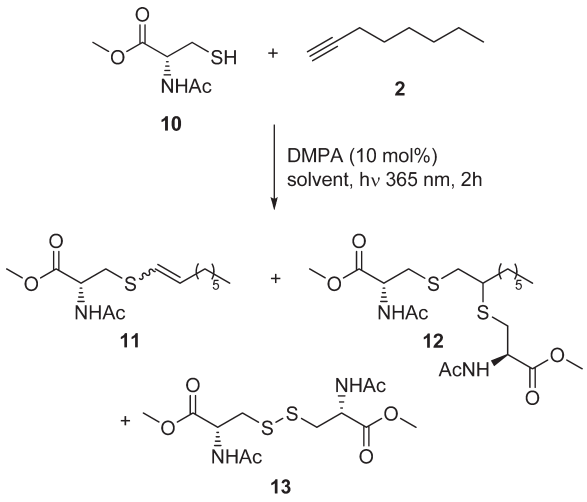

entry	**10**/**2**	solvent (*c* [M])	**11**/**12** [%][b,c]	yield **11** + **12** [%][d]
1	1:1	DMSO (0.5)	83/17	62
2	1:1	H_2O−DMSO (0.5)[e]	67/33	85
3	1:1	H_2O (0.5)	55/45	82
4	1:2	H_2O (0.5)	95/5	81
5	2:1	H_2O−DMSO (0.5)	< 5/ > 95	91
6	2:1	H_2O (0.5)[e]	< 5/ > 95	92

[a]Photoinduced reactions were carried out at r.t. with a household UVA lamp apparatus at λ_{max} 365 nm (see the Experimental Section for equipment setup). Reactions performed with **10** normally gave the corresponding cystine **13** in < 5% yield; only the reaction of entry 1 afforded **13** in ca. 20% yield. [b]Values are relative percentages and were determined by GC−MS and ^{1}H NMR analysis. [c]Adduct **11** was a 1.5:1 mixture of *Z* and *E* isomers. [d]Isolated yield calculated on the basis of the starting alkyne (entries 1−3 and 5−6) or the starting thiol (entry 4). [e]H_2O/DMSO 95:5.

It is noteworthy that our explorative study with octyne **2** and phenylacetylene **6** clearly revealed a deeply different behavior of these two alkynes toward their radical coupling reactions with thiols **1**, **10**. Indeed, phenylacetylene 6 usually gave mono/bis-sulfide adducts in notably higher (overall) yields and, furthermore, showed a distinct propensity to form monosulfide rather than bis-sulfide product. It is therefore plausible that the aromatic alkyne **6** could act as a much stronger trap for sulfur-centered radicals than the aliphatic congener **2**. This point was actually substantiated by our additional finding that the usual reaction of cysteine **10** with equimolar amounts of both alkynes **2** and **6** in DMSO could basically afford the phenylvinyl sulfide **14** at the expense of the alkylvinyl one **11** (**11**/**14** ~ 1:15, Scheme 3).

As anticipated, the ultimate goal of this study was to establish the potential role of photoinduced TYC as a click ligation tool for the direct monoglycosylation of unmodified peptides. The usefulness of this radical reaction in glycopeptide chemistry has been recently validated by the synthesis of dually glycosylated peptides by a two-step strategy, which involved first the S-propargylation of a cysteine containing peptide, and then the photoinduced coupling with excess of glycosyl thiol.[13] Undoubtedly, if peptide mono glycosylation is the target, the direct TYC of sugar alkynes with peptides bearing a free cysteine residue

appears as a more straightforward strategy. Our investigation on this complementary approach took advantage of the information gained from the above explorative study and involved peptide portions of increasing complexity. Accordingly, the coupling between the peracetylated O-propargyl β-glycoside **15** with a single cysteine residue, that is, the N-Fmoc cysteine tert-butyl ester **16**, was initially considered to establish optimal conditions for the selective monohydrothiolation pathway of such more complex substrates (Table 5).

TABLE 4. Thiol−Yne Couplings of *N*-Acetyl-L-cysteine Methyl Ester 10 with Phenylacetylene 6[a]

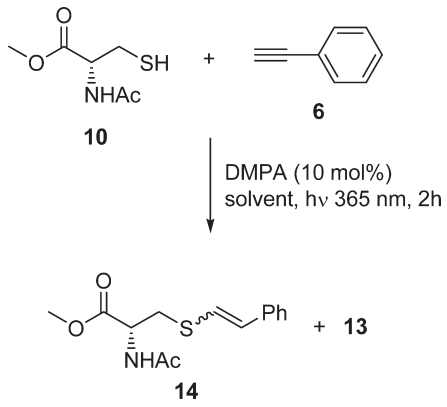

entry	**10**/**6**	solvent (*c* [M])	yield **14** [%][b,c]
1	1:1	DMSO (0.5)	60
2	1:1	H_2O−DMSO (0.5)[d]	78
3	1:1	H_2O (0.5)	88
4	2:1	DMSO (0.5)	86
5	2:1	H_2O−DMSO (0.5)[d]	91

[a]Photoinduced reactions were carried out at r.t. with a household UVA lamp apparatus at λ_{max} 365 nm (see the Experimental Section for equipment setup). Reactions performed with **10** normally gave the corresponding cystine **13** in <5% yield; only the reaction of entry 1 afforded **13** in ca. 20% yield. [b]Adduct **14** was a ~1:1 mixture of *Z* and *E* isomers. [c]Isolated yield calculated on the basis of the starting alkyne. [d]H_2O/DMSO 95:5.

The photoinduced TYC (max 365 nm, DMPA 10 mol %) of equimolar **15** and **16** proceeded smoothly under homogeneous conditions with DMF (0.5 M) as the solvent to give exclusively the monoadduct **17** (25%) as a 1.5:1 mixture of E/Z isomers (Table 5, entry 1), albeit in low yields. Complete conversion of cysteine **16** was conveniently achieved by using a 3-fold excess of sugar alkyne **15**, thus, obtaining **17** in 88% isolated yield (entry 2). It is worth noting that, owing to the set of orthogonal protective groups, the glycosyl amino acid **17** appeared to be a suitable substrate for a co-translational approach[14] to glycopeptides through N-Fmoc-based peptide synthesis.

From a mechanistic point of view, possible formation of the bis-adduct **18** seemed to be strongly inhibited by steric factors in agreement with the results reported above and previous observations on photoinduced TYC of bulky thiols.[6d] Nevertheless, due to the relevance of 'bis-armed' amino acids of type **18** in peptide chemistry,[15] the double hydrothiolation of sugar alkyne **15** with cysteine

16 was actively pursued. Thus, bearing in mind the beneficial effect of heterogeneous conditions in the model couplings of 1-octyne (Table 1, entry 5 and Table 3,entry 3),the photoinduced coupling(max 365nm, DMPA 10 mol %) of sugar alkyne **15** and cysteine **16** was initially performed in H_2O (0.5 M). Unfortunately, these conditions did not produce any results, very likely because of the 'sticky' nature of **16**, which resulted in agglomeration and hence precluded the intimate contact between the reaction partners (entry 3).

SCHEME 3. Competitive Reaction of *N*-Acetyl-L-cysteine Methyl Ester 10 with 1-Octyne 2 and Phenylacetylene 6 (1:1:1 Ratio)

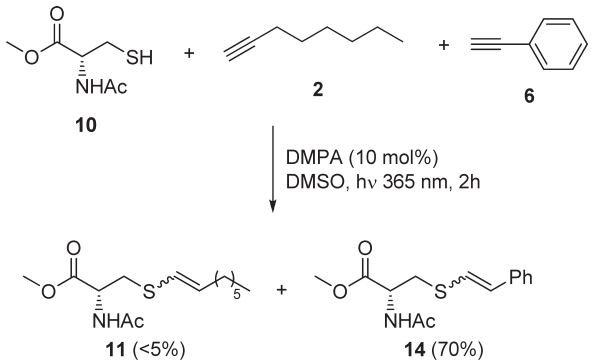

On the other hand, when equimolar **15**, **16**, and the sensitizer DMPA (10 mol %) were previously dissolved with minimal toluene, the subsequent addition of H_2O (0.01 M) resulted in the formation of organic droplets which dispersed under vigorous magnetic stirring. Irradiation of that mixture for 2 h afforded, after concentration and column chromatography, the bis-glycosylated cysteine derivative **18** as the main product (81%, d.r. ~1:1) along with small amounts of the monoadduct **17** (6%; entry 4). The selective formation of the bis-adduct **18** was finally achieved by simply using 2 equiv of cysteine **16** under the same conditions (entry 5). Although a detailed analysis of this reaction outcome goes beyond the object of this research, it can be speculated that reactants concentration into organic droplets by means of hydrophobic interactions is responsible for the observed rate acceleration of the double hydrothiolation reaction.[16,11]

SCHEME 4. Synthesis of Orthogonally Protected Bis-Armed Cysteine 20

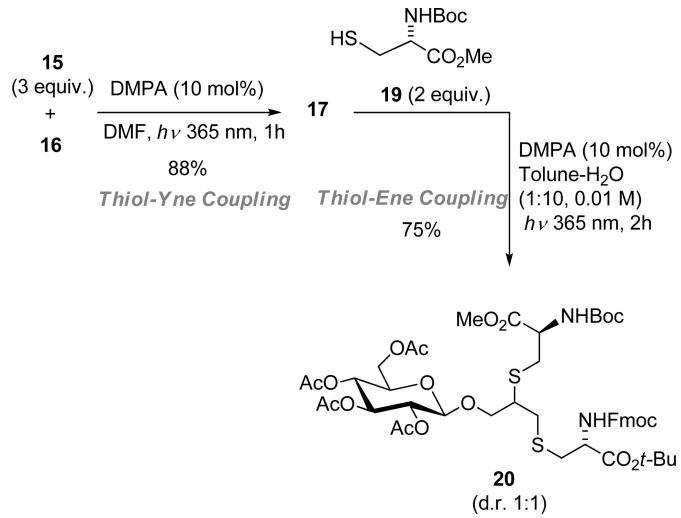

The discovery of a reaction window for both mono- and double-hydrothiolation of sugar alkyne **15** prompted us to investigate the sequential hydrothiolation of **15** using the two different cysteine derivatives **16** and **19** (Scheme 4). Indeed, we thought this proof-of-principle experiment might be of interest to establish the potential of photoinduced TYC/ TEC sequences in dual-labeling investigations.[17] Thus, the vinyl thioether intermediate **17** was first prepared by TYC of alkyne **15** with cysteine **16** under optimized conditions (Table 5, entry 2), and then subjected to the photoinduced TEC (max 365 nm, 2 h, DMPA 10 mol %) with cysteine **19** (2 equiv) in diluted water/ toluene (10:1 v/v) (0.01 M) to give the target bis-adduct **20** (d.r. ~1:1) in 66% overall yield (Scheme 4). Noteworthy, the orthogonal protection of the bis-amino acid **20** allows for differential peptide chain elongation via Boc- and Fmoc- based peptide synthesis.[15]

The investigation of 'click' equimolar glycosylation of cysteine-containing peptides via photoinduced TYC was the next step in our program. To this aim, the readily available glycosyl alkyne **21** and the natural tripeptide glutathione **22** (-L- Glu-L-Cys-Gly, GSH) in its native form were considered suitable substrates for testing the efficiency of this approach (Scheme 5). After some experimentation, full conversion of GSH **22** could be achieved under irradiation (max365nm, DMPA 10mol%, 1h) in a 19:1 H_2O-MeOH mixture[18] when using at least a 5-fold excess of sugar alkyne **21**, as it was established by LC-MS analyses

(see article). This rather disappointing, even though successful, result prompted us to synthesize an aromatic counterpart of the alkyne **21** (Scheme 5) in view of our previous discovery that an aromatic alkyne should be more effective than an aliphatic one in photoinduced TYC (Scheme 3). Accordingly, the unknown ethynylbenzyl β-D-glucopyranoside **24** was obtained by quantitative hydroxyl groups deprotection (NaOMe/MeOH) of the corresponding peracetylated derivative, which in turn was prepared, under nonoptimized conditions (45% yield), by BF_3 OEt_2-promoted glycosylation of β-D- glucose pentaacetate with ethynylbenzyl alcohol (Scheme S1). Gratifyingly, irradiation for 1 h of a mixture of glutathione **22**, DMPA (10 mol %), and sugar alkyne **24** (1.1 equiv) in H_2O-MeOH 3:1 (v/v) (0.1 M)[18] resulted in quantitative formation of the glycoconjugate **25** as judged by ^1H NMR and LC-MS analyses of the crude reaction mixture (see article).

SCHEME 5. Optimized Conditions for the Complete Glycosylation of Glutathione 22 by Sugar Alkynes 21 and 24

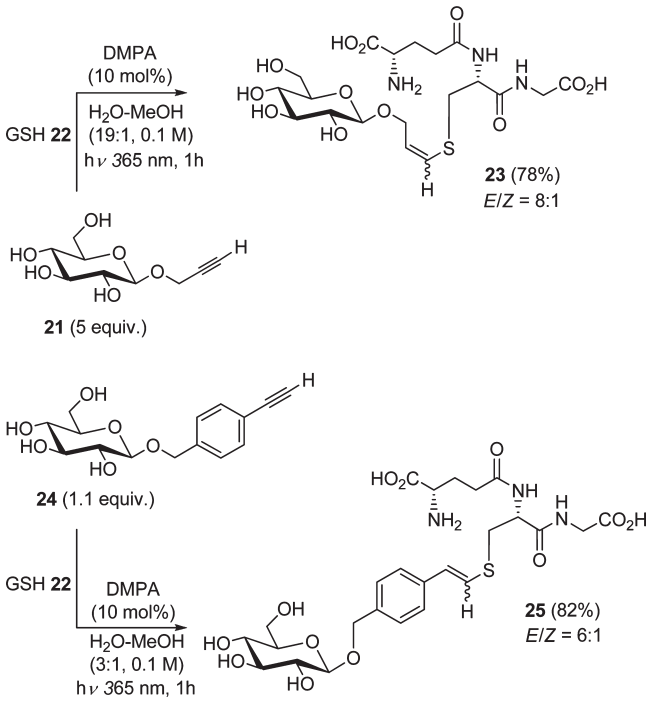

These optimal coupling conditions did not involve any significant excess of either reagents as required by a true 'click' reaction, and then allowed for a simple, rapid purification process of **25**. This compound was readily isolated by short-column chromatography with Sephadex LH20 in 82% yield as a 6:1

mixture of E/Z isomers (Scheme 5). With the pure glycopeptide **25** in hand, the stability of the vinyl thioether linkage in aqueous medium was next investigated by recording ^{1}H NMR spectra of a D_2O solution of **25** (0.03 M) over the time. Rewardingly, no degradation occurred during a week, as it was also confirmed by a final LC-MS analysis of the same solution.

SCHEME 6. Preparation of Glycopeptide 27

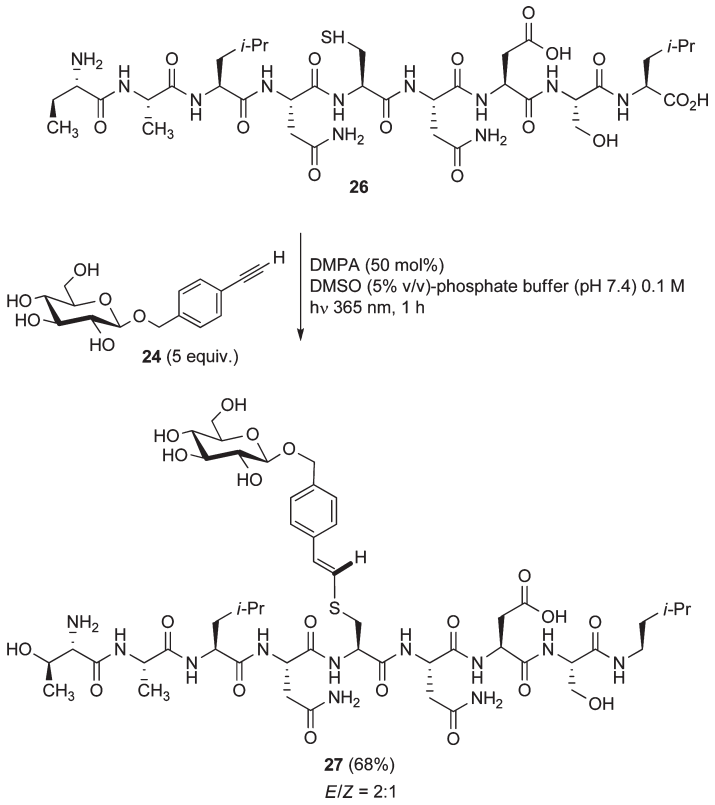

Paralleling the previous study on peptide glycosylation via photoinduced thiol-ene coupling,[19] the efficacy of the optimized thiol-yne coupling was evaluated in aqueous solutions at physiological pH with the higher synthetic nonapeptide TALNCNDSL **26**,[20] which displays a single cysteine residue as well (Scheme 6). Hence, the coupling of **24** with **26** was optimized by adding a solution of DMPA (50 mol %) and **24** (5 equiv) in DMSO (5% final volume content) to a solution of **26** in 20 mM phosphate buffer (pH 7.4) and maintaining irradiation (max 365 nm) for 1 h. Under these conditions, peptide **26** was quantitatively converted into the glycoconjugate **27**, which was obtained in 68% isolated yield (Sephadex LH20) as a 2:1 mixture of E/Z isomers. The selective attachment of **24** to the sulfhydryl group of **26** was duly confirmed by LC-MS/

MS analyses of both (E) and (Z) isomers of glycopeptide **27**. Inevitably, the use of a 5-fold excess of sugar alkyne **24** was required to drive the coupling to completion (LC-MS analysis). This result, however, appears quite satisfactory if compared to that obtained in the parallel TEC study.[19] In that occasion, even a 30-fold excess of a peracetylated allyl C-glycoside was required to achieve complete conversion of the same peptide **26**. It should be noted, however, that a detailed comparison between the two methodologies is complicated at this stage by too many variables, and therefore, it will be the object of a dedicated study.

3.3 Conclusions

Our explorative study showed that the radical alkanethiol/ terminal alkyne coupling reactions are strongly affected by the adopted experimental conditions, including thiol/alkyne molar ratio, temperature and, above all, solvent. A proper choice of the reaction conditions can hence favor highly selective occurrence of either mono- or bis-sulfide coupling product. This study also showed that an aromatic alkyne, besides being much more reactive than an aliphatic congener, has a notably enhanced propensity to form the monocoupling product exclusive of the double-coupling one. Our present observations, which are unprecedented in the reported studies of TYC reactions in the fields of bioconjugation and/or material derivatization, may possibly pave the way to new important applications of the TYC strategy in those fields. The findings were preliminarily exploited in successful glycosylation of cysteine derivatives as well as in the production of a bis-armed cysteine through dual labeling of an alkynyl sugar in a TYC/TEC sequence. Further, the appealing behavior of aromatic alkynes in TYC was rewardingly applied to glycosylation of the native form of GSH just using virtually equimolar amounts of a sugar bearing an aryla- cetylene moiety and, more importantly, to a similar glycosylation of a cysteine-containing nonapeptide under physiological conditions. Aromatic alkynes have hence become a new, attractive tag for bioconjugation studies based on the TYC ligation strategy.

3.4 Experimental Section

Photoinduced reactions were carried out in a glass vial (diameter, 1 cm; wall thickness, 0.65 mm), sealed with a natural rubber septum, located 2.5 cm away from the UVA lamp (irradiation on sample: 365 nm, 1.04 W/m^2).

General Procedure for the Thiol/Yne Radical Couplings Reported in Tables 1-4. A mixture of alkyne (0.50 mmol), thiol (0.50 mmol unless otherwise stated), 2,2-dimethoxy-2-phenylacetophenone (13 mg, 0.05 mmol), and the stated solvent (1 mL unless otherwise stated) was irradiated at room temperature for 1-2 h under magnetic stirring. The crude mixtures of reactions performed in DMSO, H_2O/DMSO, or DMF were diluted with H_2O (5 mL) and extracted with AcOEt (3 x 5 mL). The combined organic phases were washed several times with H_2O, dried (Na_2SO_4), and concentrated. The crude mixtures of the reactions carried out in [bmim][PF_6] were extracted with AcOEt (3 x 5 mL). The combined organic phases were dried (Na_2SO_4) and concentrated. For the reactions performed in toluene, the solvent was simply evaporated off. The resulting residues were eluted from a column of silica gel with the suitable elution system. Yields are reported in Tables 1-4.

(E/Z) Methyl 2-(oct-1-enylthio)acetate 3.

as a 1.2:1 mixture of E and Z isomers. GC-MS: Z-5, r.t. 8.18, m/z 216 (M^+, 25), 145 (59), 143 (39), 109 (59), 85 (47), 71 (100), 55 (44); E-5, r.t. 8.23, m/z 216 (M^+, 39), 145 (74), 143 (40), 109 (50), 85 (42), 71 (100), 55 (37). ^{1}H NMR (400 MHz): δ = 6.02-5.94 (m, 1 H, H-1'), 5.77 (ddd, 0.55 H, $J_{2',3'a}$ = 7.0 Hz, $J_{2',3'b}$ = 7.1 Hz, $J_{1',2'}$ = 14.9 Hz, H-2'(E)), 3.65 (ddd, 0.45 H, $J_{2',3'a}$ = 7.3 Hz, $J_{2',3'b}$ = 7.4 Hz, $J_{1',2'}$ = 9.5 Hz, H-2'(Z)), 3.74 (s, 3 H, OMe), 3.35 (s, 2 H, 2H-2), 2.17-2.04 (m, 2 H, 2H-3'), 1.42-1.20 and 0.92-0.80 (2 m, 11 H, 2H-4', 2H-5', 2H-6', 2H-7', 3H-8'). ^{13}C NMR (400 MHz): δ = 170.3, 134.3, 131.9, 122.7, 120.7, 52.5, 52.4, 35.1, 35.0, 33.0, 31.9, 31.7, 31.6, 29.7, 29.3, 29.0, 28.9, 28.7, 22.7, 22.6, 14.1, 14.0. ESI MS (216): 239 ($M^+ Na^+$). HRMS (ESI/Q-TOF): calcd m/z for $C_{11}H_{20}NaO_2S$ $[M+Na]^+$: 239.1082; found: 239.1087.

(R/S) Methyl 2-[(1-[(2-methoxy-2-oxoethyl)sulfanyl]methylheptyl)sulfanyl] acetate 4.

GC-MS: r.t. 11.52, m/z 322 (M^+, <1%), 263 (7), 216 (40), 203 (47), 146 (19), 143 (73), 110 (26), 107 (29), 97 (35), 87 (27), 69 (46), 55 (100). ^{1}H NMR (600 MHz): δ = 3.71 (s, 3 H, OMe), 3.70 (s, 3 H, OMe), 3.32 and 3.21 (2 d, 2 H, J = 14.5 Hz, CH_2CO), 3.25 and 3.21 (2 d, 2 H, J = 14.7 Hz, CH_2CO), 3.00-2.91 (m, 2 H, H-1a, H-2), 2.81-2.75 (m, 1 H, H-1b), 1.80-1.70, 1.50-1.40, 1.38-1.10 (3 m, 10 H, 2H-3, 2H-4, 2H-5, 2H-6, 2H-7), and 0.85 (t, 3 H, J = 7.0, 3H-8). ^{13}C NMR (600 MHz): δ = 171.2, 171.0, 51.5, 51.4, 44.8 (C-2), 37.1 (C-1), 32.7, 32.2, 31.5, 30.6, 28.0, 25.5, 21.5, 13.0. ESI MS (322): 345 (M + Na^+). HRMS (ESI/Q-TOF): calcd m/z for $C_{14}H_{26}NaO_4S_2$ $[M+Na]^+$: 345.1170; found: 345.1173.

(R/S) Methyl 2-(2-[(2-methoxy-2-oxoethyl)sulfanyl]-1phenylethylsulfanyl) acetate 8.

GC-MS: r.t. 12.05, m/z 314 (M^+, <1), 208 (55), 195 (100), 177 (18), 149 (38), 135 (29), 121 (97), 115 (20), 104 (27), 91 (25), 77 (18). ^{1}H NMR (400 MHz): δ = 7.36-7.24 (m, 5 H, Ph), 4.26 (t, 1 H, J1,2 = 7.8 Hz, H-1), 3.71 (s, 3 H, OMe), 3.67 (s, 3 H, OMe), 3.15 (d, 2 H, 2H-2), 3.14 and 3.08 (2 d, 2 H, J = 14.7 Hz, CH_2CO), 3.13 and 2.98 (2 d, 2 H, J = 15.1 Hz, CH_2CO). ^{13}C NMR (400 MHz): δ = 170.4 (2C), 139.4, 129.1, 128.5, 128.2, 128.0, 127.8, 52.2 (2C), 49.3, 37.7, 33.4, 32.6. ESI MS (314): 337 (M + Na^+). HRMS (ESI/Q-TOF): calcd m/z for $C_{14}H_{18}NaO_4S_2$ $[M+Na]^+$: 337.0544; found: 337.0548.

Methyl 2-(1-[(2-methoxy-2-oxoethyl)sulfanyl]-2-phenylethylsulfanyl)acetate 9.

GC-MS: r.t. 11.08, m/z 314 (M^+, <1), 241 (27), 223 (50), 209 (26), 177 (48), 149 (100), 135 (50), 115 (38), 103 (14), 91 (51). ^{1}H NMR (400 MHz): δ = 7.35-7.22 (m, 5 H, Ph), 4.38 (t, 1 H, $J_{1,2}$ = 7.1 Hz, H-1), 3.70 (s, 6 H, OMe), 3.45 and 3.22 (2 d, 4 H, J = 15.2 Hz, 2 CH_2CO), 3.13 (d, 2 H, 2H-2). ^{13}C NMR (400 MHz): δ = 170.6 (2C), 137.5, 129.3 (2C), 128.4 (2C), 127.0, 53.8, 52.4 (2C), 42.2, 32.4 (2C). ESI MS (314): 337 (M + Na^+). HRMS (ESI/Q-TOF): calcd m/z for $C_{14}H_{18}NaO_4S_2$ [M +Na]$^+$: 337.0544; found: 337.0549.

(2R,E/Z) Methyl 2-acetamido-3-(oct-1-enylthio)propanoate 11.

as a 1.5:1 mixture of Z and E isomers. GC-MS: Z-11, r.t. 9.41, m/z 287 (M^+, 1), 228 (22), 177 (8), 144 (16), 111 (13), 87 (26), 81 (11), 69 (38), 55 (32), 43 (100); E-11, r.t. 9.56, m/z 287 (M^+, 2), 228 (18), 177 (5), 144 (14), 111 (13), 87 (14), 81 (15), 69 (33), 55 (34), 43 (100). ^{1}H NMR: δ = 6.33 (bd, 1 H, J = 7.0 Hz, NH), 5.90-5.70 (m, 1.4 H, H-1'(E), H-1'(Z), H-2'(E)), 5.58 (ddd, 0.6 H, $J_{2',3a'}$ = 7.2 Hz, $J_{2',3'b}$ = 7.3 Hz, $J_{1',2'}$ = 9.3 Hz, H-2'(Z), 4.91-4.83 (m, 1 H, H-2), 3.75 (s, 3 H, OMe), 3.23-3.04 (m, 2 H, 2H-3), 2.17-2.00 (m, 2 H, 2H-3'), 1.42-1.20 and 0.98-0.84 (2 m, 11 H, 2H-4', 2H-5', 2-H6', 2H-7', 3-H8'). ^{13}C NMR (selected data): δ = 170.8, 169.7, 134.2, 131.4, 123.8, 121.5, 52.6, 52.5, 52.1, 36.0, 35.3, 33.1, 31.6, 31.5, 29.0, 28.9, 28.8, 28.7, 23.1, 22.6, 22.5, 14.0. ESI MS (287): 310 (M + Na^+). HRMS (ESI/Q-TOF): calcd m/z for $C_{14}H_{25}NNaO_3S$ $[M+Na]^+$: 310.1453; found: 310.1457.

Dimethyl (4R,11R)-7-hexyl-2,13-dioxo-6,9-dithia-3,12-diazatetradecane-4,11-dicarboxylate 12.

as a 1:1 mixture of C2 diastereoisomers. GC-MS: r.t. ~25 (very broad peak), m/z 320 (M^+ – N-Ac-Cys, 2%), 288 (18), 287 (13), 246 (14), 232 (17), 228 (28), 176 (34), 144 (9), 43 (100). ^{1}H NMR (400 MHz): δ = 6.64 (t, 1 H, J = 7.2 Hz, NH), 6.54 (t, 1 H, J = 7.9 Hz, NH), 4.89-4.79 (m, 2 H, H-2', H-2"), 3.78 (s, 6H, OMe), 3.10-2.91 and 2.84-2.65 (2 m, 7 H, 2H-1, H-2, 2H-3', 2H-3"), 2.07 and 2.06 (2 s, 6 H, C(O)Me), 1.78-1.60, 1.52-1.40, and 1.39-1.20 (3 m, 10 H, 2H-3, 2H-4, 2H-5, 2H-6, 2H-7), 0.88(t, 3 H, J = 6.7 Hz, 3H-8). ^{13}C NMR (400 MHz, selected data): δ = 171.3, 171.2 (2C), 170.0, 169.9, 52.7, 52.6, 52.3, 52.1, 52.0, 46.0, 38.7 (2C), 35.1, 35.0, 34.0, 33.9, 32.9, 32.7, 31.6, 29.0, 26.7, 26.6, 23.0, 22.5, 14.0. ESI MS (464): 487 (M + Na^+). HRMS (ESI/Q-TOF): calcd m/z for $C_{20}H_{36}N_2NaO_6S_2$ $[M+Na]^+$: 487.1912; found: 487.1921.

(2R,E/Z) Methyl 2-acetamido-3-(styrylthio)propanoate 14.

as a ~1:1 mixture of E and Z isomers (reported NMR spectra are for a 4:1 Z/E mixture). GC-MS: Z-14, r.t. 10.27, m/z 279 (M^+, 14), 220 (45), 161 (23), 144 (63), 134 (43), 116 (28), 115 (54), 98 (72), 91 (46), 84 (17), 77 (23), 43 (100); E-14, r.t. 10.52, m/z 279 (M^+, 14), 220 (49), 161 (25), 144 (62), 134 (47), 116 (28), 115 (61), 98 (74), 91 (51), 84 (17), 77 (25), 43 (100). ^{1}H NMR (400 MHz): δ = 7.46-7.16 (m, 5 H, Ph), 6.64 and 6.56 (2 d, 1 H, $J_{1',2'}$ = 15.6 Hz, H-1'(E), H-2'(E),

6.42 and 6.12 (2 d, 1 H, $J_{1',2'}$ = 10.7 Hz, H-1'(Z), H-2'(Z), 6.38 (d, 1 H, J = 7.1 Hz, NH), 4.97-4.88 (m, 1 H, H-2), 3.77 (s, 1.5 H, OMe), 3.72 (s, 1.5 H, OMe), 3.38-3.21 (m, 2 H, 2H-3), 2.03 (s, 3 H, C(O)Me), 2.00 (s, 3 H, C(O)Me). ^{13}C NMR (400 MHz, selected data): δ = 171.0 (E), 170.7 (Z), 170.5 (E), 169.8 (Z), 136.3, 129.4, 128.6, 128.5, 128.1, 127.3, 126.9, 126.5, 126.2, 125.5, 123.7, 60.3, 52.6, 52.4, 52.2, 37.7, 35.0, 22.9, 20.9, 14.0. ESI MS (279): 302 (M + Na^+). HRMS (ESI/Q-TOF): calcd m/z for $C_{14}H_{17}NNaO_3S$ $[M+Na]^+$: 302.0827; found: 302.0830.

(2R,E/Z) Ethyl 2-amino-3-(oct-1-enylthio)propanoate 14.

as a 2:1 mixture of Z and E isomers. GC-MS: Z, r.t. 8.43, m/z 259 (M^+, 5), 186 (85), 158 (18), 143 (21), 126 (10), 116 (22), 110 (36), 102 (75), 87 (71), 81 (29), 74 (62), 67 (33), 55 (45), 43 (100); E, r.t. 8.53, m/z 259 (M^+, 2), 186 (58), 158 (13), 143 (15), 126 (9), 116 (19), 110 (29), 102 (61), 87 (45), 81 (37), 74 (55), 67 (32), 55 (51), 43 (100). ^{1}H NMR (400 MHz): δ = 5.92-5.86 (m, 1 H, H-1'(E), H-1'(Z), 5.76 (ddd, 0.33 H, $J_{2',3a'}$ = 7.0 Hz, $J_{2',3b'}$= 7.2 Hz, $J_{1',2'}$ = 15.0 Hz, H-2'(E)), 5.58 (ddd, 0.66 H, $J_{2',3a'}$ = 6.9 Hz, $J_{2',3b'}$= 7.0 Hz, $J_{1',2'}$ = 9.2 Hz, H-2'(Z)), 4.19 (q, 2 H, J = 7.0 Hz, OCH_2CH_3), 3.68-3.64 (m, 1 H, H-2), 3.10-3.00 (m, 1 H, H-3a(E), H-3a(Z)), 2.93 (dd, 0.66 H, $J_{2,3b}$ = 7.1 Hz, $J_{3a,3b}$ = 13.8 Hz, H-3b(Z)), 2.85 (dd, 0.33 H, $J_{2,3b}$ = 7.5 Hz, $J_{3a,3b}$ = 13.9 Hz, H-3b(E)), 2.18-2.00 (m, 2 H, 2H-3'), 1.40-1.24 (m, 11 H, 2-H4', 2H-5', 2H-6', 2H-7', OCH_2CH_3), 0.92-0.84 (m, 3 H, 3H-8'). ^{13}C NMR (400 MHz, selected data): δ = 173.6, 133.7, 131.2, 123.9, 121.6, 61.2, 54.7, 54.2, 38.9, 38.2, 33.0, 31.6 (2C), 29.0, 28.8, 28.8, 28.7, 22.5, 22.4, 14.1, 13.9. ESI MS (259): 282 (M + Na^+). HRMS (ESI/Q-TOF): calcd m/z for $C_{13}H_{25}NNaO_2S$ $[M+Na]^+$: 282.1504; found: 282.1497.

(2R,E/Z)-tert-Butyl 2-(((9H-fluoren-9-yl)methoxy)carbonylamino)-3-(3'-(2",3", 4",6"-tetra-O-acetyl-β-D-glucopyranosyl)oxyprop-1-enylthio)propanoate 17.

A mixture of propargyl glycoside 15 (300 mg, 0.78 mmol), cysteine derivative 16 (103 mg, 0.26 mmol), 2,2-dimethoxy-2-phenyl-acetophenone (7 mg, 0.026 mmol), and DMF (1.5 mL) was irradiated at room temperature for 1 h under magnetic stirring, and then concentrated. The resulting residue was eluted from a column of silica gel with (i-Pr)2O and then with 9:1 $(i\text{-}Pr)_2O$ / AcOEt to give 17 (179 mg, 88%) as 1.5:1 mixture of E and Z isomers. ^1H NMR (DMSO-d_6, 120 °C, mixture of E and Z isomers): δ = 7.86 (d, 2 H, J = 7.4 Hz, Ar), 7.68 (d, 2 H, J = 7.4 Hz, Ar), 7.46-7.39 and 7.38-7.30 (2m, 4 H, Ar), 7.14 (bs, 1 H, NH), 6.36 (ddd, 0.6 H, $J_{1',3a'}$ = 0.5 Hz, $J_{1',3b'}$ = 0.6 Hz, $J_{1',2'}$ = 15.0 Hz, H-1'(E)), 6.32 (ddd, 0.4 H, $J_{1',3a'}$ = 0.5 Hz, $J_{1',3b'}$ = 0.6 Hz, $J_{1',2'}$ = 9.5 Hz, H-1'(Z)), 5.75-5.60 (m, 1 H, H-2'), 5.28-5.15 (m, 1 H, H-3"), 4.94 (dd, 0.4 H, $J_{3",4"}$ = 9.0 Hz, $J_{4",5"}$ = 9.5 Hz, H-4"(Z)), 4.92 (dd, 0.6 H, $J_{3",4"}$ = 9.0 Hz, $J_{4",5"}$ = 9.5 Hz, H-4"(Z)), 4.85-4.70 (m, 1 H, H-1", H-2"), 4.40-4.32 (m, 2 H, FmocCH$_2$), 4.30-4.06 and 4.00-3.88 (2 m, 7 H, FmocCH, H-2, 2 H-3', H-5", 2 H-6"), 3.20-2.80 (m, 2 H, 2 H-3), 2.05-1.92 (8 s, 12 H, CH_3), 1.45 (s, 9 H, t-Bu). ^{13}C NMR (mixture of E and Z isomers and conformers, selected data): δ = 170.3, 169.3, 115.6, 143.8, 141.3,128.5, 127.7, 125.1, 123.7, 120.0, 99.2, 83.2, 72.8, 71.7, 713, 69.3, 68.4, 67.2, 65.5, 61.9, 54.8, 54.1, 47.1, 37.0, 35.2, 27.9, 20.7. ESI MS (785.27): 803.6 (M + $NH4^+$). HRMS (ESI/Q-TOF): calcd m/z for $C_{39}H_{51}N_2O_{14}S$ $[M+NH4]^+$: 803.3050; found: 803.3061.

(2R,2'R/S,2"R)-tert-Butyl 2-((9H-fluoren-9-yl)methoxy)carbonylamino)-3-(1'-(2"-((9H-fluoren-9-yl)methoxy)carbonylamino)-3"-tert-butoxy-3"-oxopropylthio)-3'-(2"',3"',4"',6"'-tetra-O-acetyl-β-D-glucopyranosyl) oxypropan-2'-ylthio)propanoate 18

To a mixture of cysteine derivative 16 (155 mg, 0.39 mmol), propargyl glycoside 15 (75 mg, 0.20 mmol), and 2,2-dimethoxy-2-phenyl-acetophenone (10 mg, 0.039 mmol) in toluene (2 mL) was added H_2O (19 mL). The resulting dispersion was irradiated at room temperature for 2 h under vigorous magnetic stirring, then concentrated, and eluted from a column of silica gel with $(i\text{-}Pr)_2O$ and then with 9:1 $(i\text{-}Pr)_2O$ /AcOEt to give 18 (206 mg, 85%) as a ~1:1 mixture of C2'-diastereoisomers. ^1H NMR (DMSO-d_6, 120 °C, mixture of diastereoisomers): δ = 7.86 (d, 4 H, J = 7.4 Hz, Ar), 7.68 (d, 4 H, J = 7.4 Hz, Ar), 7.45-7.36 and

7.35-7.28 (2 m, 8 H, Ar), 7.06 (bs, 2 H, NH), 5.22 (dd, 0.5 H, $J_{3''',4'''}$ = 9.0 Hz, $J_{2''',3'''}$ = 9.5 Hz, H-3'''(diast. I)), 5.20 (dd, 0.5 H, $J_{3''',4'''}$ = 9.0 Hz, $J_{2''',3'''}$ = 9.5 Hz, H-3'''(diast. II)), 4.93 (dd, 0.5 H, $J_{4''',5'''}$ = 9.0 Hz, H-4'''(diast. I)), 4.92 (dd, 0.5 H, $J_{4''',5'''}$ = 9.0 Hz, H-4'''(diast. II)), 4.86-4.74 (m, 2 H, H-1''', H-2'''), 4.44-3.89 (m, 12 H, 2 FmocCH, 2 FmocCH$_2$, H-2, H-2'', H-3'a, H-5''', 2 H-6'''), 3.82 (dd, 0.5 H, J2',3'b = 5.0 Hz, $J_{3'a,3'b}$ = 10.5 Hz, H-3'b (diast. I), 3.70 (dd, 0.5 H, $J_{2',3'b}$ = 5.5 Hz, $J_{3'a,3'b}$ = 10.5 Hz, H-3'b (diast. II), 3.20-2.70 (m, 5 H, 2 H-3, 2 H-1'', H-2'), 2.02-1.92 (8 s, 12 H, CH_3), 1.46-1.42 (4 s, 18 H, t-Bu). ^{13}C NMR (mixture of diastereoisomers and conformers, selected data): δ = 170.6, 169.4, 155.8, 143.8, 141.3, 127.7, 127.0, 125.1, 120.0, 101.2, 100.8, 83.0, 82.9, 72.7, 72.6, 71.8, 71.0, 68.3, 67.2, 61.8, 54.6, 53.4, 47.0, 34.4, 28.0, 20.7, 20.6. ESI MS (1184.42): 1203.1 (M + NH_4^+). HRMS (ESI/Q-TOF): calcd m/z for $C_{61}H_{76}N_3O_{18}S_2$ $[M+NH_4]^+$: 1202.4560; found: 1202.4551.

(2R,2'R/S,2"R)-Methyl 2-((tert-butoxycarbonylamino)-3-(1'-(2"-((9H-fluoren-9-yl)methoxy)carbonylamino)-3"-tert-butoxy-3"-oxopropylthio)-3'-(2"',3"',4"',6"'-tetra-O-acetyl-β-D-glucopyranosyl)oxypropan-2'-ylthio)propanoate 20.

To a mixture of alkene 17 (150 mg, 0.19 mmol), cysteine derivative 19 (90 mg, 0.38 mmol), 2,2-dimethoxy-2-phenyl-acetophenone (10 mg, 0.038 mmol) in toluene (2.0 mL) was added H_2O (19 mL). The resulting dispersion was irradiated at room temperature for 2 h under magnetic stirring, and then concentrated. The resulting residue was eluted from a column of silica gel with 8:1 (i-Pr)$_2$O /AcOEt to give 20 (146 mg, 75%) as a ~1:1 mixture of C2'-diastereoisomers. ^{1}H NMR (DMSO-d$_6$, 120 °C, mixture of diastereoisomers): δ = 7.86 (d, 2 H, J = 7.4 Hz, Ar), 7.70 (d, 2 H, J = 7.4 Hz, Ar), 7.45-7.38 and 7.37-7.30 (2 m, 4 H, Ar), 7.14 (bs, 1 H, NH), 6.60 (bs, 1 H, NH), 5.35 (dd, 0.5 H, $J_{3''',4'''}$ = 9.0 Hz, $J_{2''',3'''}$ = 9.5 Hz, H-3'''(diast. I)), 5.90 (d, 0.5 H, $J_{1''',2'''}$ = 7.5 Hz, H-1''' (diast. I), 5.24 (dd, 0.5 H, $J_{3''',4'''}$ = 9.0 Hz, $J_{2''',3'''}$ = 9.5 Hz, H-3'''(diast. II)), 5.00-4.75 (m, 2.5 H, H-2''', H-4''', H-1''' (diast. II), 4.40-4.32, 4.28-4.06, 4.00-3.90, and 3.80-3.64 (4 m, 13 H, FmocCH, FmocCH2, H-2, H-2'', 2 H-3', H-5''', 2 H-6''', OCH_3), 3.10-2.80 (m, 5 H, H-3, H-1''), 2.05-1.94 (8 s, 12 H, CH_3), 1.46 (s, 9 H, t-Bu), 1.43 and 1.42 (2 s, 9 H, t-Bu). ^{13}C NMR (mixture of diastereoisomers and conformers, selected data): δ = 170.7, 169.4, 155.8, 155.2, 143.8, 141.3, 127.7, 127.1, 125.2, 120.0, 101.2,

100.8, 91.7, 83.0, 72.8, 72.6, 71.9, 71.0, 68.3, 68.2, 67.2, 61.8, 61.4, 60.4, 54.7, 53.4, 52.6, 47.0, 46.8, 45.8, 40.3, 35.9. 29.7, 28.3, 28.0, 21.0, 20.9. ESI MS (1020.36): 1038.9 (M + NH_4^+). HRMS (ESI/Q-TOF): calcd m/z for $C_{48}H_{68}N_3O_{18}S_2$ $[M+NH_4]^+$: 1038.3934; found: 1038.3922.

Glycopeptide 23.

A mixture of sugar alkyne 21 (272 mg, 1.25 mmol), reduced glutathione 22 (77 mg, 0.25 mmol), 2,2- dimethoxy-2-phenyl-acetophenone (6 mg, 0.025 mmol), MeOH (0.1 mL), and H_2O (1.9 mL) was irradiated at room temperature for 1 h under magnetic stirring, and then concentrated. The resulting white solid residue was suspended in MeOH (2 mL) and triturated with portions of MeOH (32 mL) which were pipetted off. The residue left after trituration was eluted from a column of Sephadex LH20 with 3:1 H2O-MeOH to give 23 (102 mg, 78%) as a 8:1 mixture of (E)- and (Z)-isomers (reported NMR spectra are for a 2:1 E/Z mixture). The occurrence of the E-isomer as the major compound was confirmed by analysis of the vinyl protons region of the ^{1}H NMR spectrum of the crude reaction mixture. ^{1}H NMR (300 MHz, D_2O, (E/Z)-isomers): δ = 6.25 (d, 0.66 H, J = 15.0 Hz, CH=CH (E)), 6.19 (d, 0.33 H, J = 10.5 Hz, CH=CH (Z)), 5.70-5.60 (m, 1 H, CH=CH), 4.48-4.40 (m, 1 H, H-5), 4.30 (d, 0.66 H, $J_{1''',2'''}$= 8.0 Hz, H-1'''(E)), 4.28 (d, 0.33 H, $J_{1''',2'''}$= 8.5 Hz, H-1'''(Z)), 4.22-4.00 (m, 2 H, 2 H-3''), 3.80-3.50 (m, 6 H, 2 H-2, H-10, H-5''' 2 H-6'''), 3.34-3.04 (m, 4 H, H-1'a, H-2''', H-3''', H-4'''), 2.94-2.82 (m, 1 H, H-10 b), 2.40-2.30 (m, 2 H, 2 H-8), 2.02-1.94 (m, 2 H, 2 H-9).^{13}C NMR (75 MHz, D2O, (E/Z)-isomers; selected data): δ = 174.7, 174.6, 173.8, 173.6, 172.1, 172.0, 129.7, 129.0, 128.3, 124.8, 124.4, 101.1, 100.7, 75.9, 75.8, 75.7, 72.9, 69.5, 69.4, 65.6, 60.6, 53.7, 52.9, 41.7 31.1, 25.9. ESI MS (525): 526 (M + H^+). HRMS (ESI/Q-TOF): calcd m/z for C19H32N3O12S $[M + H]^+$, 526.1707; found, 526.1701. The LC- MS analysis of the reaction mixture was performed to establish the full conversion of glutathione and confirm the E/Z ratio of 23 (see Figure S1)

Glycopeptide 25

A mixture of sugar alkyne 24 (79 mg, 0.27 mmol), reduced glutathione 22 (75 mg, 0.24 mmol), 2,2- dimethoxy-2-phenyl-acetophenone (6 mg, 0.024

mmol), and MeOH (0.5 mL), and H_2O (1.5 mL) was irradiated at room temperature for 1 h under magnetic stirring, and then concentrated. The resulting residue was eluted from a column of Sephadex LH20 with 1:1 H_2O-MeOH to give 25 (120 mg, 82%) as a 6:1 mixture of (E)- and (Z)-isomers. The occurrence of the E-isomer as the major compound was confirmed by analysis of the vinyl protons region of the ^{1}H NMR spectrum of the crude reaction mixture. ^{1}H NMR (400 MHz, D_2O, (E)-isomer): δ = 7.40-7.20 (m, 4, H, Ar), 6.72 and 6.54 (2 d, 2 H, J = 15.6 Hz, CH=CH), 4.74 and 4.57 (2 d, 2 H, J = 11.7 Hz, 2 H-2'), 4.56-4.50 (m, 1 H, H-5), 4.36 (d, 1 H, $J_{1''',2'''}$ = 8.0 Hz, H-1'''), 3.77 (dd, 1 H, $J_{5''',6'''}$a = 2.0 Hz, $J_{6'''a,6'''b}$ = 12.5 Hz, H-6'''a), 3.74 (s, 2 H, 2H-2), 3.58 (dd, 1 H, $J_{5''',6'''b}$ = 5.5 Hz, H-6'''b), 3.57 (t, 1 H, J = 7.0 Hz, H-10), 3.40-3.10 (m, 5 H, H-2''', H-3''', H-4''', H-5''', H-1'a), 3.03 (dd, 1 H, $J_{1'b,5}$ = 8.0 Hz, J1'a,1'b = 14.5 Hz, H-1'b), 2.36-2.28 (m, 2 H, 2 H-8), 2.05-1.90 (m, 2 H, 2 H-9). 1H NMR (400 MHz, D_2O, (E)-isomer; selected data): δ = 6.49 and 6.22 (2 d, 2 H, J = 10.8 Hz, CH=CH), 4.37 (d, 1 H, $J_{1''',2'''}$ = 8.0 Hz, H-1'''). ^{13}C NMR (D_2O, (E/Z)-isomers; selected data): δ = 174.9, 173.8, 172.4, 116.7, 135.9, 129.5, 129.0, 127.3, 126.0, 124.3, 101.3, 76.1, 76.0, 73.3, 71.3, 69.9, 61.0, 54.0, 53.7, 41.8, 33.8, 31.4, 26.1. ESI MS (601.19): 619.9 ($M + NH_4^+$). HRMS (ESI/Q-TOF): calcd m/z for $C_{25}H_{39}N_4O_{12}S$ $[M+NH_4]^+$: 619.2280; found: 619.2275.

The LC-MS analysis of the reaction mixture was performed to establish the full conversion of glutathione and evaluate the E/Z ratio of 25 (see Figure S2).The LC MS/MS analysis of 25 was also performed to confirm the selective glycosylation of the cysteine residue of glutathione.

Glycopeptide 25

A solution of sugar alkyne 24 (13.8 mg, 0.047 mmol) and DMPA (1.2 mg, 4.71 μmol) in DMSO (0.25 mL) was added to a solution of peptide 26 (10.0 mg, 9.41 μmol) in 20 mM phosphate buffer (pH 7.4, 5.0 mL). The resulting solution was irradiated at room temperature for 1 h under magnetic stirring, and then lyophilized. The resulting residue was eluted from a column of Sephadex LH20 with H_2O to give 27 (8.0 mg, 68%) as a 2:1 mixture of (E)- and (Z)-isomers but slightly contaminated by excess sugar alkyne (reported ^{1}H NMR spectrum is for a ~1:2 E/Z mixture). The occurrence of the E-isomer as the major compound was confirmed by analysis of the vinyl protons region of the ^{1}H NMR spectrum of

the crude reaction mixture. ^{1}H NMR (400 MHz, D_2O, (E/Z)- isomers, selected data): δ = 6.64 and 6.58 (2 d, 066 H, J = 13.5 Hz, CH=CH(E)), 6.44 and 6.165 (2 d, 1.32 H, J = 9.5 Hz, CH=CH- (Z)). The LC-MS analysis of the reaction mixture was performed to establish the full conversion of peptide 26 and confirm the E/Z ratio of 27 (see Figure S4). The LC MS/MS analyses of peptide 26 and glycopeptide 27 were performed to confirm the selective glycosylation of the cysteine residue of 26

3.5 Bibliography

[1] M. Minozzi, A. Monesi, D. Nanni, P. Spagnolo, N. Marchetti and A. Massi, J. Org. Chem., 2011, 76, 450-459.

[2] van Dijk, M.; Rijkers, D. T. S.; Liskamp, R. M. J.; van Nostrum, C. F.; Hennink, W. E. Bioconjugate Chem. 2009, 20, 2001–2016.

[3] **a)** Ogawa, A.; Obayashi, R.; Ine, H.; Tsuboi, Y.; Sonoda, N.; Toshikazu, H. J. Org. Chem. 1998, 63, 881– 884. For another recent example of radical monothiolation of arylacetylenes, see: **b)** Beauchemin, A.; Gareau, Y. Phosphorus, Sulfur, Silicon Relat. Elem. 1998, 139, 187–192. It is worth emphasizing that a higher reactivity (kinetic constant of more than one order of magnitude higher) of phenylacetylene with respect to an alkyl congener (1-propyne) has been also reported for addition of alkyl (methyl) radicals, see: **c)** Fischer, H.; Radom, L. Angew. Chem., Int. Ed. 2001, 40, 1340–1371.

[4] **a)** Benati, L.; Montevecchi, P. C.; Spagnolo, P. J. Chem. Soc., Perkin Trans. 1 1991, 2103–2109. and references therein. **b)** Benati, L.; Montevecchi, P. C.; Spagnolo, P. J. Chem. Soc., Perkin Trans. 1 1992, 1659–1664. **c)** Benati, L.; Capella, L.; Montevecchi, P. C.; Spagnolo, P. J. Chem. Soc., Perkin Trans. 1 1995, 1035–1038. **d)** Benati, L.; Capella, L.; Montevecchi, P. C.; Spagnolo, P. J. Org. Chem. 1995, 60, 7941–7946. **e)** Montevecchi, P. C.; Navacchia, M. L. J. Org. Chem. 1997, 62, 5600–5607. **f)** Montevecchi, P. C.; Navacchia, M. L. J. Org. Chem. 1998, 63, 537–542. **g)** Montevecchi, P. C.; Navacchia, M. L.; Spagnolo, P. Tetrahedron 1998, 54, 8207–8216. **h)** Montevecchi, P. C.; Navacchia, M. L.; Spagnolo, P. Eur. J. Org. Chem. 1998, 1219–1226. **i)** Leardini, R.; Nanni, D.; Zanardi, G. J. Org. Chem. 2000, 65, 2763–2772. We recently exploited addition of sulfanyl radicals to alkynes as a novel tin-/metal-free method to generate assorted kinds of radicals, see: **j)** Benati, L.; Calestani, G.; Leardini, R.; Minozzi, M.; Nanni, D.; Spagnolo, P.; Strazzari, S. Org. Lett. 2003, 5, 1313–1316. **k)** Benati, L.; Leardini, R.; Minozzi, M.; Nanni, D.; Scialpi, R.; Spagnolo, P.; Zanardi, G. Synlett 2004, 987–990. **l)** Benati, L.; Bencivenni, G.; Leardini, R.; Minozzi, M.; Nanni, D.; Scialpi, R.; Spagnolo, P.; Zanardi, G. J. Org. Chem. 2006, 71, 3192– 3197. **m)** Bencivenni, G.; Lanza, T.; Leardini, R.; Minozzi, M.; Nanni, D.; Spagnolo, P.; Zanardi, G. Org. Lett. 2008, 10, 1127–1130.

[5] Under these conditions, the reaction vessel actually warmed up to 35-40 C. Anyway, strictly identical results were obtained with reaction mixtures kept at 25 °C by simultaneous air-cooling with compressed air.

[6] **a)** Fairbanks, B. D.; Scott, T. F.; Kloxin, C. J.; Anseth, K. S.; Bowman, C. N. Macromolecules 2009, 42, 211–217. **b)** Chen, G.; Kumar, J.; Gregory, A.; Stenzel, M. H. Chem. Commun. 2009, 6291–6293. **c)** Chan, J. W.; Hoyle, C. E.; Lowe, A. B. J. Am. Chem. Soc. 2009, 131, 5751–5753. **d)** Hensarling, R. M.; Doughty, V. A.; Chan, J. W.; Patton, D. L. J. Am. Chem. Soc. 2009, 131, 14673–14675. **e)** Konkolewicz, D.; Gray-Weale, A.; Perrier, S. J. Am. Chem. Soc. 2009, 131, 18075–18077. **f)** Lowe, A. B.; Hoyleb, C. E.; Bowman, C. N. J. Mater. Chem. 2010, 20, 4745–4750. **g)** Fairbanks, B. D.; Sims, E. A.; Anseth, K. S.; Bowman, C. N. Macromolecules 2010, 43, 4113–4119. **h)** Chan, J. W.; Shin, J.; Hoyle, C. E.; Bowman, C. N.; Lowe, A. B. Macro- molecules 2010, 43, 4937–4942. **i)** Hoogenboom, R. Angew. Chem., Int. Ed. 2010, 49, 3415–3417.

[7] All the vinyl sulfides were formed as mixtures of E- and Z-isomers: see the Experimental Section for details. Studies on the stereoselective formation of the kinetic (Z) or thermodynamic (E) product are currently underway.

[8] Reactions carried out in water were heterogeneous mixtures, whereas those carried out in water/DMSO 95:5 were normally homogeneous.

[9] Both in water and in the ionic liquid the 8/9 ratio is ca. 2:1.

[10] a) Chapter before, b) Lanza, T.; Minozzi, M.; Monesi, A.; Nanni, D.; Spagnolo, P.; Chiappe, C. Curr. Org. Chem. 2009, 13, 1726–1732.

[11]For a recent discussion about organic synthesis “on water”, see: Chanda, A.; Fokin, V. V. Chem. Rev. 2009, 109, 725–748.

[12] We cannot exclude that polar factors may also play an additional role in the overall thiolation reaction, see: Escoubet, S.; Gastaldi, S.; Vanthuyne, N.; Gil, G.; Siri, D.; Bertrand, M. P. J. Org. Chem. 2006, 71, 7288–7292.

[13] Lo Conte, M.; Pacifico, S.; Chambery, A.; Marra, A.; Dondoni, A. J. Org. Chem. 201075, 4644–4647.

[14] McGarvey, G. J.; Benedum, T. E.; Schmidtmann, F. W. Org. Lett. 2002, 4, 3591–3594.

[15] For leading references on the synthesis of bis-amino acids, see: (a) Li, C.; Tang, J.; Xie, J. Tetrahedron 2009, 65, 7935–7941. For an interesting application, see: (b) Schafmeister, C. E.; Brown, Z. Z.; Gupta, S. Acc. Chem. Res. 2008, 41, 1387–1398.

[16] Pirrung, M. C.; Das Sarma, K.; Wang, J. J. Org. Chem. 2008, 73, 8723–8730.

[17] For an outstanding example, see: van Kasteren, S. I.; Kramer, H. B.; Jensen, H. H.; Campbell, S. J.; Kirkpatrick, J.; Oldham, N. J.; Anthony, D. C.; Davis, B. G. Nature 2007, 446, 1105–1109.

[18] Homogeneous conditions were required to achieve good conversions of GSH **22**

[19] Dondoni, A.; Massi, A.; Nanni, P.; Roda, A. Chem.—Eur. J. 2009, 15, 11444–11449.

[20] This compound was kindly provided as trifluoroacetic salt by UFPeptides S.r.L. (University of Ferrara).

CHAPTER 4

Theorical approach for radical additions Computational Methods

4.1 Theoretical approach

This chapter is focused on the computational methods adopted in this thesis. All calculations presented here have been performed within the density functional theory (DFT) formulation of the quantum mechanics. The reason is that DFT is one of the most computationally efficient first principle methods to calculate atomic structures and electronic states in a wide variety of materials. Furthermore, it allows for dynamics, thus offering a versatile tool for performing finite-temperature simulations. More recently, DFT-based dynamics has been combined with methods suitable to sample chemical reaction paths and applied successfully to complicated chemical, catalytic and biochemical reactions.

This chapter is organized as follows. Theoretical and practical aspects of DFT calculations are described in sections X.X and X.X, respectively. The basics of the first principles (DFT-based) dynamics are presented in section X.X. Finally, in the latter section, the free energy sampling technique, known as Blue Moon Ensemble, used to inspect chemical reaction pathways and to work out free energy barriers is briefly discussed in view of its applications.

4.1.1 Density Functional Theory

The density functional theory (DFT) was originally proposed in the early 60s by Hohenberg and Kohn (1964)[1], and Kohn and Sham (1965)[2] with important contributions also from the group of Pople[3] (Pople et al. 1981, Pople et al. 1989, Johnson et al. 1993). Its importance in the advancement of computational quantum chemistry and related fields was internationally acknowledged by the Nobel Prize in Chemistry in 1998 awarded jointly to Walter Kohn and John A. Pople. The DFT is a formulation of the many-body quantum mechanics in terms of an electron density distribution, $\rho(\mathbf{x})$, which describes the ground state of a general system composed of interacting electrons and classical nuclei at given positions $\{\mathbf{R}_I\}$. Several excellent books and review articles have been published on the fundamentals of DFT (Parr and Yang[4], Marx and Hutter[5]). For this reason, I limit the discussion to the basic details necessary

to what has been done in this thesis and refer the reader to the rich literature, part of which is cited in the references listed at the end of this chapter. The first step in DFT consists in giving an explicit form for the electron density distribution; in a way similar to the hypotheses introduced in the HF approach, also here single-particle wavefunctions $y_i(x)$ are used to express the many-body mathematical function $\rho(\mathbf{x})$. The major difference and, at the same time, dramatic simplification, is the fact that not even the specific analytic form of the complex function $\psi_i(\mathbf{x})$ matters, but only its square modulus, so that the electron

$$\rho(\mathbf{x}) = \sum_{i=1}^{N^{occ}} f_i |\psi_i(\mathbf{x})|^2 \qquad (1)$$

density readsThis expression is clearly a single Slater determinant constructed from the single-particle wavefunctions representing all the N^{occ} occupied orbitals. The coefficients f_i are the integer occupation numbers, and they are equal to 1 in the case in which the spin is explicitly considered (spin-unrestricted) or equal to 2 if the spin is neglected and energy levels are considered as doubly-occupied (spin-restricted). Furthermore, the wavefunctions $\psi_i(\mathbf{x})$ are subject to the orthonormality constraint.

$$\int \psi_i^*(\mathbf{x})\psi_j(\mathbf{x})d^3x = \delta_{ij} \qquad (2)$$

as in any quantum mechanics approach. The Kohn-Sham (KS) DFT total energy of the system in its ground state is then written as

$$E^{KS}[\{\psi_i\}] = E_k[\{\psi_i\}] + E_H[\rho] + E_{xc}[\rho] + E_{el}[\rho] + E_{II} \qquad (3)$$

In Eq. (3) the first three terms on the right-hand side (E_k, E_H, E_{xc}) describe all the electron-electron interactions, the fourth term (E_{el}) refers to the electron-nucleus interaction and the fifth one (E_{II}) the nucleus-nucleus interaction. (exactly *as sketched in* ***Fig. 4***. Let's revise briefly the explicit form and the meaning of each one of these terms. E_k is the Schrödinger-like kinetic energy expressed in terms of the single-particle wavefunctions $\psi_i(\mathbf{x})$ as

$$E_k[\{\psi_i\}] = \sum_{i=1}^{N^{occ}} f_i \int d^3x \psi_i^*(x) \left(-\frac{1}{2}\right) \qquad (4)$$

and it is completely diagonal both in the index *i* and in the argument **x** of the wavefunctions, as in a non-interacting system of N^{occ} electrons. We remark, in passing, that this expression for the kinetic energy does not depend on the density $r(x)$ but directly on the wavefunctions. The second term, E_H, is the Hartree energy already encountered in the HF approach, it accounts for the Coulomb electrostatic interaction between two charge distributions and is written as

$$E_H[\rho] = \iint d^3x\, d^3y \frac{\rho(\mathbf{x})\rho(\mathbf{y})}{|\mathbf{x}-\mathbf{y}|} \qquad (5)$$

This is generally computed via the associate Poisson equation solved for the Hartree potential

$$V_H(\mathbf{x}) = \int d^3y \frac{\rho(\mathbf{y})}{|\mathbf{x}-\mathbf{y}|} \qquad (6)$$

The exchange interaction and the electron correlations due to many-body effects are represented by the term $E_{xc}[\rho]$, whose exact analytical expression is unfortunately unknown; this represents in a sense a limit of the DFT. There are good approximations derived from the homogeneous electron gas limit for the exchange interaction[6]. Namely, the pure exchange part of the functional, $E_x[\rho]$ can be written in the so-called local density approximation (LDA) as

$$E_x[\rho] = -\frac{3}{2} \qquad (7)$$

This is the simplest possible form and the name comes from the fact that an interacting but homogeneous electron distribution is assumed, in which the (unknown) density is given by the local density $\rho(\mathbf{x})$ at a specific point **x** in the inhomogeneous system. Similarly, the LDA version of the correlation energy, originally proposed by Kohn and Sham[2] and successively improved by Perdew and Zunger (1981)[7], reads

$$E_c[\rho] = \int d^3x\, \rho(\mathbf{x}) \varepsilon_c(\rho(\mathbf{x})) \qquad (8)$$

where the explicit analytic form of the function $\varepsilon_c(\rho(\mathbf{x}))$ comes from a parameterization of the results of random phase approximation calculations. Due to the insufficiency of a simple LDA approximation in the treatment of many real systems, such as proteins and nucleic acids, non-local approximations including the gradient of the density, $\nabla \rho(\mathbf{x})$ are often adopted and the exchange-correlation functional becomes

$$E_{xc}[\rho, \nabla\rho] = \int d^3x\, \varepsilon_{xc}(\rho(\mathbf{x}), \nabla\rho(\mathbf{x})) \qquad (9)$$

In practical applications, however, the gradient enters only with its modulus $|\nabla \rho(\mathbf{x})|$, thus adding only a modest computational cost to DFT calculations. These generalized gradient corrections (GGA) are indeed a bit arbitrary, in the sense that they do not represent a regular perturbation expansion as, for instance, in the case of MP2 corrections. Nonetheless, they are generally based on solid physical and mathematical argumentations and anyhow their accuracy can be assessed *a posteriori* by test calculations and comparisons with both exact results and experiments[3c]. As far as the exchange term is concerned, the original work of Becke[6] represents a milestone in the field and it is still regarded as a standard. It was subsequently refined and improved by the same author[8] with remarkable success in a wealth of applications. Also correlations, have received special attention from several research groups, sometimes including also the exchange part into a single functional[9]. Among all the possible functional forms for the exchange and correlation functional, the ones that have been most widely used in the applications of DFT DFT for chemistry and aqueous solution is the Becke exchange in combination with the Lee, Yang and Parr correlation, termed BLYP[6,9e] in the literature. This is also the choice done in the simulations treated in this chapter. Indeed, as far as it has been checked over the years, BLYP provides a better performance in terms of geometrical parameters and relative energies for a wide variety of organic and inorganic molecules[10], two of the main ingredients in proteins and nucleic acids. In general, the explicit form adopted to describe the exchange and correlation

interactions represents a delicate step in the set-up of the simulation framework and must be carefully tested and benchmarked. As a word of warning, let us also stress the fact that no one of the present versions of E_{xc} included van der Waals interactions. In the cases in which they are dominant, such as, for instance, in the base pair stacking of DNA and RNA, special corrections ad hoc must be included[11], although they are not entirely (or not at all) self-consistent with the DFT formulation.

The analytic form of the electrostatic interaction between the two sets of variables, electrons and nuclei, is simply given by the Coulomb attraction between a point-like charge at nuclear positions $\mathbf{R}_I$ and the electron density distribution,

$$E_{eI}[\rho] = -\int d^3x \sum_{I=1}^{M} \frac{Z_I \rho(\mathbf{x})}{|\mathbf{x} - \mathbf{R}_I|} \qquad (10)$$

where Z_I is the charge of the I^{th} nucleus. However, for most of the applications that will be discussed in the following paragraphs, this expression turns out to be computationally expensive. In fact, in a large protein or nucleic acid system there are two different length scales that come into play: a small one for the core electrons, characterized by rapidly varying wavefunctions, especially in the region very close to the nucleus, and a longer one for the valence electrons that form chemical bonds and vary more smoothly. Clearly, in an all-electron calculation, the first one would dominate and add a computational workload that would make impractical dynamical simulations, and often even static optimizations, of large biomolecules. Provided that the model system is small enough and long dynamical quantum simulations are not required, it is certainly possible to use and all-electron DFT approach. However, one can observe that core electrons are generally inert and do not participate to chemical bonds. This crucial observation led to the use of pseudopotentials. Namely, core electrons are eliminated and a potential describing the core-valence interaction is built by fitting to the all-electron solutions of the Schrödinger or Dirac equation for the single atom of the chemical species considered[12]. Alternatively, one can consider the inner electron wavefunctions close to the nuclei as frozen orbitals and

describe them with appropriate angular momentum projectors[13]. In a pseudopotential (PP) approach, the electron-nucleus interaction is rewritten as

$$E_{el}[\rho] = \int d^3x\, V_{ps}(\mathbf{x} - \mathbf{R}_I) \times \rho(\mathbf{x}) \qquad (11)$$

The elimination of the core electron from the calculation allows one to get rid of the short length scale problem. The computational cost can be further reduced, provided that a separable form is chosen for the pseudopotential[14] such as

$$V_{ps}(\mathbf{r}) = V_{loc}(\mathbf{r}) + \sum_{l,m} \phi_{lm}(\mathbf{r}) V_{NL}^{lm} \phi_{lm}^{*}(\mathbf{r}) \qquad (12)$$

where $\mathbf{r} = \mathbf{x} - \mathbf{R}_I$ and on the right-hand side we have separated the PP into a local term $V_{loc}(\mathbf{r})$, depending only on the position $\mathbf{r}$, and a non-local (NL) part represented by a sum over all the orbital angular momenta l,m. The functions $\phi_{lm}(\mathbf{r}) = f_l(r)Y_{lm}(\Omega)$ are eigenfunctions of the atomic Hamiltonian in which the core-valence interaction has been replaced by the PP, $f_l(r)$ indicates the radial part of the solution, whereas the angular dependence is represented by the spherical harmonics $Y_{lm}(\Omega)$. Several analytical forms for the PPs have been reported over the years[15] and widely used in applications ranging from gas-phase molecules, to solid state system and soft matter. In general they are *norm-conserving*. The meaning of this definition is that the square norm of the wavefunction is preserved in the pseudopotential construction. In fact, a general PP (radial) wavefunction $\phi^{PP}(r)$ is nodeless and matches the all-electron one $\phi^{AE}(r)$ only beyond a certain distance r_0 from the nucleus, called cut-off radius,

$$\begin{cases} \phi^{AE}(r) = \phi^{PP}(r) & \forall r > r_0 \\ \phi^{AE}(r) \neq \phi^{PP}(r) & \forall r < r_0 \end{cases} \qquad (13)$$

Nonetheless, the norm of the wavefunction is conserved in the sense that

$$\int_0^\infty \left|\phi^{AE}(r)\right|^2 r^2 dr = \int_0^\infty \left|\phi^{PP}(r)\right|^2 r^2 dr \qquad (14)$$

This rather stringent condition can be released as shown by Vanderbilt (1990)[13a], leading to the so-called ultra-soft pseudopotentials. On the other

hand, an augmented charge has to be added in order to conserve the total charge density as obtained upon integration of the square modulus wavefunction. As a final observation, let us point out that in some cases the presence of a core electron charge density distribution can be properly accounted for via the introduction in the pseudopotential of a non-linear core correction[16].

Finally, the fifth and last term in right-hand side of Eq. (3) is simply the Coulomb interaction between two classical nuclei *I* and *J* and is written as where Z_I and Z_J must be intended as the net valence charge only in a PP approach.

$$E_{II} = \sum_{I<J}^{M} \frac{Z_I Z_J}{|\mathbf{R}_I - \mathbf{R}_J|} \qquad (15)$$

The total energy E^{tot} of the ground state of such a system of interacting electrons and nuclei can then obtained by minimizing the KS functional with respect to the single-particle orbitals $\psi_i(\mathbf{x})$,

$$E^{\text{tot}} = \min_{\{\psi_i\}} E^{\text{KS}}[\rho] \qquad (16)$$

which, in practice, means solving the KS Schrödinger-like equations given by the variational derivative of the KS functional with respect to the single-particle wavefunctions $\psi_i(\mathbf{x})$,

$$\frac{\delta E^{\text{KS}}[\rho]}{\delta \psi_i^*} \equiv f_i H^{\text{KS}} \psi_i(\text{x}) = f_i \varepsilon_i \psi_i(\text{x}) \qquad (17)$$

A question that at this point is still unanswered is "what is $\psi_i(\mathbf{x})$?". In a way similar to what has been done in the case of HF, also in DFT approaches we need to select a proper basis set on which orbitals can be expanded. One possible choice is to adopt a Slater or Gaussian set of functions, as successfully done in many quantum chemistry approaches. An alternative choice, and rather popular in the physics community, is represented by plane waves (PW). In this expansion, the single-particle wavefunctions $\psi_i(\mathbf{x})$ become:

$$\psi_i(\mathbf{x}) = \sum_{\mathbf{G}=0}^{\mathbf{G}^{\max}} c_i(\mathbf{G}) e^{i\mathbf{G}\cdot\mathbf{x}} \qquad (18)$$

where the Hilbert space spanned by the plane waves exp(i**Gx**) is truncated at a suitable cut-off generally expressed as an energy and measured in Rydberg, E_{cut} = $(\mathbf{G}^{max})^2/2$. The advantage of plane waves is that they do not depend on the atomic positions $\mathbf{R}_I$, the accuracy can be systematically (variationally) improved by increasing the cut-off and they form a complete orthonormal basis-set. The first property is useful in the calculation of the forces required for instance in dynamics, since Pulay forces are exactly zero, and the Hellmann-Feynman theorem[17],

$$\frac{\partial E}{\partial \mathbf{R}_I} = \langle \psi \,|\, \frac{\partial \hat{H}}{\partial \mathbf{R}_I} \,|\, \psi \rangle \qquad (19)$$

Furthermore, the calculations of gradients $\left(\nabla\psi_i(\mathbf{x}) = \sum_{\mathbf{G}} i\mathbf{G}c_i(\mathbf{G})e^{i\mathbf{G}\cdot\mathbf{x}}\right)$ or Laplace operators $\left(\nabla^2\psi_i(\mathbf{x}) = -\sum_{\mathbf{G}} G^2 c_i(\mathbf{G})e^{i\mathbf{G}\cdot\mathbf{x}}\right)$, such as the electronic kinetic energy, is reduced to simple products in the Fourier space; the use of the fast Fourier transform (FFT) makes the calculation straightforward and distributable in parallel processing[18]. As a word of warning, since often radicals are involved in the reactions studied here, we checked all the results with self-interaction corrections.

4.1.2 Car-Parinello Method

Most of the quantum chemical applications are static calculations of the electronic structure performed either on stable experimental configurations or on stationary points obtained via geometry optimization. These are indeed instructive and rich of information. Nonetheless, finite temperature and entropy effects are two of the dominant features in chemical reactions, particularly in solution, and the role of the explicit solvent is far from negligible. In this respect, the so called first principles molecular dynamics (FPMD) has represented a huge step forward in quantum simulations of condensed phases in general and, more recently, in biological systems. In practice, the interactions among atoms, instead of being described by an analytic function of the atomic coordinates $\mathbf{R}_I$, is directly computed from the total energy E^{tot}, which is simultaneously a function

of the electron wavefunctions and of the atomic coordinates in the sense specified at the beginning of this paragraph. The interactions are supposed to be electrostatic, i.e. dependent just on the charges and positions of the particles and not on their velocities; in particular, the Born-Oppenheimer (BO) approximation, at a given instant t in time, consists in an optimization of the electronic structure at the corresponding (fixed) nuclear positions $\mathbf{R}_I(t)$. Then the nuclear forces are computed as gradients of the total energy with respect to the ionic position and the variables $\mathbf{R}_I(t)$ updated to $\mathbf{R}_I(t+\delta t) = \mathbf{R'}_I(t')$. The set of equations that one has to solve iteratively reads

$$M_I \ddot{\mathbf{R}}_I = -\nabla_{\mathbf{R}_I} \min_{\{\psi_i\}} E^{\mathrm{tot}}\left[\{\psi_i\}, \{\mathbf{R}_I\}\right] \qquad (20)$$

$$\frac{\delta E^{\mathrm{tot}}}{\delta \psi_i^*} \equiv H^{\mathrm{tot}} \psi_i(\mathbf{x}) = \varepsilon_i \psi_i(\mathbf{x}) \qquad (21)$$

and imply the recalculation of the electronic ground state after each displacement of the atoms. The BO approximation assumes that electrons stay "frozen" on their ground state, whereas nuclei move and for this reason it is referred to as "adiabatic approximation".

An alternative to this scheme has represented a real breakthrough in first principles dynamical simulations: the Lagrangean-based method proposed by Car and Parrinello in 1985[19]. Two major problems arise in FPMD: On one hand one has to integrate the equations of motion for the nuclear positions, which represent the long time scale part to the problem. On the other hand, one has to propagate dynamically the smooth time-evolving (ground state) electronic subsystem. The Car-Parrinello molecular dynamics (CPMD) is able to satisfy this second requirement in a numerically stable way and makes an acceptable compromise for the time step length of the nuclear motion. The formulation is an extension of a classical molecular dynamics Lagrangean in which the electronic degrees of freedom are added to the system, along with any other dynamical variable $q_\alpha(t)$, such as a thermostat[20] or a barostat[21].

$$\mathcal{L}^{\mathrm{CP}} = \frac{1}{2}\sum_I M_I \dot{\mathrm{R}}_I^2 + \sum_i \mu \int d^3x \left|\dot{\psi}_i(\mathrm{x})\right|^2 + \frac{1}{2}\sum_\alpha \eta_\alpha \dot{q}_\alpha^2 - E^{tot}\left[\rho, \{\mathrm{R}_I\}, q_\alpha\right]$$

$$+\sum_{ij}\lambda_{ij}\left(\int d^3x \psi_i^*(\mathrm{x})\psi_j(\mathrm{x}) - \delta_{ij}\right) \qquad (22)$$

The first three terms in the right-hand side of Eq. (21) are the kinetic energies of the nuclei, of the electrons and of the additional dynamical variables, the fourth one is the total energy, in practice the DFT functional in the applications that will be discussed, and the last addendum is the orthonormality constraint for the wavefunctions. The kinetic energy for the electronic degrees of freedom is the novelty of the CPMD approach. The fictitious mass μ assigned to the orbitals $\psi_i(\mathbf{x})$ is the parameter that controls the speed of the updating of the wavefunctions with respect to the nuclear positions and, for this reason, it determines degree of adiabaticity of the two subsystems, electrons and nuclei. A rigorous mathematical proof has been given[22], showing that the CPMD trajectory $\{\mathbf{R}^{\mathrm{CP}}(t)\}$ stay close to the BO one $\{\mathbf{R}^{\mathrm{BO}}(t)\}$ and the upper bound is given by $|\mathbf{R}^{\mathrm{CP}}(t) - \mathbf{R}^{\mathrm{BO}}(t)| < C\,\mu^{1/2}$, where C is a positive constant. This is nothing else but a strategy to update on-the-fly the wavefunctions when ions undergo a displacement. The related Euler-Lagrange equations of motion read.

$$\mu\ddot{\psi}_i(\mathbf{x}) = -\frac{\delta E^{\mathrm{tot}}}{\delta \psi_i^*} + \sum_j \lambda_{ij}\psi_j(\mathbf{x}) \qquad (23)$$

$$M_I \ddot{\mathbf{R}}_I = -\nabla_{\mathbf{R}_I} E^{\mathrm{tot}} \qquad (24)$$

$$\eta_\alpha \ddot{q}_\alpha = -\frac{\partial E^{\mathrm{tot}}}{\partial q_\alpha} \qquad (25)$$

Let us observe that it is straightforward to give a Hamiltonian, instead of a Lagrangean, formulation of the CPMD method, via a simple Legendre transform. Despite the fact that the method dates back to more than a quarter of century,

applications to proteins and nucleic acids became possible only in the late 90s, when large systems could be computationally afforded.

4.1.3 Blue Moon

One of the earliest techniques for sampling rare events and related free energy landscapes, also in the sense of the historical development, was the Blue Moon[22]. For all the details, we refer the reader to the cited publications. Just to summarize the essential points, let us recall that in a quantum dynamical simulation, the method rely on the identification of a reaction coordinate, or order parameter, $\xi = \xi(\mathbf{R}_I)$ of a given subset of atomic coordinates (Lagrangean variables) $\mathbf{R}_I$ able to track the chemical reaction on which one wants to focus. The simplest example is represented by the distance between two atoms that are expected to form or break a chemical bond as in all the cases studied here. This analytical function is added to, e.g., a Car-Parrinello Lagrangean as a holonomic constraint,

$$\mathcal{L} = \mathcal{L}^{CP} + \lambda_k \times \left[\zeta(\mathbf{R}_I) - \zeta_k\right] \qquad (27)$$

where λ_k is a Lagrange multiplier and ξ_k is a given assigned value of $\xi(\mathbf{R}_I)$ that one wants to sample. For each sampled value, a constrained dynamics is performed and then the average constraint force f_ξ computed as the time average

$$f_\xi = \langle \lambda_k \rangle_t = \frac{\partial F}{\partial \xi} \qquad (28)$$

turning out to be the gradient of the free energy F along ξ. The free energy profile of the reaction is then computed as

$$\Delta F = \int_{\xi_0}^{\xi_f} f_\xi \, d\xi \qquad (29)$$

where ξ_0 is the initial value of the reaction coordinate and ξ_f the final one.

4.2 Introduction of our problem

The main target of the present set of simulations has been the radical reaction. The reactions were realized in laboratory in several usual and unusual environments, namely toluene, benzene, ionic liquids or even simple water[23]. The general reaction mechanism is shown Scheme 1

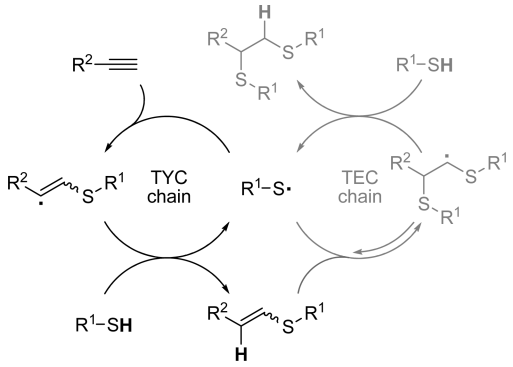

Scheme 1. Mechanisms of TYC and TEC Radical Chains

In the first step, on which we focused, is the thio-radical addiction to the electron-rich system named TYC; this step proceeds with the formation of a β-sulfanylvinyl radical (see Figure. 1). The specific thio-radical selected is the methyl thioglycolate, the smallest molecule used during the synthesis work. For electron rich molecules, attention has been paid to terminal alkyne, in particular 1-octine; the approach is equivalent to alkene TEC, characterized by mono and bis adduction during the different synthesis. The β-sulfanylvinyl formed readily abstracts hydrogen from thiols in solution, to regenerate the chain-carrier (R1-S·), sulfur-centered radical intermediate, with simultaneous formation of vinyl sulfide mono adduct (TYC chain).

The second reaction step (TEC) could not be studied within the limits of the present thesis. In such a step, the mono adduct can undergo further addition of another sulfanyl radical to give an α,β-disulfanyl-disubstituted alkyl radical that can subsequently abstract hydrogen from the thiol to give the final bis-sulfide bis-adduct (TEC chain, Scheme 1). Our studies, instead, were pursued by focusing on the crucial intermediates Vinil-E and Vinil-Z.

4.3 Computational Section

First-principles dynamical simulations have been performed with the CPMD package version 3.15.1[24]. The simulated systems were always placed in cubic or orthorhombic supercells (of lateral sizes in the range of 10-20 Å) on which periodic boundary conditions were applied whenever the solvent was present. In the cases in which reactions in vacuum were studied, these periodic boundary conditions were released and the system treated as isolated. On the other hand, the solvated conditions have been reproduced by periodic boundary conditions anb surrounding the solute molecule (or molecules) with a number of water molecules sufficient to reproduce at least 2-3 hydration shells, keeping the density of the solvent water to the experimental liquid density (0.99 g/cm^3).

Valence electrons are expanded in a plane-wave basis set with an energy cut-off of 70 Ry. All the calculations presented here, since they involve radicals or, in general, unpaired electrons have been performed in the spin-unrestricted local spin density approximation (LSD), thus allowing for a correct treatment of the open-shell cases. The core-valence interaction was expressed in terms of Trouiller-Martins norm conserving pseudopotentials for C, O and S, whereas a von Barth-Car norm conserving pseudo- potential was used for H atoms. The Kleinman–Bylander factorization was used for the nonlocal part and the BLYP gradient corrections mentioned at the beginning of this chapter were used for the exchange-correlation functional. The integration time step was set to 3.0 a.u. (0.12 fs) for vacuum system, and 4.0 a.u in case of solution (0,096 fs). This choice is driven by the necessity to keep into account the fast H stretching modes, which are a bit slowed down in solution, due to the presence of the hydrogen bond network of water, hence allowing for a slightly larger time step. A fictitious electron mass of 380-400 a.u. ensured good control of the constants of motion during the dynamics.

The simulations have been performed for total times ranging from 0.5 ps for Vinyl to more than 5.0 picoseconds for the inspection of reaction pathways within the Blue Moon ensemble approach.

The temperature was set to 300 K (i.e. 26-27 °C) and controlled with a Nosé-Hoover thermostat[25] after an initial equilibration phase where a velocity

rescaling algorithm was used to thermalize the system. An example is reported for the case of the β-sulfanylvinyls, where simulations have been performed on the E and Z configurations, which are experimentally known to co-exist and between which our solute can easily switch during its exploration of the phase space.

Has also explicated local spin density approximation (LSD) to split the calculation for all valence electrons present in the calculation and not consider the valence orbital like close shell.

In all the constrained dynamics simulations, done within the Blue Moon scheme[23], the reaction coordinate was chosen to be the distance between the atoms involved in the reactions. Specifically: (i) for thio-radical addictions the reaction coordinate adopted was the distance of the S atom of the thio-radical molecule (methyl-thioglycolate, R-S·) from the terminal carbon of the alkyne (C). (ii) Analogously for the H transfer, although some intrinsic difficulties imposed a slight variation; namely, in an initial stage, the distance between the S atom of thiol-molecule (R-SH) and the radical carbon center of β-sulfanylvinyl (C·) was used as a constraint, just to approach the two reacting molecules preventing artificial de-hydrogenation which could be induced by constraints on H. In fact, the bond between S and H is rather weak, and risk could break (artificially) apart if an uncareful constraint, corresponding to a pulling force, is applied. Only in a second stage, when the molecules were eventually separated by about 3.0 Å we switched to the H-C distance constraint.

All molecules have been constructed and sketched with the ChemBioDraw version 12.0.3 or MarvinSketch version 5.3.8 in 2D, and subsequently transformed in 3D system by MarvinSpace or MarvinView version 5.3.8. The 3D coordinate has been transported in CPMD input file. These structure were used as initial configurations and both wavefunctions and geometries were initially fully optimized before each dynamical run. Data were visualized and analyzed using the VMD software[26], gnuplot[27] and XmGrace

4.4 Result and Discussion

Reaction conditions: no solvent

Thiyl-radical addiction

The calculations discussed here focus on the addition of methylthiyl-radical to 1-octyne (Figure 1, a).

After an initial unconstrained CPMD dynamics, needed to equilibrate the system, the free energy profile was computed with the Blue Moon ensemble approach, using as a reaction coordinate (RC) the distance $d_{S\text{-}C}$ = |R(S)- R(C)| show in Figure 1a. For each fixed constraint value, simulations were run for about 1–1.5 ps and thirty points; each value was characterized by different RC values, ranging from 7.14 Å to 1.85 Å. At the end of the constrained dynamics simulations, all constraint on the final reaction product were released and a free dynamics was performed to confirm the stability of the bond formed. On the reactants side, the simulation started with a planar angle configuration between C_α and S·, as shown in Figure 1a. After few femtoseconds we observed the thiol radical moving in a position in which the two reactants form on average a 90° angle, a position compatible with the generally accepted reaction pathway always assumed as a starting point in all former ab-initio calculations.[28] This is an important result that suggests that our reactants seem to rearrange spontaneously in such way as to allow for the studied reaction to occur without imposing any ad-hoc geometry which could bias the whole simulation.

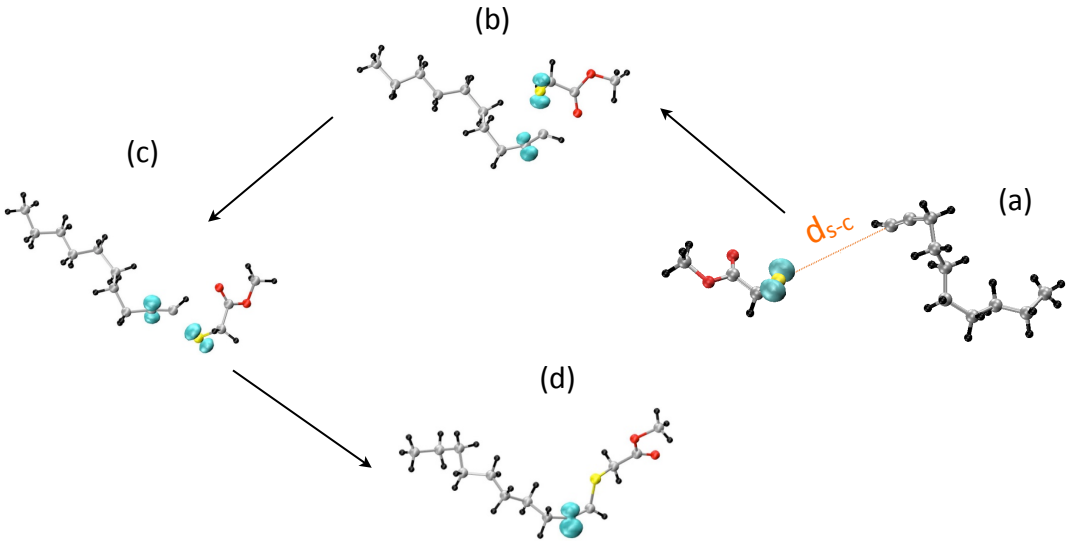

Figure 1. Localization of Spin in the key point of simulation show in Figure 2

In such a process the thiol radical aligns onto the plane of the C-C triple bond with formation of the β-sulfanylvinyl radical, whose formation requires an activation energy of 10.5 kcal/mole; Figure 1d shows the whole reaction pathway.

During the simulation the interaction between the two reaction centers (Figure 2, upper panel) is positive (> 0 au), that is the forces between the two atoms are repulsive, until the transition state is reached; afterwards, the forces becomes attractive (< 0 au) to form the stable sulfanylvinyl radical. The constraint force returns repulsive when the distance between the atoms further decreases. The lower panel of Figure 2 shows, the free total energy involved in the reaction, with the maximum indicating the transition state.

Figure 1, in which the cyan surfaces represent spin density distribution, clearly show that the transition state can be attained through two different approaches, i. e. with the sulfanyl radical coming closer to the C-C triple bond on either sides with respect to the hydrocarbon chain of the alkyne, hence forming Z- and E-β-sulfanylvinyl radicals (structures **b** and **c**). It is worth noting that, both in the transition states and in the final intermediate, the spin distribution is correctly predicted to be on the internal carbon of the C-C unsaturated bond.

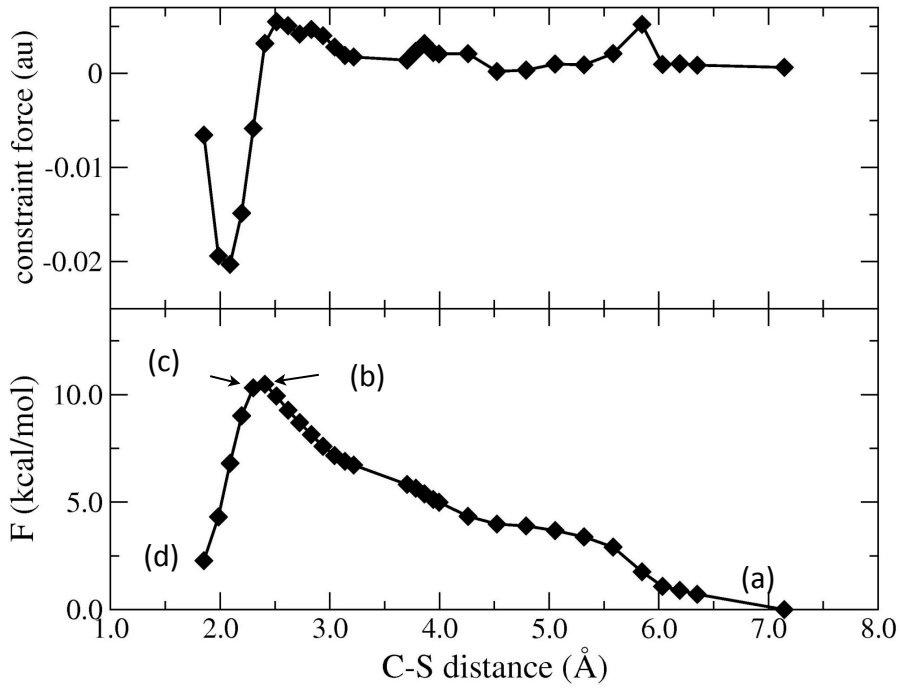

Figure 2. thiol-radical addition path way. Is also represented the localization of Spin in the key point of simulation. Initial state C-S distance 7.0 Å, Transition state, between 2.0 and

Calculations afforded the thermodynamically less stable Z-vinyl radical (Structure **d**) but this point is of no importance as far as the stereochemical outcome of the reaction is concerned, since, as previously reported, E- and Z-vinyl radicals are known to interconvert very rapidly into each other.

β-sulfanylvinyls (E and Z) have been simulated for 0.4-0.7 ps, to observe the interchangeability between the two structures. Figure 3 shows the temperature of the Vinyl interconversion system as a function of the simulation step for the (NVT) calculation using a Nosé-Hoover thermostat for temperature control. In the initial stage, a velocity-rescaling algorithm was used to attain thermal equilibrium (after red line), and then a canonical thermostat of the type indicated above was adopted. Figure 4 shows the corresponding energies calculated step by step during the simulation.

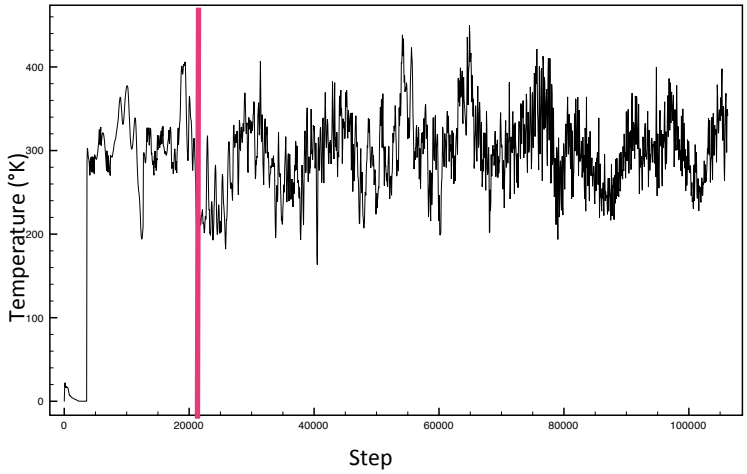

Figure 3. Simulation with Nosé-Hoover thermostat. After an initial rescaling

Car-Parrinello-like simulations critically depend on the ability to control the drift of the electronic wave functions away from the instantaneous Born-Oppenheimer (BO) ground state and, to ensure a good degree of adiabaticity of the CPMD method during the simulation, a very good control of the electron fictitious kinetic energy must be ensured. Figure 4 shows in red the EKS Kohn-Sham energy, equivalent to the potential energy in classical MD; in green the EHAM energy of the total CP-Hamiltonian, that must be conserved during the simulation; in blue the total classical energy (ECLAS), i. e. the difference between the EHAM and the electron kinetic energy (EKINC).

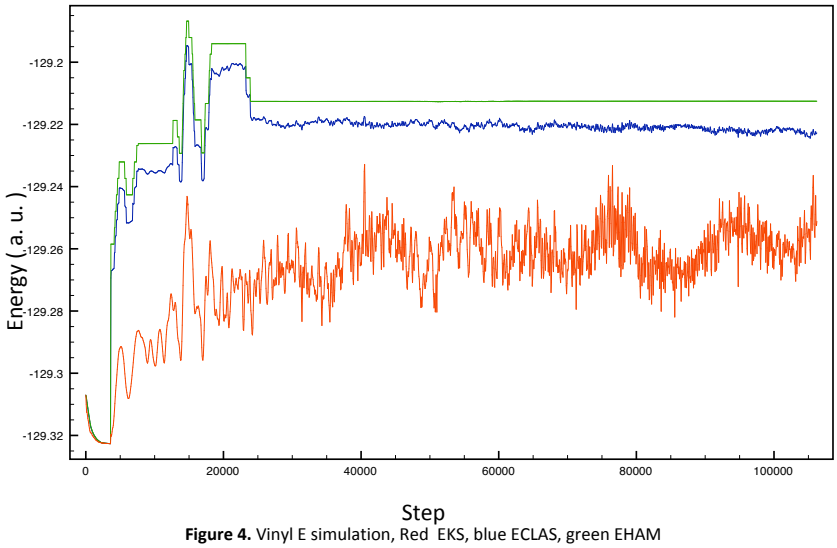

Figure 4. Vinyl E simulation, Red EKS, blue ECLAS, green EHAM

Figures 3 and 4 report comparable results, showing that the two vinyl structures are able to interconvert into each other at 300 K, giving Z/E lifetime

ratios of about 2/1 and 4/1 starting from the E- and Z-configuration, respectively (Figure 5).

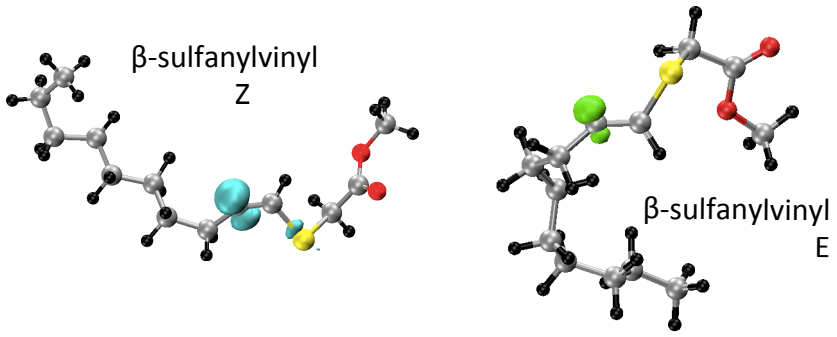

Figure 5. β-sulfanylvinyl E and β-sulfanylvinyl Z.

Hydrogen transfer: vinyl sulfide mono adduct formation

The simulation in total took more than 3.0 ps. By accosting the β-sulfanylvinyl radical (Figure 6, **a**), and the thiol molecule (Figure 6, **b**) we expected, at a proper distance, the hydrogen thiol to be transferred to the β-sulfanylvinyl radical, giving the final vinyl sulfide mono adduct.

We performed twenty-one calculations of different RC values, from 5.00 Å - to 2.40 Å, for the distance between the thiol and the vinyl radical, in particular between the thiol sulfur atom and the vinyl carbon radical.[29] Heuster and Kalvoda[30] proposed, for hydrogen transfer between C and O, a C-O distance of less than 2.8 Å. Houk et al.[31] found for the analogous transition-state geometry a C-O distance of 2.48 Å. Sulfur has larger size and a more diffused electron cloud than carbon or oxygen atoms; indeed Jørgensen et al.[32] calculated for C-S H-transfer a C–H···S distance in the transition state close to 3.0 Å with a C–H···S angle close to 130°. Subsequently Himo[33] confirmed those data, and proposed for hydrogen atom transfer from cysteine to glycyl radical a C-S distance close to 3.0 Å.

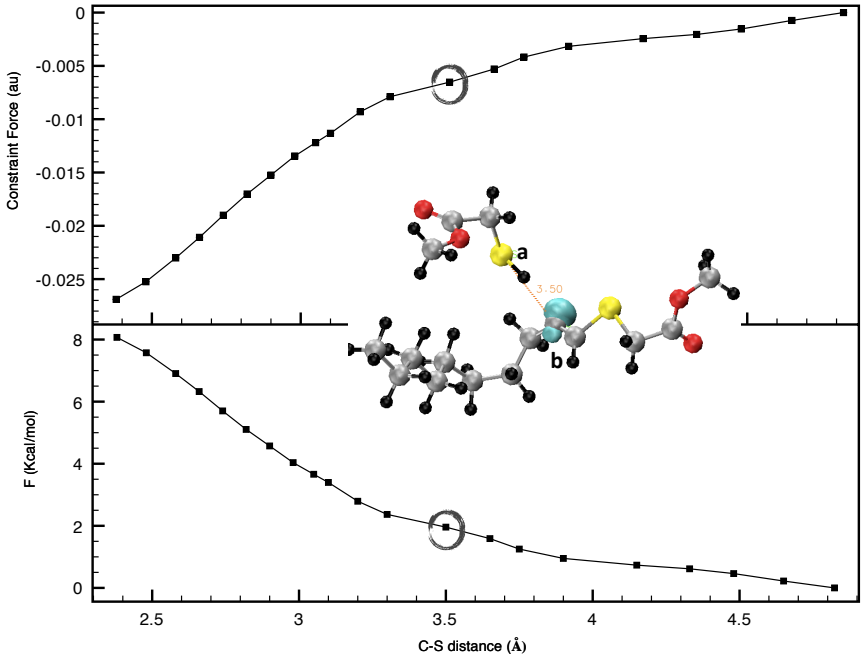

Figure 6. Hydrogen transfer. Constrained simulations between C-S

As shown in Figure 6, our first simulation did not give the expected results, since, instead of hydrogen transfer, the formation of a new bond between carbon and sulfur occurred. Therefore, starting from the geometry calculated for a C-S distance of 3.5 Å (circled point in Figure 6), a parameter in line with Himo and Jørgensen, we initially restarted the simulation with a double constraint involving both the C-S and the C-H bonds. After few femtoseconds the former constraint was eliminated and the simulation carried out with the latter only.

Simulation was performed for twenty points more, with the C··H distance ranging from 2.70 Å to 1.30 Å. At nearly 1.70 Å, a transition state was observed, and the final formation of the C-H bond was observed at 1.50 Å (Figure 7, Ts and Fs).

The thiol molecule is shown to approach the vinyl radical with a C=C-H angle of about 90° to 120°. In the transition state the C•-S distance during hydrogen transfer was found to be 3.07 Å, in line with previous results.[32,33] In the vacuum, the activation energy for hydrogen transfer from methyl thioglycolate to 1-octyne was calculated as ~4,7 kcal/mol.

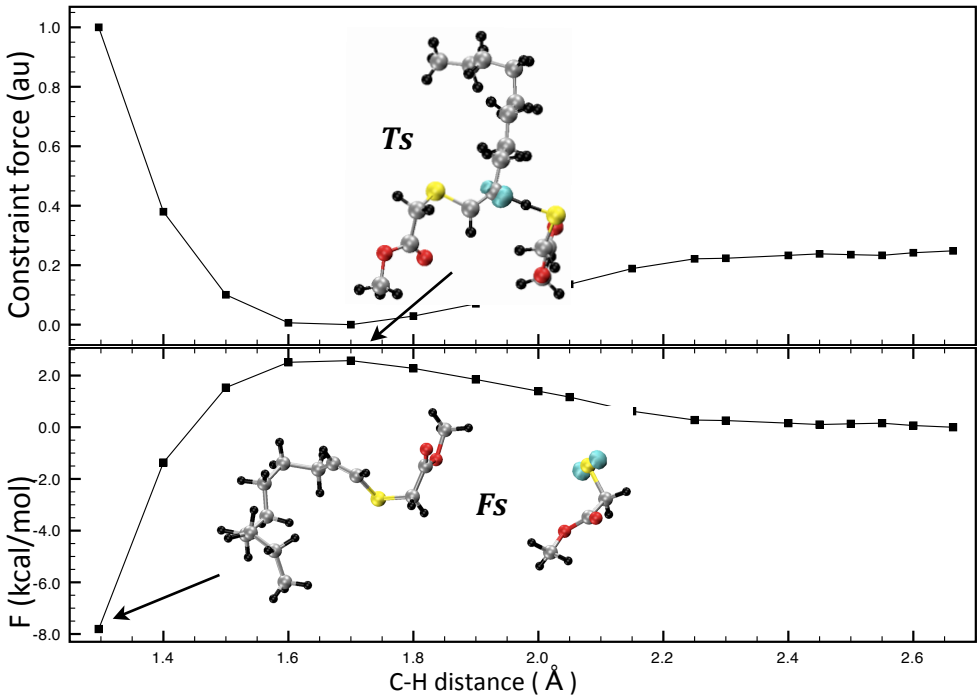

Figure 7. Hydrogen transfer. Constrained simulations between C-H, after initial constraint C-S

To conclude this section it is worth pointing out that, during the simulations shown above, all molecules/intermediates were completely free to move in the space, with the only exceptions of the constraints explained above. That means that vinyl radicals were free to interconvert between their E- and Z-configurations. After hydrogen transfer, calculations predicted formation of the Z-vinyl sulfide, that is the expected kinetic product.

Reaction conditions: solvent (water)

There are different types of effects induced by the solvent. Solvent molecules can be part of the reaction, like for instance in hydrolysis reactions. In this case, the only way to model the situation is, of course, to include the parts that are needed in the quantum calculation. The same applies to short-range solvent effects, where, for instance, strong hydrogen bonds are known to form or break during the course of the reaction. Other methods use the dielectric constant to emulate the solvent.

CPMD calculations fill the calculation box with molecules of the solvent taken into consideration. Therefore we initially built a simulation box characterized by similar dimensions with respect to the previous simulations, but filled with so many water molecules as to obtain the normal water density

value of 0,99 g/cm^3 at RT. After an initial free dynamics of 1.0 -2.0 ps, we needed to eliminate some water molecules to ensure a constant pressure value of the reaction vessel.

Thiyl-radical addiction

Simulations of about 1–1.5 ps were performed for twenty points of different RC values.

Figure 8 (lower panel) shows the free energy of the reactants (red line) and the total energy (black line) for the solvated system; the upper panel reports the interaction force between the two reaction centers. We can observe that, close to 4.0 Å, the total energy decreases of few kilocalories/moles in correspondences with a calculated structure where there is a proton sharing between the thiyl radical and the terminal carbon of the alkyne Figure 8 a.

Although more constrained by the solvent molecules with respect to the vacuum, the thiyl radical was observed to be able to move rapidly in a position orthogonal to the carbon-carbon triple bond, analogously to what predicted in the vacuum. Also in this case preferential formation of the Z-vinyl radical was observed. The transition state was located between 2.2 Å and 2.5 Å (Figure 8 b) and the activation barrier for formation of the β-sulfanylvinyl radical (Figure x c) was calculated as 6.8 kcal/mol (17.0 kcal/mol for the total energy).

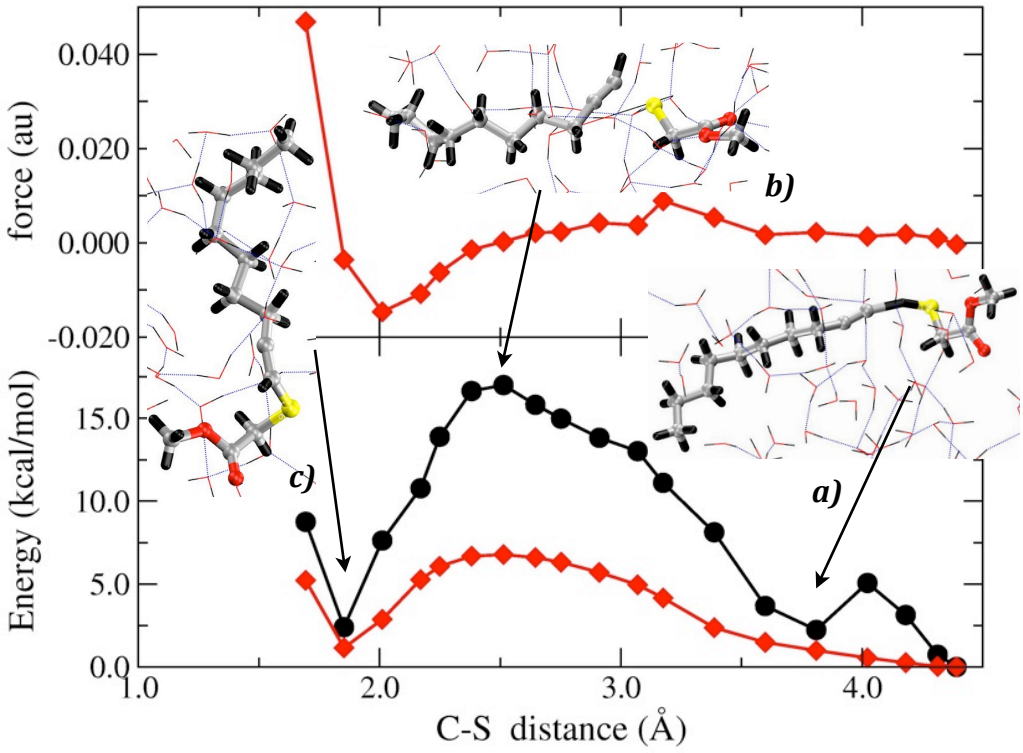

Figure 8. Thiol-radical addition path way in solution. a) Proton sharing, b)Transition state c) Final state.

Hence, the solvent effect in lowering the activation energy for addition of the thiyl radical to the alkyne can be estimated as approximatively 4.0 kcal/ mole.

As far as E/Z interconversion is concerned, the results in water are comparable with those obtained in the vacuum. This means that vinyl radicals, although more constrained by the solvent, are able to flip and interconvert very rapidly at 300 K: Z/E lifetime ratios were about of about 1/1 and 2/1 starting from the E- and Z-configuration, respectively (Figure 9). This result would suggest that water could influence the carbon chain mobility in such a way as to favour vinyl radical interconversion, although this is a preliminary result that has to be supported by further, more sound experimental data. This result is however in line with the data obtained for additions of thiyl radicals to alkynes carried out in water (Chapter 4, Table 3).

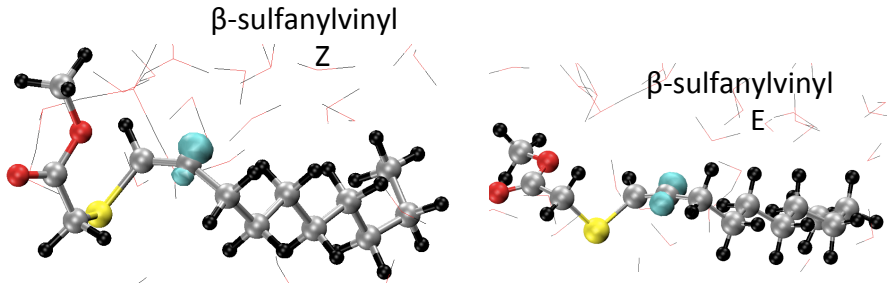

Figure 9. β-sulfanylvinyl E and β-sulfanylvinyl Z solvated in water.

Hydrogen transfer: vinyl sulfide mono adduct formation

After an initial unconstrained simulations of 0.5 ps, the thiol was observed to perform a spontaneous hydrogen transfer to the vinyl radical. Figure 10 shows the transition state structure (**b**) and the activation energy can be evaluated as lower than 2.5 kcal/mole at 300 K. This can only be an evaluation, since that value is comparable to the the error bar of the method. However it can be inferred that hydrogen transfer from a thiol to a vinyl radical seems to be a quasi-spontaneous process at room temperature in water.

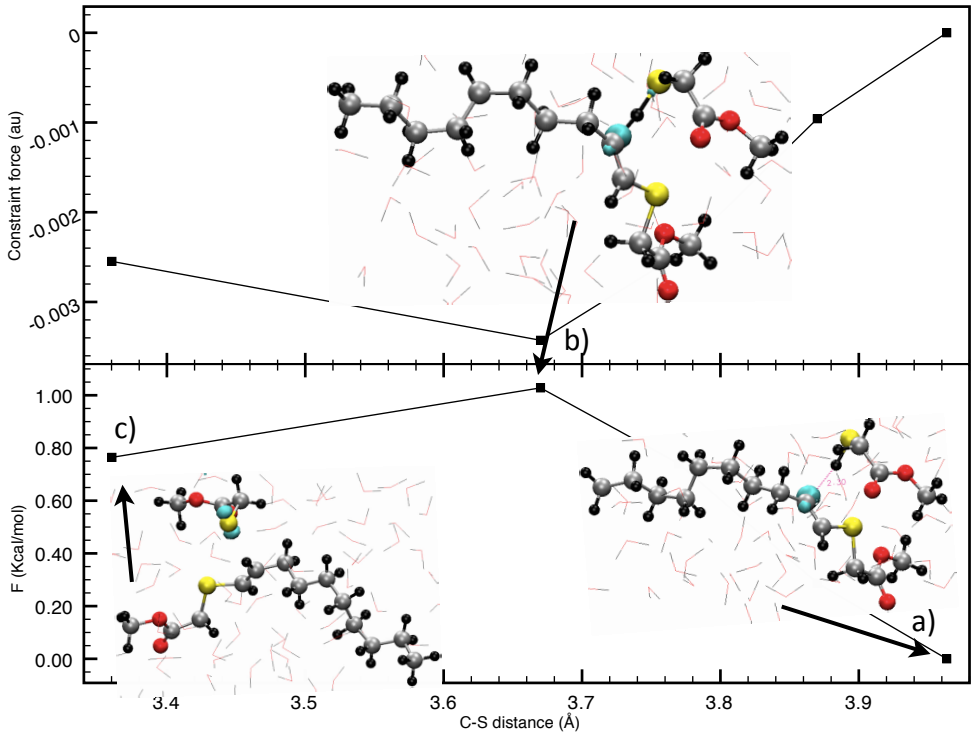

Figure 10. Hydrogen transfer. Constrained simulations between C-S

Mulliken population Analysis

Performing Mulliken charge density analyses during the simulations, allows for studying charge evolution along the reaction pathway.

Graphic 1 shows the trends obtained by analyzing thiyl-radical addition in the vacuum and in water and shows the main atoms involved in the reaction (Figure 11) and their charge evolution (Table 1).

The only significant modification of the charge distribution moving from the reactants to the product through the transition state was observed for the sulfur atom and, unexpectedly, for the sp^3 carbon atom linked to the C-C triple bond. In the transition state the sulfur atom shows a propensity for assuming a partial negative charge and this result is in line with the polar characteristics of many transition states involved in radical reactions. Of course, the presence of water as the solvent can have a very beneficial effect by stabilizing charge separation in the transition state. The development of the positive charge on the carbon atom is instead much more puzzling and currently we don't have any explanation for this unprecedented datum.

Graphic 2 shows the analogous trends obtained for hydrogen transfer from the thiol moiety to the vinyl radical. Data are summarized in Table 2 and the involved atoms are labelled in Figure 12. A first, notable difference between the two reaction conditions (vacuum and water) is a strong charge separation in the reactants atoms (IS) before hydrogen transfer in the vacuum; this situation rapidly evolves towards a more uniform charge distribution even before the transition state is reached. In water it seems the solvent effect could decrease the local charge throughout the whole system, hence decreasing Coulomb interactions. Under these conditions, the only important trend is that of the carbon atom that is the terminus of hydrogen transfer: this atom increases its positive charge by approaching the transition state, as requested by polar effects in hydrogen atom transfers, and then becomes more and more negative by coming closer to the final state, as a result of conjugation with the sulfur atom. At the same time, the thiol sulfur lowers its positive charge in approaching the transition state, although the effect is much smaller than expected. The fact that in water the electron distribution of the initial state is much closer to that of the

transition state with respect to the vacuum conditions could suggest that the system would not require such an important rearrangement to be transformed into the products as in the vacuum: this hypothesis may well give an explanation for the calculated very low activation barrier for hydrogen transfer in aqueous solution.

Dec_Mulliken	A	B	C	D	E	F
	Vacuum					
Initial State	-0,279	-0,050	-0,239	-0,417	0,475	0,131
TS_2_41	-0,039	0,034	-0,172	-0,408	0,452	0,063
Final State	-0,279	0,023	-0,295	-0,407	0,470	0,210
	Water					
Initial State	-0,283	-0,021	-0,236	-0,413	0,475	0,121
TS	0,273	0,022	-0,218	-0,372	0,448	-0,050
Final State	-0,287	0,063	-0,328	-0,417	0,478	0,297

Table1. Mulliken spin densities on different atoms take in consideration.

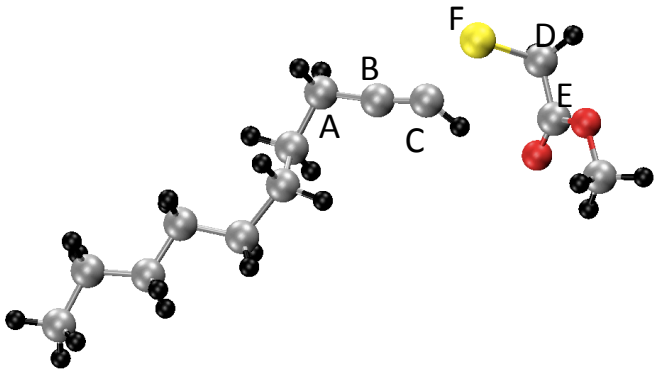

Figure 11. Atoms take in consideration in Table 1

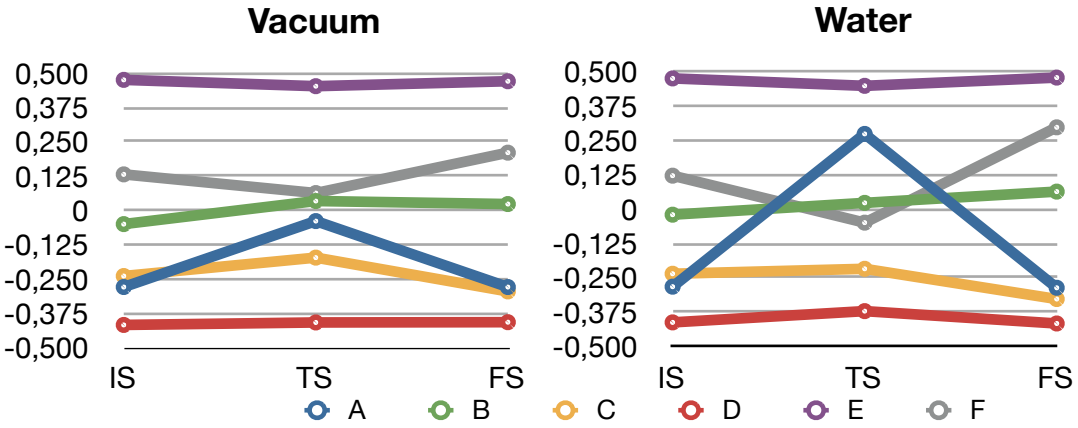

Graphic 1. Mulliken spin densities of Table 1

Quench_Mulliken	A	B	C	D	E	F
			Vacuum			
Initial State	-0,830	0,498	-0,884	0,884	0,394	0,110
TS_150	-0,247	0,059	-0,325	0,266	0,159	0,098
TS_160	-0,293	0,151	-0,311	0,220	0,070	0,040
TS_170	-0,290	0,162	-0,343	0,275	0,037	0,042
Final State	-0,264	-0,132	-0,251	0,244	0,222	0,187
			Water			
Initial State	-0,301	0,127	-0,342	0,267	0,076	0,096
TS_G_74501	-0,275	0,174	-0,272	0,194	0,050	0,080
TS_G_75401	-0,293	0,115	-0,277	0,265	0,096	0,034
TS_G_75741	-0,275	-0,084	-0,273	0,301	0,149	0,178
Final State	-0,236	-0,123	-0,270	0,271	0,155	0,190

Table2. Mulliken spin densities on different atoms take in consideration for Hydrogen Transfer

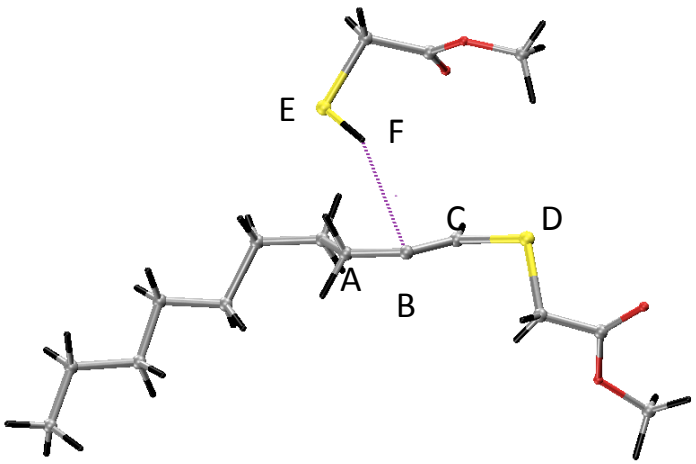

Figure 12. Atoms take in consideration in Table 2

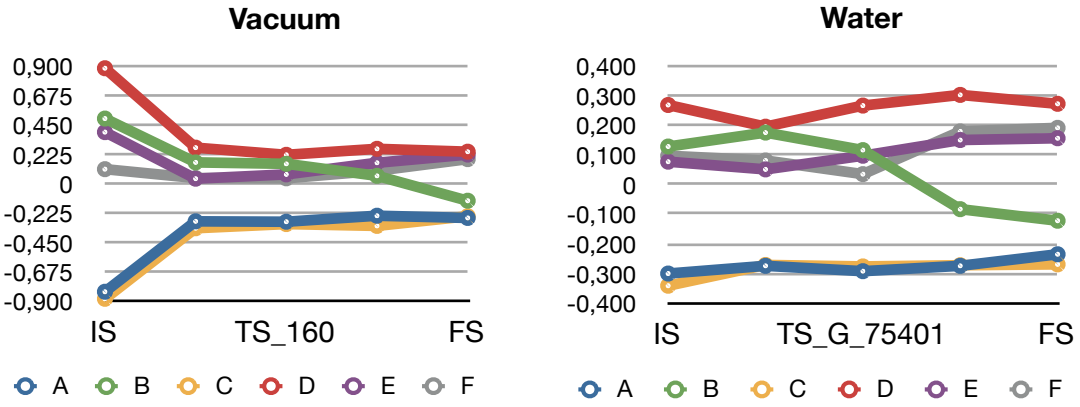

Graphic 2. Mulliken spin densities of Table 2

4.5 Conclusion

CPMD calculations were carried out in order to get some more insight into the mechanism of the thiol/yne coupling (TYC), particularly the solvent effect. The model reaction, i.e. addition of methyl thioglycolate to 1-octyne, was considered in its two steps: i) addition of the corresponding sulfanyl radical to the alkyne, followed by ii) hydrogen atom transfer from the starting thioglycolate to the resulting β-sulfanyl-substituted vinyl radical. Simulations gave, for the first step, an activation barrier in the vacuum of 10.5 kcal/mol, with the two possible final intermediates, the E- and Z-vinyl radicals, rapidly interconverting at 300 K, as expected on the basis of previous results. The activation energy of the second step was calculated as 4.7 kcal/mol, suggesting that the rate-determining step of the whole TYC reaction is addition of the sulfanyl radical to the alkyne.

In water the corresponding barriers were found to be 6.8 kcal/mol and ca. 2 kcal/mol, respectively, with the latter being an estimated value since the results of calculations were inside the error bar of the method. Neverthelss, this data suggest that both sulfanyl radical addition to the alkyne and, above all, hydrogen transfer to the resulting vinyl radical are significantly faster in water with respect to vacuum. This could be the result of charge stabilization by the water molecules, which, in the case of the hydrogen transfer step, seems to prevent a major reorganization for the system to pass through the transition state. In the addition step, on the contrary, the very similar charge distributions in reactants and products together with the significant charge development in some of the atoms directly involved in the reaction suggests formation in water of a transition state with a major charge separation: this is a situation that is commonly believed to accelerate many radical reactions, especially, like in our case, in the presence of heteroatoms that can tolerate that charge distribution. A faster addition step in water may well justify the better results obtained in that environment for TYC reactions but also a faster hydrogen transfer step may account for the preferred production of reduction products (vinyl sulfides) when the intermediate vinyl radicals may evolve by different routes.

It is however worth pointing out that, before saying that, with respect to vacuum, the effect of water in accelerating our reactions resides in its polar character or its ability to give raise to hydrogen bondings (and not, for instance, simply to entropic and/or micellar effects), it will be crucial to carry out analogous calculations in the presence of another non-polar, aprotic solvent such as benzene. Those calculations are currently underway.

4.6 Bibliography

[1] P. Hohenberg and W. Kohn, Physical Review 1964, 136, B864.

[2] W. Kohn and L. J. Sham, Physical Review 1965, 140, A1133.

[3] **a)** D. J. DeFrees, B. A. Levi, S. K. Pollack, W. J. Hehre, J. S. Binkley and J. A. Pople, Journal of the American Chemical Society 1979, 101, 4085-4089. **b)** Raghavachari, K., G. W. Trucks, M. Head-Gordon, and J. A. Pople, 1989, Chem. Phys. Lett. 157, 479. **c)** Johnson B G, Gill P M W and Pople J A 1993,J. Chem. Phys. 98 5612–26.

[4] R. G. Y. Parr, W., Density-functional theory of atoms and molecules, New York: Oxford University Press., New York, 1988, p. 333.

[5] H. J. Marx D., Modern Methods and Algorithms of Quantum Chemistry,J. Grotendorst (Ed.), John von Neumann Institute for Computing, Ju¨lich, NIC Series 2000, 1, 301-449.

[6] A. D. Becke, Physical Review A 1988, 38, 3098.

[7] J. P. Perdew and A. Zunger, Physical Review B 1981, 23, 5048.

[8] **a)** A.D Becke. J. Chem. Phys., 98 (1993), p. 5648; **b)** A.D. Becke, J. Chem. Phys. 98, 1372 (1992).

[9] **a)** J. P. Perdew, Phys. Rev. B 33, 8822 (1986); **b)** J.P. Perdew and Y. Wang, Phys. Rev. B 45, 13244 (1992);**c)** J.P. Perdew, K. Burke and M. Ernzerhof, Phys. Rev. Lett. 77, 3865 (1996); 78, 1396 (1997); **d)** S.J. Vosko, L. Wilk and M. Nusair, Can. J. Phys. 58, 1200 (1980); **e)** C. Lee, W. Yang and R. G. Parr, Phys. Rev. B 37, 785 (1988);**f)** F.A.Hamprecht, A.J.Cohen, D.J.Tozer and N.C. Handy, J. Chem. Phys. 109, 6264 (1998) **g)** A. J. Cohen and N. C. Handy, J. Chem. Phys. 117, 1470 (2002). H) X. Xu and W. A. Goddard III, Proc. Natl. Acad. Sci. USA, 101, 2673 (2004).

[10] F. A. Hamprecht, A. J. Cohen, D. J. Tozer, and N. C. Handy, J. Chem. Phys. 109, 6264 (1998).

[11] **a)** T. Schwabe and S. Grimme, Phys. Chem. Chem. Phys. 9, 3397 (2007). **b)** P. L. Silvestrelli, Phys. Rev. Lett. 100, 053002 (2008).

[12] **a)** D. Vanderbilt. Phys. Rev. B, 41:7892, 1990.; **b)** P. E. Blochl. Phys. Rev. B, 50:17953, 1994.

[13] L. Kleinman and D. M. Bylander, Physical Review Letters 1982, 48, 1425-1428.

[14] **a)** G. B. Bachelet, D. R. Hamann and M. Schlter, Physical Review B 1982, 26, 4199-4228. **b)** R. Stumpf X. Gonze and M. Scheffler. Analysis of separable potentials. Phys. Rev. B, 44:8503, 1991. **c)** N. Troullier and J. L. Martins, Phys. Rev. B 43, 1993 (1991).

[15] S. G. Louie, S. Froyen, and M. L. Cohen, Phys. Rev. B 26, 1738 (1982).

[16] R. P. Feynman, Physical Review 1939, 56, 340-343.

[17] W.H. Press, S.A. Teukolsky, W.T. Vetterling & B.P. Flannery (1992)

[18] R. Car and M. Parrinello, Physical Review Letters 1985, 55, 2471.

[19] **a)** S. NosÈ, J. Chem. Phys. 1984, 81, 511. **b)** W. G. Hoover, Physical Review A 1985, 31, 1695.

[20] **a)** H. Andersen, J. Chem. Phys. 1980, 72, 2384. **b)** M. Parrinello and A. Rahman, Physical Review Letters 1980, 45, 1196.

[21] F. A. a. S. Bornemann, Num. Math., 78 (3). 1998, 359-376.

[22] G. Ciccotti and J. P. Ryckaert, Computer Physics Reports 4, 346-392.

[23] **a)** Lanza, T.; Minozzi, M.; Monesi, A.; Nanni, D.; Spagnolo, P.;Chiappe, C. Curr. Org. Chem. 2009, 13, 1726–1732. **b)** M. Minozzi, A. Monesi, D. Nanni, P. Spagnolo, N. Marchetti and A. Massi, J. Org. Chem., 2011, 76, 450-459

[24] CPMD Consortium (2010) CPMD Consortium page.www.cpmd.org

[25] Martyna J, Klein ML, Tuckerman M (1992) Nosé–Hoover chains: the canonical ensemble via continuous dynamics. J Chem Phys 97:2635–2643

[26] Humphrey W, Dalke A, Schulten K (1996) VMD: visual molecular dynamics. J Mol Graph 14:33–38

[27] http://www.gnuplot.info/

[28] **a)** T. L. Jacobs,G. E. Illingworth Jr., The Addition of Thiyl Radicals to Allenic Hydrocarbons',The Journal of Organic Chemistry 1963 28 (10), 2692-2698, **b)** T. Kawamura, M. Ushio, T. Fujimoto, T. Yonezawa, Electron Spin Resonance Study on Intermediate Free Radicals in the Addition of Thiols to Unsaturated Compounds, Journal of the American Chemical Society / 93:4, February 24, 1971, 909 **c)** Y. A. Borisova, A. K. Dyusengalievb, G. A. Orazovab, and T. P. Serikovb, Quantum-Chemical Study of the Photochemical Addition Reaction of Dialkyl Disulfides with Olefins, PETROLEUM CHEMISTRY, Vol. 49, No. 2009

[29] A. F. Shestakov, T. G. Denisova, E. T. Denisov,à and N. S. Emeľ yanova, Reactions of intramolecular hydrogen abstraction, Russ.Chem.Bull., Int.Ed., Vol. 51, No. 4, April, 2002.,

[30] Heusler, K.; Kalvoda, J. Angew. Chem., Int. Ed. Engl. 1964, 3, 525-596

[31] Houk K. N., Tucker J. A., Dorigo A. E., Quantitative Modeling of Proximity Effects on Organic Reactivity, Acc. Chem. Res., Vol. 23, No. 4, 1990

[32] Ma, L., Jørgensen, A.-M. M., Sørensen, G. O., Ulstrup,J. & Led, J. J. J. Am. Chem. Soc. 122, 9473–9485 (2000).

[33] F. Himo, C–C bond formation and cleavage in radical enzymes, a theoretical perspective, Biochimica et Biophysica Acta 1707 (2005) 24–33

List of Publications

- Spagnolo, P., Nanni, D., Chiappe, C., Minozzi, M., Lanza, T., Monesi, A., "**Radical Additions of Thiols to Alkenes and Alkynes in Ionic Liquids**" Curr. Org. Chem., 2009, 13, pp. 1726 - 1732

- T. Lanza, M. Minozzi, A. Monesi, D. Nanni, P. Spagnolo, G. Zanardi, I**mproved Radical Approach to N-Unsubstituted Indol-2-one and Dihydro-2-quinolinone Compounds Bearing Spirocyclic Cyclohexanone/Cyclohexadienone Rings**, Adv. Synth. Catal. 2010, 352, 2275 – 2280

- M. Minozzi, A. Monesi, D. Nanni, P. Spagnolo, N. Marchetti and A. Massi, **An Insight into the Radical Thiol/Yne Coupling: The Emergence of Arylalkyne-Tagged Sugars for the Direct Photoinduced Glycosylation of Cysteine-Containing Peptides,** J. Org. Chem., 2011, 76, 450-459.